UNIVERSITY OF CALIFORNIA, SAN DIEGO

The Foraging Sorties Hypothesis: Evaluating the Effect of Gut Dynamics on Copepod Foraging Behavior

A dissertation submitted in partial satisfaction of the requirements for the degree

Doctor of Philosophy

in

Oceanography

by

Erdem Mustafa Karaköylü

Committee in charge

Professor Peter J. S. Franks, Chair
Professor Jules S. Jaffe, Co-chair
Professor Ian Abramson
Professor David Checkley
Professor James J. Leichter
Professor Mark D. Ohman

2010

ProQuest LLC
789 East Eisenhower Parkway
P.O. Box 1346
Ann Arbor, MI 48106-1346

The Dissertation of Erdem Mustafa Karaköylü is approved, and it is acceptable in quality and form for publication on microfilm and electronically:

_____

_____

_____

_____

_____

Co-chair

_____

Chair

Universiy of California, San Diego

2010

DEDICATION

To my parents, Meral and Nuri, who supported me in everything I undertook; to my dear wife Kate, who stood by me in good times and bad, long before we were married; last but not least, to my daughter Eva, who gives a sense to it all.

TABLE OF CONTENTS

LIST OF ABBREVIATIONS

chl: Chlorophyll

FS: Foraging Sorties

GTT: gut throughput time

MISCIS: Multi-spectral Copepod Imaging System

Phaeo: Phaeopigment

PLIF: Planar Laser Imaging Fluorometer

PMG: Posterior mid-gut

rfu: Relative fluorescence unit

SF: Stationary feeding

UMG: Upper mid-gut

LIST OF FIGURES

LIST OF TABLES

ACKNOWLEDGMENTS

I would like to acknowledge Professor Peter Franks for his multiple roles as chair of my committee, mentor and source of support for academic as well as non academic issues.

I would also like to acknowledge members of the Franks and Ohman Labs, for providing an arena where I could test ideas, and present results. Their constructive criticisms were invaluable.

Special thanks go to Professor Jules Jaffe and members of his Lab, specifically Dr. Paul Roberts and Fernando Simonet, for their technical and logistical assistance. Their help made this work possible.

Chapter 1, in full, is a reprint of the material as it appears in Limnology and Oceanography Methods 2009, Karaköylü, Erdem; Franks, Peter J. S., Tanaka, Yuji, Roberts, Paul, L. D., Jaffe, Jules S. The dissertation author was the primary investigator and author of this paper.

Chapter 3, in full, is currently being prepared for submission for publication of the material. Karaköylü, Erdem; Franks, Peter J. S. The dissertation author was the primary investigator and author of this material.

Chapter 4, in full is currently being prepared for submission for publication of the material. Karaköylü, Erdem; Franks, Peter J. S. The dissertation author was the primary investigator and author of this material.

VITA

1997	Bachelor of Arts, Eastern Mediterranean University
2001	Bachelor of Science, Florida Institute of Technology
2001 – 2003	2nd Lieutenant, Commando, Turkish Armed Forces
2003 - 2010	Research Assistant, University of California San Diego
2008	Teaching Assistant, University of California San Diego
2009	Master of Science, University of California, San Diego
2010	Doctor of Philosophy, University of California, San Diego

PUBLICATIONS

"Copepod feeding quantified by planar laser imaging of gut fluorescence" Limnology and Oceanography Methods vol. 7, pp, April 2009

ABSTRACT OF THE DISSERTATION

The Foraging Sorties Hypothesis: Evaluating the Effect of Gut Dynamics on Copepod Foraging Behavior

by

Erdem Mustafa Karaköylü

Doctor of Philosophy in Oceanography

University of California, San Diego, 2010

Professor Peter J.S. Franks, Chair

Professor Jules S. Jaffe, Co-chair

While the diel vertical migration of copepods has been known for over a century, the details of this migration remain elusive. Field studies in Dabob Bay, a fjord in Puget Sound, Washington State (U. S. A.) show that copepods found in food-

poor layers had gut contents similar to copepods found in food-rich layers. Two hypotheses have been proposed to explain these observations; the stationary feeding hypothesis and the foraging sorties hypothesis. The stationary feeding hypothesis states that copepods with food in their guts were feeding in the layers where they were captured. The foraging sorties hypothesis predicts that copepods migrate into food-rich layers, where they feed to saturation, in brief bouts that lasts several tens of minutes. They then sink out as they digest. Once their gut is cleared the return to the shallow layer and repeat the cycle. In both cases feedback from the gut during feeding is critical. The present work has two components. The first consists of a series of laboratory experiments where I use a planar laser imaging fluorometer to quantify the dynamics of food movement through the guts to determine the time scales that are likely to dictate feeding behavior of individual copepods and their resulting vertical distribution. The second component of this work consists in deploying a profiling multi-spectral imaging system. This system is used to record individual copepod location in the water column and to quantify their corresponding gut content. Used in conjunction with an IBM, partially based on the laboratory work, I show that stationary feeding and foraging sorties hypotheses are feasible strategies. Furthermore I show that dominance of one strategy over the other will depend greatly on the interaction between the copepods' physiology and the environment they experience. Thus, prediction of the general foraging pattern may be possible from knowledge of the hydrographic structure.

CHAPTER 1

Copepod feeding quantified by planar laser imaging of gut fluorescence

Erdem M. Karaköylü, Yuji Tanaka, Peter J. S. Franks, Paul L. D. Roberts, Jules S. Jaffe.

Published in Limnology and Oceanography Methods 2009 vol. 7, pp 33-41

Abstract

We present a new method for quantifying the feeding of individual copepods, using a planar sheet of laser to stimulate the fluorescence of phytoplankton ingested by the copepod. The fluorescence is imaged with a sensitive CCD camera, giving two-dimensional images of the copepod's gut with 20 x 20 μm spatial resolution. Using tethered copepods, we have obtained >3 h long time series of copepod gut fluorescence with images every 15-20 s. The same individual copepod can be used for multiple experiments, obviating the problems of individual variability as a source of error. Initial data reveal two distinct patterns of variability as material moves through two functionally different gut compartments; these patterns reflect processes occurring in each compartment. The upper (anterior) mid-gut shows higher variability and less repeatability than the posterior mid-gut where undigested material is aggregated into a fecal pellet and evacuated at regular intervals. Variability in the upper mid-gut is likely due to factors such as intermittence of feeding and relatively complex mixing dynamics. In the posterior mid-gut, mixing dynamics are much simpler, and the variability of the upper compartment is integrated over the time scale of pellet formation.

Introduction

Copepods constitute a fundamentally important link between primary producers and higher trophic levels in the ocean. Their activities exert a significant control over biogeochemical cycles, through feeding, metabolism, defecation, and vertical migration. Feeding by herbivorous copepods often follows a diel rhythm, as visual predators force the copepods to avoid the euphotic zone, typically restricting feeding to nighttime hours (Zaret and Suffern 1976; Dagg et al., 1997). While this pronounced diel rhythm has been noted for decades (Marshall 1924; Fuller 1934; Petipa 1958; Duval and Geen 1976), feeding and foraging behaviors at shorter time and space scales are poorly understood. Recent technological advances have begun to reveal the microscale (<1 m) structure of the phytoplankton (Franks and Jaffe 2001, 2008; McManus et al. 2003), and laboratory experiments have shown that copepods are capable of altering their behavior in response to microscale gradients in phytoplankton concentration (Tiselius 1992; Leising and Franks 2002; Bochdansky and Bollens 2004). In spite of this growing knowledge of copepod behavior, the actual feeding dynamics of these animals are largely unknown on the time scales over which they forage (tens of minutes to hours).

Both field studies (Boyd *et al.* 1980; Båmstedt 1988; Båmstedt *et al*. 1992) and laboratory experiments (Mackas and Burns 1986; Mobley 1987) have revealed considerable variability in individual feeding behavior of herbivorous copepods, within broad diel feeding rhythms. Such variability is likely the result of alternating hunger and satiation thresholds rather than the availability of food (Simard *et al*. 1985; Ishii 1990). Hunger and satiation thresholds result from the interaction of ingestion, digestion, and

egestion. Thus the gut dynamics are important in determining copepod foraging behavior and local concentration of the organisms.

Here, we introduce a new method of imaging *in vivo* laser-induced fluorescence from phytoplankton pigments within copepod guts. This allows the generation of long (hours), well-resolved (tens of seconds) time series of ingestion, food movement in the digestive tract, and egestion, for individual copepods.

Materials and Procedures

Laser sheet

Gut pigment fluorescence was excited by illumination from a 532 nm wavelength diode-pumped solid-state 3 W laser (Melles Griot 58-GSS-309). The laser was collimated to produce a 2 mm diameter beam with less than 2 mrad divergence. This beam passed through a mechanical shutter (NM Laser LS200) that allowed the beam to be remotely switched on and off by the user. After the shutter, the beam passed through two Powell lenses (Powell 1987) that expanded it along two orthogonal axes to produce a slab of laser light approximately 1 cm wide and 10 cm high at the target copepod's location. One advantage of the Powell lens method is that it yields a sheet of nearly uniform intensity without the need for scanning mirrors or complex optics (Christensen and Morris 1998). The divergence of the laser beam produced by each Powell lens could be adjusted between 1° and >90°, with each lens operating on an orthogonal axis. To produce a sheet of thickness y_1 and height y_2 (here 1 cm and 10 cm respectively, Fig. 1-1), at a distance d between the center of the lens farthest from the copepod and the copepod, the divergences can be calculated by solving

$$y_1 = 2d\tan\frac{\theta_1}{2} \quad (1)$$

$$y_2 = 2(d - d_1)\tan\frac{\theta_2}{2} \quad (2)$$

where d_1 is the distance between the lens centers when placed in series. To minimize the variation in sheet dimensions in the sample chamber, we chose θ_1 to be as small as possible (1°) and solved for d and θ_2, giving $\theta_2 = 10°$ and $d = 57$ cm.

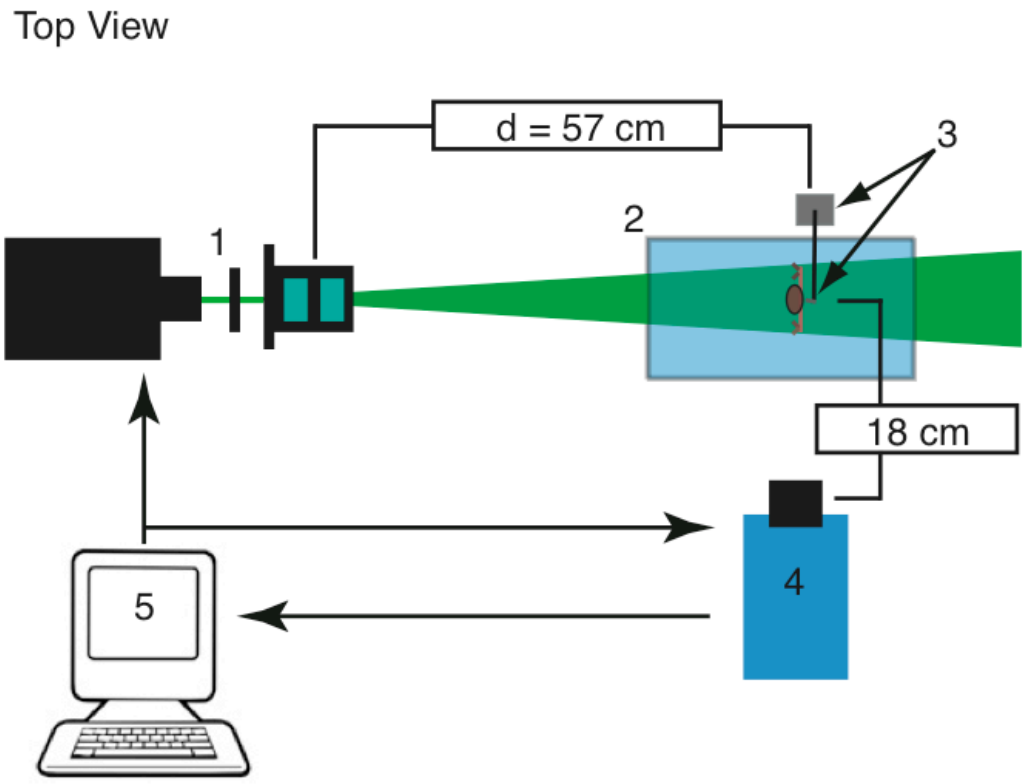

Figure 1-1: *Top view of the experimental setup*. 1: Laser, collimator, shutter and Powell lens assembly; 2: Tank and filtered seawater; 3: Micromanipulator & tethered copepod; 4: CCD camera; 5: Computer controlling laser and camera, and receiving images from camera.

Camera

The stimulated fluorescence was imaged with a scientific grade 1376 x 1000 pixel CCD camera (Cooke Corp. Sensicam QE) through a Nikkor 50 mm f/1.8 lens. Fluoresced (red) light passed through a 680 nm bandpass filter with a 20 nm bandwidth (Omega Optical 3rd Millenium) that was positioned behind the objective. In order to maintain a focused image the lens was moved 1.5 cm away from the CCD sensor, and toward the target, using a set of 5 mm C-mount spacers. The 18 cm distance separating the camera objective from the target area yielded a 2 x 2 cm field of view at the image plane, a depth of field that was roughly twice as large as the typical thickness of the copepods under study, and a resolution of 20 x 20 μm per pixel.

Copepod preparation

Most experiments were conducted at Scripps Institution of Oceanography (La Jolla, CA), with additional experiments at the University of Washington's School of Oceanography (Seattle, WA). For the Scripps portion of the work, adult female *Calanus pacificus* were captured in the morning of November 2005, within 5 km of the Scripps Pier (La Jolla, CA). Slow vertical tows from 70 m depths were made with a 505 μm mesh net with a 1 m diameter opening and a solid "live" cod end. The cod end had small side openings covered by 505 μm mesh to reduce turbulence that might damage animals. The contents of the cod end were distributed into 1 L glass jars partially filled with 0.2 μm filtered sea water and carried back to the lab in a cooler filled with cooled water. In Washington, adult female *C. pacificus* were collected in Dabob Bay (Puget Sound, WA), using a 1 m diameter Puget Sound type closing net, fitted with a 571 μm mesh and a "live" cod end. The net was towed vertically from 160 m to the surface on the morning of

May 8, 2006. Retrieval rate was approximately 10 m/min to reduce the risk of damaging the captured animals. The contents of the cod end were immediately decanted into 4 L plastic jars, pre-filled with seawater from the R/V Barnes' seawater system. The jars were kept in a cooler with until arrival at the lab.

Copepods were kept cool in the dark prior to sorting; usually 2 to 6 h. Sorted adult female *Calanus pacificus* were tethered to an acetone-bleached human hair using a small drop of cyanoacrylate glue (*cf.* Haury, 1976). The hair was attached to a platinum wire that extended from a glass or plastic rod. Tethered copepods were starved for at least 12 h before an experiment, in an incubator set to the experimental temperature, with a day/night light cycle that corresponded to the local day length.

Imaging chamber

Copepods were imaged in a 30 x 20 x 10 cm Plexiglas tank (Fig. 1-1). The tank was filled with filtered seawater. Using a chiller powering a closed circulation system placed in the tank, we adjusted the water temperature to within ±0.5°C of the desired temperature.

A tethered copepod was positioned inside the imaging chamber in the field of view of the camera. The tether rod was held by a 3-axis Kanetec micromanipulator; the copepod was oriented in an upright resting position (Fig. 1-2).

In experiments carried out at Scripps, copepods were offered a monoculture of the diatom *Thalassiosira weissflogii* at a concentration of at least 4,000 cells/ml, so that food was not limiting (Frost 1972). Food used for the Washington experiments consisted of water collected from the chlorophyll maximum in Dabob Bay, where the copepods had been captured. The food was initially in a small beaker where a magnetic stir bar kept the particles homogeneously distributed in the beaker. Phytoplankton were transferred by

means of a peristaltic pump and a thin tube running from the beaker to the tip of a pipette suspended about 1 cm above and less than 0.5 cm in front of the copepod's first antennae. The delivery speed was adjusted so that the cells produced a thin stream past the copepod, about 0.1 mL min^{-1}. Food was thus continuously available to the copepod, which was allowed to feed *ad libitum* while being imaged. The stream of cells was far enough from the copepod that uneaten phytoplankton usually did not distort the gut fluorescence signal.

Image acquisition

The camera was synchronized to the laser via a pulsed controller. The laser pulse duration and the length of the interval between pulses were set according to the requirements of the experiment. These requirements were to 1) obtain images that resolved the spatial distribution of pigment in the copepod gut, 2) avoid pixel saturation at high gut content (high fluorescence intensities), and 3) use a pulse intensity-frequency combination that would not induce behavioral artifacts in the imaged copepod. We found that pulse duration of 30-100 ms at intervals of 15-20 s gave satisfactory results with a green (532 nm) laser. At higher pulse frequencies, the laser flash was found to disturb the animal to the point where, at a 1 s interval, the animal ceased feeding and jumped repeatedly.

Once positioned, the copepod was left in the dark for 15-30 minutes before the experiment began. The imaging began with the first laser pulse. A minimum of 5 images of the copepod was taken before the peristaltic pump controlling food addition was turned on. These images were used as "blanks" during processing, providing an estimate of the background signal from the copepod and the surrounding medium.

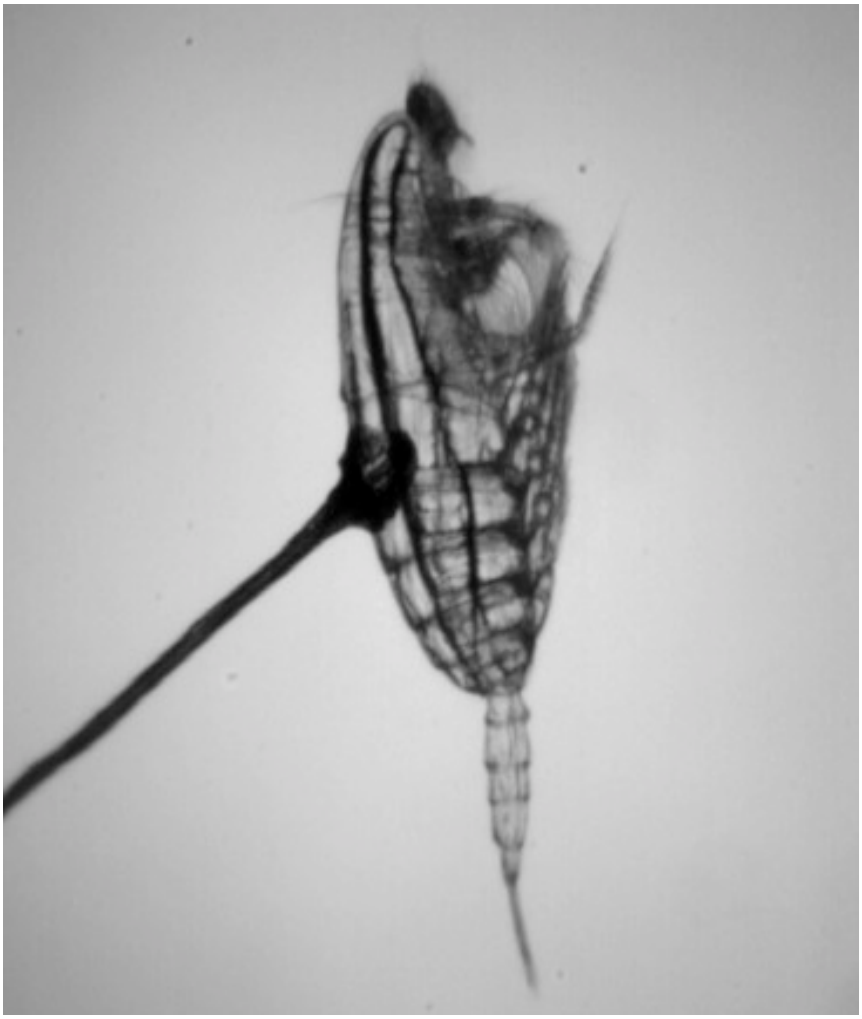

Figure 1-2**:** *A tethered Calanus pacificus CV*. Data shown in this paper come from experiment conducted using adult females only. Part of the tether – a human hair – and the glue drop on the back of the copepod are also visible.

Image processing

Images were processed using Matlab (The Mathworks). Images from the PLIF system contained signals from the phytoplankton in the copepod's gut, as well as free phytoplankton in the stream passing the copepod. To quantify the gut dynamics we

focused on fluorescence signal in the mid-gut where digestion takes place (Brunet et al. 1994). A composite image, constructed by summing all the images acquired during an experiment, revealed the various sections of the gut (Fig. 1-3). For our analyses the mid-gut was divided into two distinct compartments (Gauld 1957; Dagg and Wyman 1983; Penry and Frost 1990). The first spans mid-gut zones I and II (Arnaud et al. 1980), designated here as the 'upper mid-gut' or UMG. The second is the posterior mid-gut (zone III, *op. cit.*), here referred to as PMG. The fluorescence in the UMG and PMG was calculated by integrating the pixel intensities over these areas in each image. This procedure generated time series of fluorescence for both sections of the copepod's gut; the sum of both yielded a time series of bulk gut fluorescence. When an apparently anomalous feature such as an unexpected single-point peak or trough was found in the time series, the corresponding image was inspected. These anomalies usually indicated a copepod jumping or a free food particle that altered the gut signal by traveling in front of the imaging plane. In such cases the corresponding data point was replaced by an average of its two surrounding neighbors. These contaminated images were rare and accounted for less than 2% of any given data set.

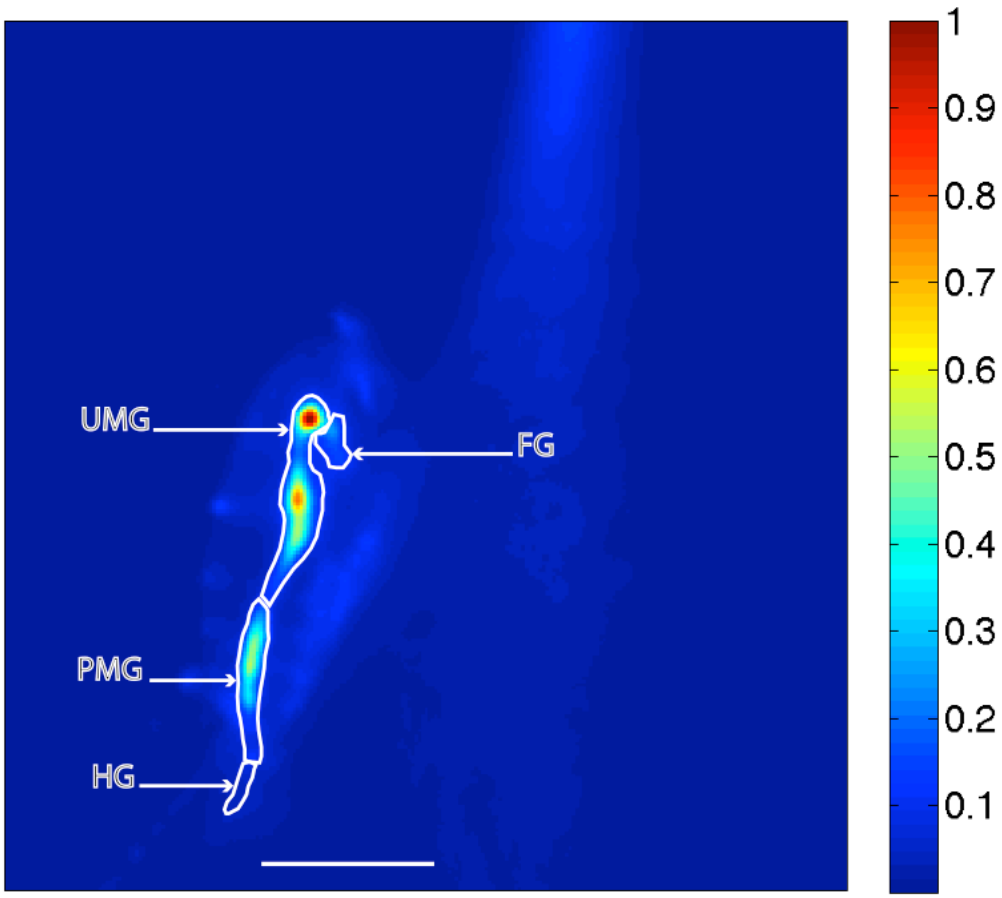

Figure 1-3: *Fluorescence distribution inside a copepod's gut.* The flow of cells is visible in front of the animal. Gut sections are as described in the text. FG: foregut; UMG: upper mid-gut; PMG: posterior mid-gut; HG: hindgut. The color bar shows the relative pigment fluorescence intensity within these regions. Scale bar is 1 mm.

Extracted gut pigment content vs. imaged gut fluorescence intensity

To relate the imaged gut fluorescence to the extracted gut pigment content, we conducted experiments in which *C. pacificus* from Dabob Bay were imaged for varying amounts of time (up to one hour), at 12 °C. Their food was supplied from bottle samples acquired at the chlorophyll maximum layer (chlorophyll *a* concentration 55.04 mg m^{-3}, phaeopigment concentration 5.59 mg m^{-3}, Pierson *pers. comm.*) in Dabob Bay. At the end of each experiment the copepod was transferred immediately to 90% acetone for 24 hours

(Kleppel et al. 1988). The pigment extracted from each copepod was quantified using a Turner Designs TD-700 bench fluorometer with a 1 mL cuvette adaptor. The total amount of *a*-phorbin (chlorophyll *a*, phaeophytin *a* and phaeophorbide *a*) pigments extracted, expressed as chlorophyll *a* equiv. ind^{-1} (Båmstedt et al. 2000) was compared to the bulk gut pigment fluorescence signal calculated from the last fluorescence image acquired during the corresponding experiment.

Assessment

Using our laser-induced gut fluorescence system, we acquired spatially and temporally resolved images of copepod gut fluorescence. Experiments reported here were designed to:

1) Determine the relationship between imaged fluorescence intensity and the corresponding gut pigment content;
2) Compare the new method with published results from classical gut clearance experiments;
3) Quantify feeding rhythms and evaluate the feasibility of the method for revealing the characteristic time scales and gut processes that could affect a copepod's feeding behavior over minutes to hours.

Comparison with extracted gut pigment

The calibration runs confirmed that the fluorescence signal detected by the CCD camera and integrated over the copepod's gut was linearly related to the extracted gut pigment content ($R^2 = 0.70$, $p < 0.005$, $n = 13$) (Fig. 1-4A). Phaeopigment *a* (phaeophytin *a* and phaeophorbide *a*; Stearns 1986) made up most of the pigment in the gut (Fig 1-4B;

Currie 1962; Shuman and Lorenzen 1975). The observed linearity of the response of the imaging system to gut pigment content suggests that the imaged fluorescence is a reliable measure of food present in the copepod gut. Some variability is possible due to shifting distributions of gut pigment as food boluses travel down the digestive tract.

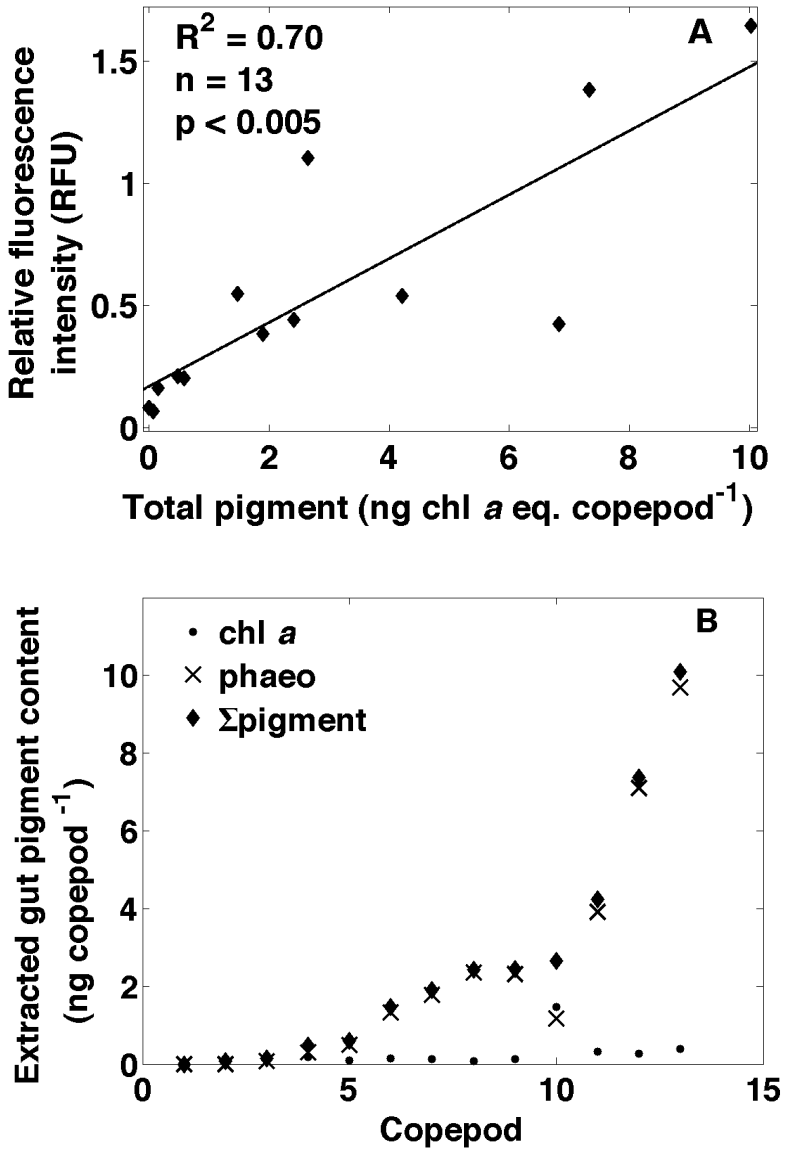

Figure 1-4: *Calibration of the PLIF method with pigment extraction.* (A) Total PLIF-measured fluorescence (relative fluorescence units or RFU) vs. acetone-extracted pigment. Each point represents an individual copepod. (B) Relative amounts of chlorophyll *a* (chl *a*), phaeopigment *a* (phaeo), and total chl *a* pigment (Σpigment) making up the individual gut pigment content for 13 copepods.

Gut clearance rate

The decay rate of gut fluorescence in copepods whose food supply has been removed gives a measure of the gut clearance rate. This rate provides a characteristic time scale of copepod food processing, and has been used to estimate grazing rate. Daily algal intake can be calculated (Kiørboe et al. 1985) with the underlying assumption that ingestion matches egestion, i.e. feeding is at steady state. In traditional experiments, recently feeding copepods were incubated in seawater devoid of food; the time elapsed for ingested food to clear the gut was quantified by removing individual copepods at fixed intervals and extracting their gut pigments. To obtain similar data from a single copepod, we used our PLIF, imaging a tethered copepod at 12 °C feeding on a stream of phytoplankton. After a few hours, food injection was stopped and imaging continued.

After the food supply was terminated, the fluorescence intensity integrated over the gut of the copepod *F(t)* decayed with time *t* (Fig. 1-5). The decay in fluorescence was fitted with an exponential function representing a first-order kinetic reaction:

$$F(t) = F(0)e^{-rt} \tag{3}$$

(e.g. Kiørboe et al. 1982; Kiørboe and Tiselius 1987), from which the decay rate r (min^{-1}) was determined (Fig. 1-5). The resulting value of $r = 0.0257$ min^{-1} at 12 °C is comparable to values of 0.0218 - 0.0392 min^{-1} for *Centropages hamatus* at 10-15 °C (Kiørboe et al. 1982), 0.027 min^{-1} for *Calanus pacificus* at 13-15 °C (Flint et al. 1991), and 0.0104 - 0.0220 min^{-1} for *Calanus finmarchicus* at 6.1-9.0 °C (Durbin et al. 1995).

This correspondence of our measurements with previous work suggests the PLIF system gives a realistic picture of the gut dynamics of herbivorous copepods. An important difference from the classic gut clearance method is that fluorescence imaging allows us to calculate the decay rate from successive measurements of one copepod. This represents a characteristic of the individual, rather than an average over a population and its associated variability.

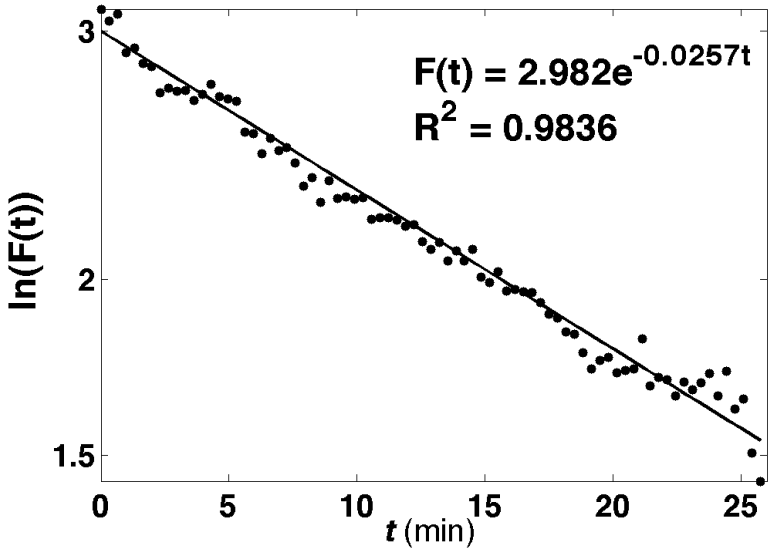

Figure 1-5: *Time series of the decay of gut fluorescence from a single copepod.* The copepod was fed for a few hours; food addition was interrupted at t = 0, while imaging continued. The line is a linear fit to the log-transformed data using equation (3), giving a decay rate of r = 0.0257 min^{-1}, equivalent to a gut transit time of about 40 min.

Feeding rhythms

In the UMG there are two competing mechanisms that affect the integrated fluorescence signal. Ingestion increases the signal; digestion decreases the signal as material is processed and moved along the gut tract. Within ~20 min of the onset of feeding the UMG signal peaks to its highest level during an experiment (Fig. 1-6A). This is most likely a starvation response (Runge 1980, Tiselius 1998) and lasts a few tens of minutes to an hour. Other peaks of lower intensity, each separated by up to a few tens of minutes, follow this initial peak. One explanation for these broad fluctuations is the discontinuous ingestion of material, while the gut contents are being continuously digested. Such discontinuous ingestion is in agreement with known copepod feeding intermittence (Koehl and Strickler 1981, and refs. therein). There are also shorter, tens of seconds to minute scale fluctuations; a close examination of a sequence of corresponding image fames suggest these are due to local changes in pigment concentration caused by relatively complex food mixing patterns in the UMG (Penry and Frost 1990), in both the axial and radial direction (Penry and Jumars 1986, 1987).

In contrast to the variability of the UMG signal, The PMG signal shows striking temporal regularity. At relatively constant intervals, and rapidly (10s of seconds or less) following a defecation event, a discrete transfer of material takes place from the UMG to the PMG, marked by an initial peak in the PMG signal (Fig 1-6B-F). Once transfer is completed no further exchange is visible between the UMG and the PMG. Then the pellet is evacuated usually causing downward spike, followed by another peak that indicates the next pellet has been transferred to the PMG. While the fecal pellet is still in the PMG, the fluorescence signal decays. This may be attributable to a loss in pigment by enzymatic

degradation within the pellet (Nott *et al.* 1985). The temporal regularity of this evacuation/transfer cycle is not visibly affected by the fluctuations in the UMG signal.

Our observations support a number of studies that focused on individual copepod feeding. Paffenhöfer (1994) looked at the variability in the duration between defecation intervals of tethered individuals, which he argued were an indicator of feeding activity. However, in a later study Paffenhöfer *et al.* (1995) tracked and filmed free-swimming copepods, recording ingested cell numbers and pellet evacuation intervals. They found that variability in ingestion rate was greater than that of pellet evacuation rate. In a critique of Paffenhöfer (1994), Dagg (1995) pointed out that even in the case of highly variable gut content fecal pellet production rates could remain relatively constant while the amount of material contained in pellets varied (see also Dagg and Walser 1986, and refs. therein). To quantify pellet content and relate defecation to feeding activity, one would have to collect them sequentially, in the order they were produced. We speculate that the PMG data may give us some indication about the variability in the fecal pellet content. Because fluorescence intensity is used as a proxy for the amount of material imaged, the peaks in the PMG signal constitute a relative index of the amount of material transferred from the UMG. If so, then the combination of evacuation rate and pellet content may be used as an indicator of *in vivo* gut turnover. More work is required before we can draw any conclusions.

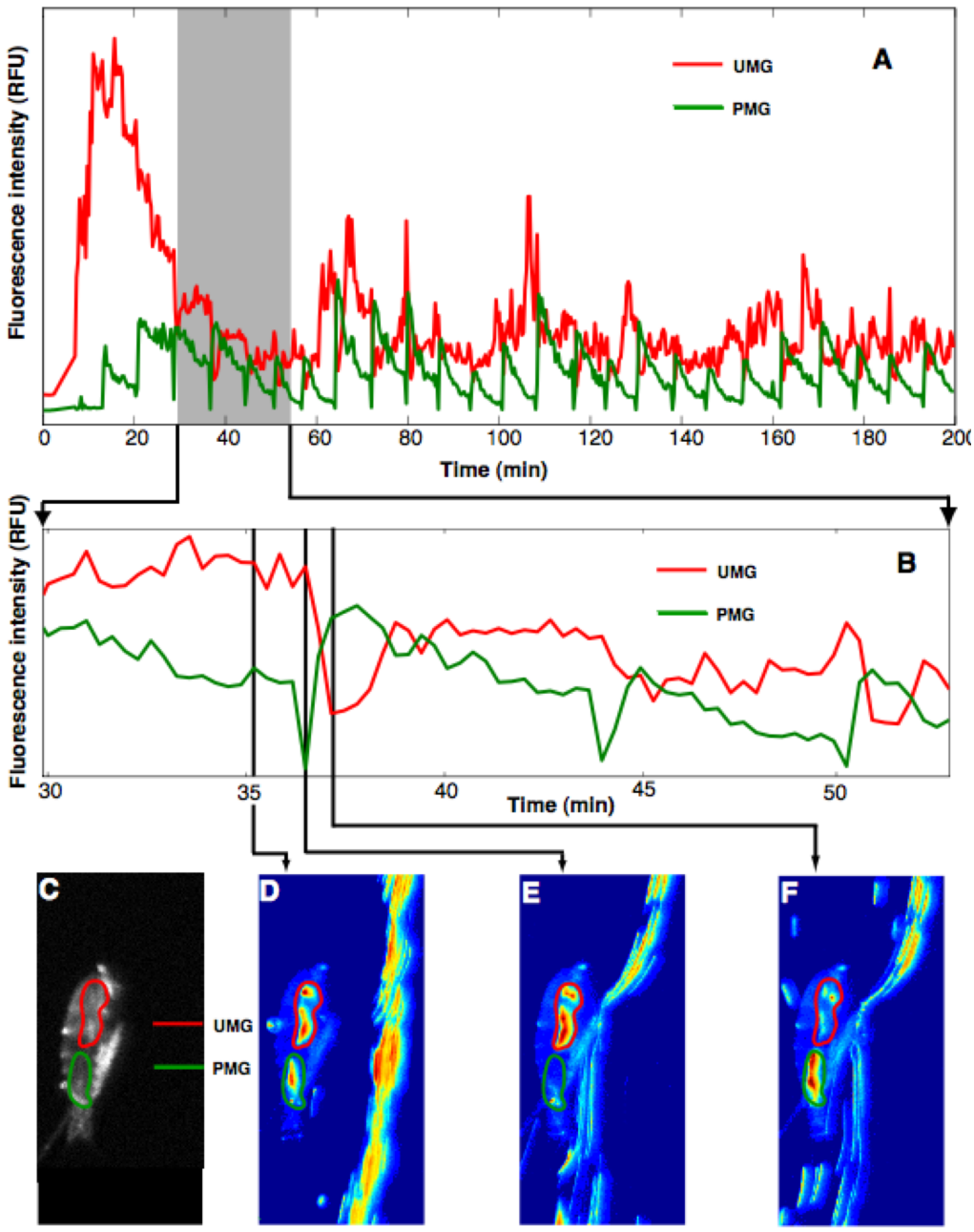

Figure 1-6: *Time series of gut fluorescence from a single copepod at 12 °C.* (A) 3.3 h time series of fluorescence from two distinct sections of the mid-gut; ———: UMG; ———: PMG. Shaded region shows the section expanded in panel (B). (C) Tethered copepod with outlined UMG and PMG regions. (D)-(F) Selected images showing cells entrained in feeding current, and the flow of ingested matter through UMG and PMG. Black arrows link frames to the time series.

Discussion

We have presented an optical approach to quantify and image the gut fluorescence of individual copepods feeding on phytoplankton. While measuring feeding indices using multiple individuals probably remains the more practical approach in field applications, an awareness of the effect of individual variability is nevertheless critical. Tseitlin (1994) has shown that the interpretation of such pooled data could become unreliable because of individual differences. A number of studies have addressed this issue resulting in a better appreciation for the variability in individual feeding behavior (*e.g.* Turner *et al.* 1993, Paffenhöfer 1994, Paffenhöfer *et al.* 1995). However, we still lack a good understanding of the gut dynamics that take place between ingestion and evacuation. Yet gut dynamics regulate the flow of material through the gut, thereby determining further ingestion and the associated feeding behavior of a copepod.

Using our PLIF technique we were able to image the flow of ingested phytoplankton pigment as it was moved through the gut of a live copepod. The resulting time series from different gut compartments are a first quantification of live copepod gut dynamics during feeding. These data enable some interesting observations: the short-term fluctuations in the UMG signal indicate that even continuously available food is not continuously ingested; the temporal regularity in the PMG signal, seemingly unaffected by the UMG fluctuations, shows that digestion is continuous; the fluctuations in the amount of matter that is regularly transferred to the PMG suggest a variable gut turnover. These observations suggest alternating bouts of feeding and satiation with reduced or no feeding. If they occur in the wild, such changes in feeding activity could have important implications for copepod feeding dynamics and vertical movement in the water column.

For example, particle-feeding copepods such as *C. pacificus* take advantage of their negative buoyancy to enhance the effect of the feeding currents they create during feeding bouts (Strickler 1982); interruptions in feeding result in sinking. Thus the copepod's vertical position varies continuously as a result of short-term changes in feeding activity (Gauld 1966; Pearre 1973, 2003; Mackas and Bohrer 1976; Rudyakov and Tseitlin 1982; Cowles and Strickler 1983; Leising *et al.* 2005). Tarling and Johnson (2006) suggested that krill undergo multiple vertical migrations throughout the night according to the fullness of their gut. If gut fullness affects feeding and consequently swimming of copepods, then they too may demonstrate multiple vertical migrations at night. In an environment where food and predators co-occur in surface layers, feeding rhythms and consequent vertical motions will alter predation risk and food intake. There could be biogeochemical consequences depending on where copepods release fecal pellets and excreta relative to the pycnocline as a result of such alternating vertical displacement (Dagg *et al.* 1989; Longhurst *et al.* 1990). We believe our approach can be of significant help in formulating and testing models of copepod behavior that include feeding, digestion and egestion.

A particular advantage of the method described here is that copepods can be kept alive and used in multiple different experimental treatments on the same individual. We are currently analyzing data from experiments exploring the effect of temperature on gut dynamics.

The use of the of *in vivo* gut fluorescence does not need to be restricted to the lab, but can also be used in the field. While tracking individual copepods *in situ* for long times may not be feasible, we have coupled a laser-induced gut fluorescence detection

system to a plankton imaging device that can be deployed *in situ.* This system provides information on both the local concentration of copepods, and the fluorescence intensity of their guts. We are currently analyzing data collected by such a system, recently deployed in Dabob Bay (Puget Sound, WA).

Comments and recommendations

To relate the imaged gut fluorescence to gut pigment content, it is essential to calibrate the system with measurements of extracted pigments, and retain the system configuration after calibration. Even the use of Powell lenses does not guarantee that the laser sheet will be perfectly even; spatial fluctuations in intensity that can be detected by the CCD camera can occur. To mitigate these spatial variations in incident irradiance, copepods should always be imaged at the same location in the laser field. The camera should be focused for the first experiment and its settings should be left unchanged thereafter. In subsequent experiments, focusing should be done by moving the copepod relative to the camera, rather than adjusting the camera objective. This is straightforward with the micromanipulator holding the tether.

The use of a tether increases the artificiality of the experiment. However, in view of the promising results obtained here, we hope further research can be conducted to develop instrumentation that can similarly assess gut content remotely in freely swimming animals.

Chapter 1, in full, is a reprint of the material as it appears in Limnology and Oceanography Methods 2009, Karaköylü, Erdem; Franks, Peter J. S., Tanaka, Yuji,

Roberts, Paul, L. D., Jaffe, Jules S. The dissertation author was the primary investigator and author of this paper.

References

Arnaud, J., M. Brunet, and J. Mazza 1980. Structure et ultrastructure comparées de l'intestin chez plusieurs espèces de Copépodes Calanoides (Crustacea). Zoomorphol. 95: 213-233.

Båmstedt, U., D.J. Gifford, X. Irigoien, A. Atkinson, and M. Roman. 2000. Feeding. In: Harris, R., Wiebe, P., Lenz, J.,Skholdal, H.R., Huntley, M. [eds.]. ICES Zooplankton Methodology Manual, Academic Press.

————, H. C. Eilertsen, K. S. Tande, D. Slagstad, and H. R. Skjoldal. 1992. Copepod grazing and its potential impact on the phytoplankton development in the Barents Sea. Polar Res. 10: 339-353.

————. 1988. Ecological significance of individual variability in copepod bioenergetics. Hydrobiol. 167/168: 43-59

Bochdansky, A. B., and S. M. Bollens. 2004. Relevant scales in zooplankton ecology: Distribution, feeding, and reproduction of the copepod *Acartia hudsonica* in response to thin layers of the diatom *Skeletonema costatum*. Limnol. Oceanogr. 49: 625-636.

Boyd, C. M., S. L. Smith, and T. J. Cowles. 1980. Grazing patterns of copepods in the upwelling system off Peru. Limnol. Oceanogr. 25: 583-596.

Christensen, K. A., and M. D. Morris. 1998. Hyperspectral Raman microscope imaging using Powell lens line illumination. Appl. Spectrosc. 52(5): 1145-1147.

Currie, R. I. 1962. Pigments in zooplankton feces. Nature 193: 956-957

Dagg, M. J., B.W. Frost, and J. A. Newton. 1997. Vertical migration and feeding behavior of *Calanus pacificus* females during a phytoplankton bloom in Dabob Bay, U.S. Limnol. Oceanogr. 42: 974-980.

Dagg, M.J. 1995. A comment on 'Variability due to feeding activity of individual copepods' (Paffenhöfer, 1994). J. Plank. Res. 17: 903-905.

————, B. W. Frost, and W. E. Walser Jr. 1989. Copepod diel migration, feeding, and the vertical flux of pheopigments. Limnol. Oceanogr. 34: 1062-1071.

———— and W. E. Walser Jr. 1986. The effect of food concentration on fecal pellet size in marine copepods. Limnol. Oceanogr. 31: 1066-1071.

————, and K. D. Wyman. 1983. Natural ingestion rates of the copepods *Neocalanus plumchrus* and *N. cristatus* calculated from gut contents. Mar. Ecol. Prog. Ser. 13: 37-46.

Durbin, E. G., S. L. Gilman, R. G. Campbell, and A. G. Durbin. 1995. Abundance, biomass, vertical migration and estimated development rate of the copepod *Calanus finmarchicus* in the southern Gulf of Maine during late spring. Cont. Shelf Res. 15: 571-591.

Duval, W. S., and G. H. Geen. 1976. Diel feeding and respiration in zooplankton. Limnol. Oceanogr. 21: 823-829.

Flint, M.V, A.V. Drits, and A.F. Pasternak. 1991. Characteristic features of body composition and metabolism in some interzonal copepods. Mar. Biol. 111:199-205.

Franks, P. J. S., and J. S. Jaffe. 2001. Microscale distributions of phytoplankton: initial results from a two-dimensional imaging fluorometer, OSST. Mar. Ecol. Prog. Ser. 220: 59-72.

————, and J. S. Jaffe. 2008. Microscale variability in the distributions of large fluorescent particles observed *in situ* with a planar laser imaging fluorometer. J. Mar. Sys. 69: 254-270.

Frost, B. W. 1972. Effects of size and concentration of food particles on the feeding behavior of the marine planktonic copepod *Calanus pacificus*. Limnol. Oceanogr. 17: 805-815.

Fuller, J. L. 1934. Feeding rate of *Calanus finmarchicus* in relation to environmental conditions. Biol. Bull. 72: 233-246

Gauld, D. T. 1966. The swimming and feeding of planktonic copepods, p. 313-334. In H. Barnes, [ed.], Some Contemporary Studies in Marine Science. Allen and Unwin.

————. 1957. A peritrophic membrane in calanoid copepods. Nature 179: 325-326.

Haury, L. 1976. Method for restraining living planktonic crustaceans. Fish. Bull. 74: 220-221.

Kiørboe, T., and P.T. Tiselius, 1987. Gut clearance and pigment destruction in a herbivorous copepod, *Acartia tonsa*, and the determination of in situ grazing rates. J. Plank. Res. 9: 525-534.

————, F. Møhlenberg, and H. U. Riisgård. 1985. *In situ* feeding rates of planktonic copepods: a comparison of four methods. J. Exp. Mar. Biol. Ecol. 88: 67-81.

————, F. Møhlenberg, and H. Nicolajsen, 1982. Ingestion rate and gut clearance in the planktonic copepod *Centropages hamatus* (Lilljeborg) in relation to food concentration and temperature. Ophelia 21: 181-194.

Kleppel, G. S., R. E. Pieper, and G. Trager. 1988. Variability in the gut contents of individual *Acartia tonsa* from waters off Southern California. Mar. Biol. 97: 185-190.

Koehl, M.A.R. and R.J. Strickler. 1981. Copepod feeding currents: Food capture at low Reynolds number. Limnol. Oceanogr. 26: 1062-1073.

Leising, A. W., J. J. Pierson, S. Cary, and B. W. Frost. 2005. Copepod foraging and predation risk within the surface layer during night-time feeding forays. J. Plank. Res. 27: 987-1001.

————, and P. J. S. Franks. 2002. Does *Acartia clausi* (Copepoda: Calanoida) use an area-restricted search foraging strategy to find food? Hydrobiol. 480: 193-207.

Longhurst, A. R., A. W. Bedo, W. G. Harrison, E. J. H. Head, and D. D. Sameoto. 1990. Vertical flux of respiratory carbon by oceanic diel migrant biota. Deep-Sea Res. 37: 685-694.

Mackas, D.L. and K. E. Burns. 1986. Poststarvation feeding and swimming activity in *Calanus pacificus* and *Metridia pacifica*. Limnol.Oceanogr. 31: 383-392.

————, and R. Bohrer. 1976. Fluorescence analysis of zooplankton gut contents and an investigation of diel feeding patterns. J. Exp. Mar. Biol. Ecol. 25: 77-85.

Marshall, S. 1924. The food of *Calanus finmarchicus* during 1923. J. Mar. Biol. Assoc. U.K. 13: 473-479.

McManus, M.A., A. L. Alldredge, A. H. Barnard, E. Boss, J. F. Case, T. J. Cowles, P. L. Donaghay, L. B. Eisner, D. J. Gifford, C. F. Greenlaw, C. M. Herren, D. V. Holliday, D. Johnson, S. MacIntyre, D. M. Gehee, T. R. Osborn, M. J. Perry, R. E. Pieper, J. E. B. Rines, D. C. Smith, J. M. Sullivan, M. K. Talbot, M. S. Twardowski, A. Weidemann, and J. R. Zaneveld. 2003. Characteristics, distribution and persistence of thin layers over a 48-hour period. Mar. Ecol. Progr. Ser. 261: 1-19.

Mobley, C.T. 1987. Time-series ingestion rate estimates on individual *Calanus pacificus* Brodsky: interactions with environmental and biological factors. J. Exp. Mar. Biol. Ecol. 114: 199-216.

Nott, J.A., E.D.S. Corner, L.J. Marvin, and S.C.M. O'Hara. 1985. Cyclical contributions of the digestive epithelium to faecal pellet formation by the copepod *Calanus helgolandicus*. Mar. Biol. 89: 271-279.

Paffenhöffer, G.A., M. H. Bundy, K. D. Lewis, and C. Metz. 1995. Rates of ingestion and their variability between individual calanoid copepods: direct observations. J. Plank. Res. 17: 1573-1585.

————. 1994. Variability due to feeding activity of individual copepods. J. Plank. Res. 16: 617-626.

Pearre, S. 2003. Eat and run? The hunger/satiation hypothesis in vertical migration: history, evidence and consequences. Biol. Rev. 78: 1-79.

————. 1973. Vertical migration and feeding in *Sagitta elegans* Verrill. Ecology 54:300-314.

Penry, D.L., and B. W. Frost. 1990. Re-evaluation of the gut-fullness (gut fluorescence) method for inferring ingestion rates of suspension-feeding copepods. Limnol. Oceanogr. 35: 1207-1214.

————, and P. A. Jumars. 1987. Modeling animal guts as chemical reactors. Am. Nat. 129: 69-96.

————, and P. A. Jumars. 1986. Chemical reactor analysis and optimal digestion. Biosci. 36: 310-313.

Petipa T.S. 1958. The diurnal feeding rhythm of the copepod crustacean *Acartia clausi* Giesbrecht. Dokl. Akad. nauk SSSR 120: 435-437.

Powell, I. 1987. Design of a laser-beam line expander. Appl. Opt. 26: 3705-3709.

Rudyakov, Y.A. and V. B. Tseytlin. 1982. Modeling of feeding processes and formation of a vertical distribution of a copepod cohort. Oceanol. 22: 465-470.

Runge, J.A. 1980. Effects of hunger and season on the feeding behavior of *Calanus pacificus*. Limnol. Oceanogr. 25: 134-145.

Shuman, F.R., and C. J. Lorenzen. 1975. Quantitative degradation of chlorophyll by a marine herbivore. Limnol. Oceanogr. 20: 580-586.

Stearns, D.E. 1986. Copepod grazing behavior in simulated natural light and its relation to nocturnal feeding. Mar. Ecol. Progr. Ser. 30: 65-76.

Strickler J.R. 1982. Calanoid copepods, feeding currents, and the role of gravity. Science 218: 158-160.

Tarling, G.A., and M. L. Johnson. 2006. Satiation gives krill that sinking feeling. Curr. Biol. 16: R83-84.

Tiselius, P. 1998. Short term feeding responses to starvation in three species of small calanoid copepods. Mar. Ecol. Progr. Ser. 168: 119-126.

————. 1992. Behavior of *Acartia tonsa* in patchy food environments. Limnol. Oceanogr. 37: 1640-1651.

Tseitlin, V.B. 1994. Simulating measurements of copepod gut passage time. Oceanol. 34: 66-71.

Turner, J.T., P. A.Tester, and J. R. Strickler. 1993. Zooplankton feeding ecology: A cinematographic study of animal-to-animal variability in the feeding behavior of *Calanus finmarchicus*. Limnol. Oceanogr. 38: 255-64.

Zaret, T.M. and J.S. Suffern. 1976. Vertical migration in zooplankton as a predator avoidance mechanism. Limnol. Oceanogr. 21: 804-813.

CHAPTER 2

Individual variability of gut dynamics in continuously feeding *Calanus pacificus* (Copepoda: Calanoida)

Abstract

Highly resolved time series of gut content were obtained for individual adult Calanus pacificus females while they fed on saturating levels of phytoplankton. The gut contents were quantified remotely using a recently introduced gut fluorescence imaging system, sensitive enough to differentiate among midgut compartments. Images were acquired every 15 seconds during experiments lasting 4-6 hours at 12 °C. Feeding copepods revealed a factor of 25 intra- and inter-individual variations in gut content. Calculated gut throughput times were around 20 min but were similarly highly variable among and within individuals, ranging from 10 to 50 min. Ingestion rates, estimated from time series of gut throughput time and gut content, varied between ~0.91 and 3.68 μg C h^{-1}. Much of the intra-individual variability seems to occur because pre-starved individuals process food at a rate that gradually increases as they feed. Systematic fluorescence decay was detected in one of the gut compartments and could be an indicator of digestion; decay rates were negatively correlated with gut throughput time.

The inter- and intra-individual variability revealed by our results suggests that average measurements of gut throughput time and other indicators of digestion may not be sufficient to describe the trophic interactions that shape population dynamics. In particular, the averaging process may obscure the more actively feeding individuals that may contribute disproportionately to these interactions.

Introduction

Grazing involves a complex interaction of food availability, food capture and handling, intake need, and digestive performance. It is also a fundamental link between primary producers and heterotrophs, influencing trophic interactions and nutrient cycling. In the last 30 years, there has been considerable development in the theoretical understanding of digestive performance (see review by Yearsley et al. 2001), allowing for a more complete formulation of gut processes. Not taking gut processes into account can lead to erroneous estimates of ecosystem-level dynamics, as shown for instance by a reformulation of NPZ models by Mitra et al. (2007). Flynn (2009) has also shown that ecosystem models with environment-sensitive gut dynamics have flexible trophic linkages that dampen unrealistic oscillations.

An important diagnostic of digestive performance that has lately received attention is the time food spends in the gut, referred to as gut throughput time (*GTT*). *GTT* affects the efficacy and efficiency of digestive processes on gut content. This in turn determines the amount and stoichiometry of nutrients retained and assimilated by the organisms, and the characteristics of matter they evacuate (Mitra and Flynn 2007, Wolesensky et al. 2005). Several approaches have been used to estimate *GTT*. One consists in dividing the gut content by the pellet evacuation rate, where the gut content is quantified as number of fecal pellets (e.g. Besiktepe and Dam 2002). This requires visually estimating pellet volume relative to gut volume; a process that is labor intensive and time consuming, and has to be simplified by the estimation of an average ratio. Another common approach to estimate *GTT* is the gut clearance method (Mackas and Bohrer 1976), in which previously fed copepods are incubated in food-free water while

they clear their guts; the inverse of the estimated average clearance rate is taken as the *GTT*. While this method is relatively easy to use and is particularly suitable for measurements at sea, it remains problematic for a number of reasons. First, this method requires many copepods to gain a single estimate of *GTT*. However, individuals may show variability in initial gut content, fraction of gut content evacuated with each pellet, and frequency of evacuation. Tseitlin (1994) showed that individual variability of initial gut content could compromise the experimental outcome. Second, gut clearance rate experiments require that animals be transferred to food-free media, thus interrupting any feeding activity. However, feeding activity determines *GTT* (e.g. Baars and Oosterhuis 1984), and *GTT* measured via the gut clearance method represents unsteady and temporary conditions, during which gut replenishment in response to evacuation cannot occur. How gut clearance rate measured during fasting relates to *GTT* during feeding remains unclear, and *GTT* is best measured during feeding. Finally, *GTT* is in all likelihood highly variable even in constant conditions, and the value of a single estimate of throughput time with no knowledge of its statistical properties is unclear. A third approach has been to track the progression through the gut of visually traceable food such as charcoal (McCullough et al. 1979), dye particles (Wotton et al. 1995), and naturally colored prey (e.g. conspicuously red diaptomid copepods; Murtaugh 1984). While this is appropriate for one-time measurements, making multiple *GTT* measurements during feeding to assess variability is difficult.

Here we use a planar laser imaging fluorometer to collect sequential images of the distribution of phytoplankton pigment in different copepod midgut compartments (Karaköylü et al. 2009). We use this data to construct highly resolved (one image every

15 s), several hours-long time series of gut fluorescence in individual copepods that were exposed to a continuous and saturating food source. We analyzed these time series to quantify *GTT*, and other characteristics of gut dynamics. The specific goals of this study were threefold: (1) To quantify differences among individuals and identify common patterns in changes of gut content over minute to hour scales, given the continuous availability of food at saturating levels; (2) To quantify individual differences and identify common patterns in GTT; (3) To determine whether digestive performance varied in relation to (1) and (2), over the 4-6 hours of a typical experiment.

Methods

The experiments consisted of feeding individual copepods with a continuous source of phytoplankton while repeatedly imaging fluorescing pigments to infer changes in the distribution of material throughout the gut and quantify gut dynamics. A brief description follows; the method is described in detail in Karaköylü et al. (2009).

Preparation

12 adult female Calanus pacificus, collected in a single net tow in November of 2006, offshore from La Jolla, California (USA) were maintained at 12 °C on a diet of *Thalassiosira weissflogii* for 10 days. Prior to an experiment, an individual was tethered (glued to an acetone-washed human hair) and starved for about 18 hours.

Image Acquisition

During the experiments, the tethered copepod was placed in a temperature-controlled tank, and its tether held in place by a micromanipulator (Fig. 2-1).

Food (*T. weissflogii*) was offered to the copepod in the form of a continuous stream, injected in front of the animal. This approach stopped free cells from interfering with the imaging process, while ensuring a continuous food source.

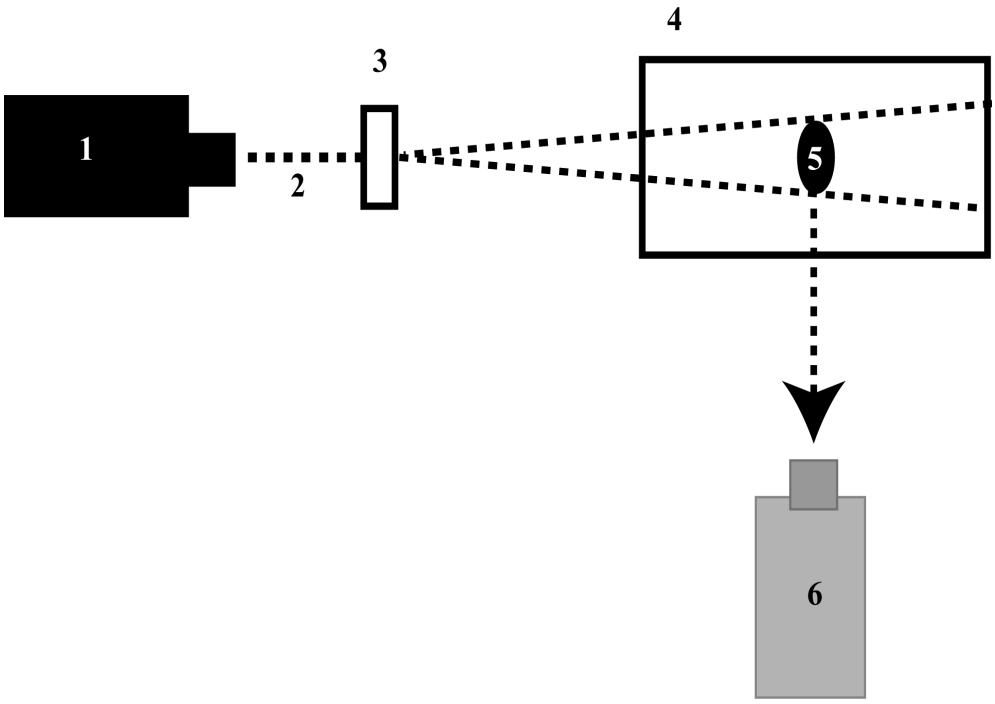

Figure 2-1: *Experimental setup.* 1: Laser; 2: Beam; 3: Powell lens assembly; 4: Tank; 5: copepod; 6: CCD camera.

A green 532 nm 3W laser (Melles Griot 58-GSS-309) beam was expanded into a sheet with a pair of Powell lenses. A tethered copepod was placed into this laser sheet, which was capable of inducing fluorescence from phytoplankton pigment in free as well as ingested cells. Calibration runs have shown the fluorescence response of this system to be linearly related to the extracted gut pigment (Karaköylü et al. 2009). Because

continuous illumination disturbed the copepod, the laser was pulsed with a 30 ms on/15 s off cycle.

A scientific grade 1376 x 1000 pixel Charge Coupled Device camera (Cooke Corp. Sensicam QE), equipped with a Nikkor 50 mm f/1.8 lens and a 680 nm bandpass filter was coupled to the laser pulse. This setup yielded sequences of images at the rate of 1 image every 15 s, taken without interrupting the copepod's feeding. Each acquired image corresponded to a snapshot of the distribution of pigment in the copepod's gut.

Image Analysis

By averaging all the images collected during a given experiment, we were able to identify two principal gut compartments where food resided significantly longer (Fig. 2-2). These compartments are the upper mid-gut (UMG), where ingested food is accumulated for digestion, and the posterior mid-gut (PMG), where fecal pellets are produced prior to evacuation. For each image, we integrated the fluorescence signal over each individual compartment. This yielded time series of the amount of material each gut compartment contained over the course of the experiment; these time series were then analyzed to detect potential gut rhythms and quantify gut dynamics.

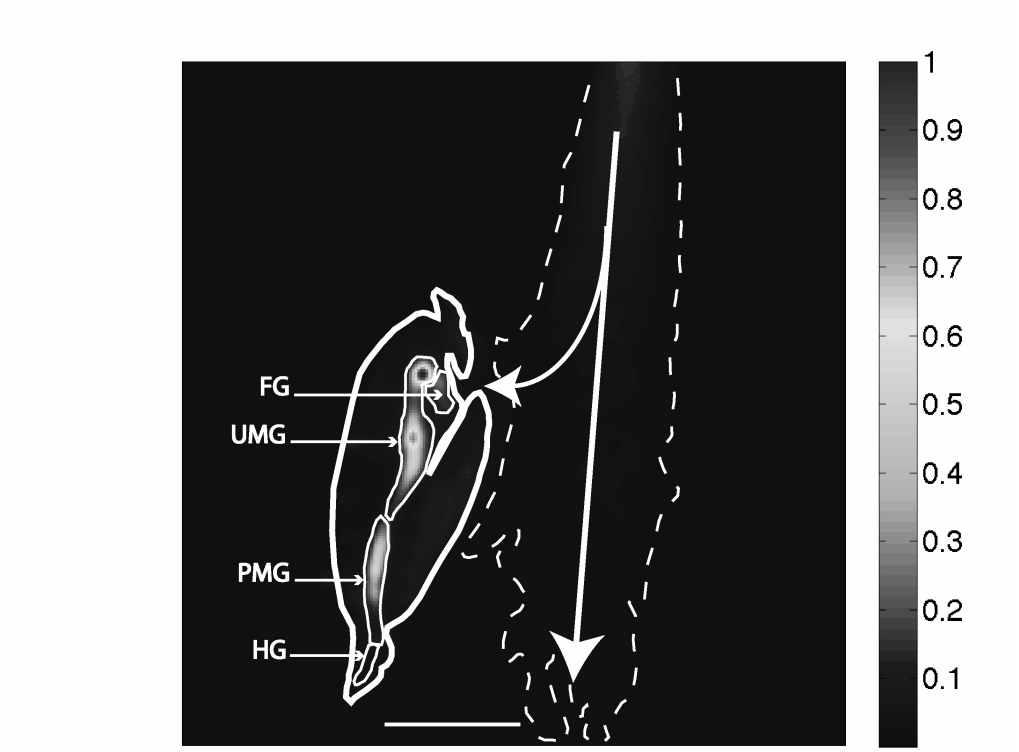

Figure 2-2: *Average of all images acquired during one experiment.* The copepod outline and that of the phytoplankton flow (dashed line) are shown in white. Gut compartments are labeled as follows: FG - foregut, UMG- upper mid-gut, PMG - posterior mid-gut, HG - hindgut. Scale bar is 1 mm. Grayscale bar is normalized fluorescence signal intensity.

Gut Throughput Time

Because evacuation is critical in calculating *GTT*, understanding the relationship between evacuation and total gut content is necessary. Our first step in examining gut dynamics consisted of calculating a PMG fraction; i.e. the integrated fluorescence of the PMG divided by the integrated fluorescence of the gut. We repeated this procedure for

each copepod and computed an average (over all copepods) PMG fraction time series. We then calculated individual *GTT* time series for each copepod. We based our approach on potential gut content reduction, taking the gut content at a particular time and quantifying how much material was evacuated in multiple subsequent defecation events. Specifically, at each transfer event of a bolus from the UMG to the PMG, we measured total gut content. Then, using the magnitude and timing of subsequent evacuation events, we calculated how long it would take a copepod to reduce this amount of gut content by a factor of 1/e (i.e. the time taken to reach ~ 37% of the original gut content, or the e-folding scale). This facilitates comparison of our results with previous studies where gut clearance, usually based on an exponential pigment loss model (Mackas and Bohrer 1976), is the more common approach. Mathematically this is structured as: Given G^*, the gut content at some time t*, find the number of evacuation events n such that

$$\sum_{k=1}^{n} P_k \geq G^*(1-e^{-1}) \tag{1}$$

corresponding to elapsed time t_n:

$$t_n = \sum_{k=1}^{n} t_k \tag{2}$$

Here, k is the index of evacuation events occurring at times t_k, subsequent to t^*, and P_k is the magnitude of the peaks in PMG fluorescence that mark the transfer of material from the UMG to the PMG prior to those events, indicating the amount that was transferred.

Once the condition in equation (1) was met, we calculated gut throughput time from (2) as:

$$GTT = t_n - t^* \quad (3)$$

The above was repeated as long as there were enough subsequent evacuation events to account for G^* in (1), yielding time series of individual copepod *GTT* that span several hours.

Ingestion rate and total ingestion

To convert the gut fluorescence signal to pigment content the gut contents of two copepods were extracted immediately after their respective experiment was terminated and matched to the last images recorded. Problems with our equipment prevented us from conducting more extractions; however, we assumed this still made for an acceptable conversion given the linear equivalence between the laser induced signal and gut pigment found earlier (cf. Karaköylü et al. 2009). Assuming ingestion was matched by gut transit (Mackas and Bohrer 1976) and digestion (Durbin and Campbell 2007), we calculated the ingestion rate *I* using gut content *G* and *GTT* from (3) such that,

$$I = G \, x \, GTT^{-1}. \quad (4)$$

This allowed multiple estimations of ingestion rate in the course of an experiment. Using a carbon (C) to chl ratio of 66 (by weight) for *T. weissflogii* (Strzepek and Price 2000), we integrated these data to estimate individual accrued ingestion at the end of a 4-hour feeding period.

Results

Description of the data

Out of the 12 copepods tested, 10 yielded usable time series. One animal refused to eat, while the other could not on account of a peristaltic pump malfunction. Both copepods were nevertheless re-used later in another batch of experiments not reported here. The sum of the integrated fluorescence from the UMG plus PMG is referred to as bulk gut content, or simply gut content (Fig. 2-3A). The UMG contributed the most to the bulk gut content (Fig. 2-3B). Both bulk and UMG signals were irregular with occasional peaks and troughs of varying amplitude. One obvious pattern visible in both bulk gut content and UMG was an initial peak (in the first 10's of minutes) of higher magnitude than subsequent peaks. In contrast, the PMG signal was much more regular (Fig 2-3C), showing a repeating cycle (Fig 2-3D) with small variations in amplitude. This pattern consisted of a rapid (tens of seconds) increase that culminated in a peak, marking a bolus transfer to the PMG from the UMG. The signal then decayed almost monotonically, even though there was no further transit of material into or out of the PMG, until the bolus was evacuated as a fecal pellet. This decay in the PMG fluorescence signal was in good agreement with an exponential decay model for all the animals tested; for all fits $r^2 > 0.70$, $p < 0.05$. The sharp trough that marked the evacuation of the bolus as a fecal pellet interrupted the exponential fluorescence decay in the PMG. A new transfer of material from the UMG immediately followed this evacuation from the PMG. Often this transfer happened less than 15 s after the evacuation so that the trough marking the evacuation did not reach zero in our data.

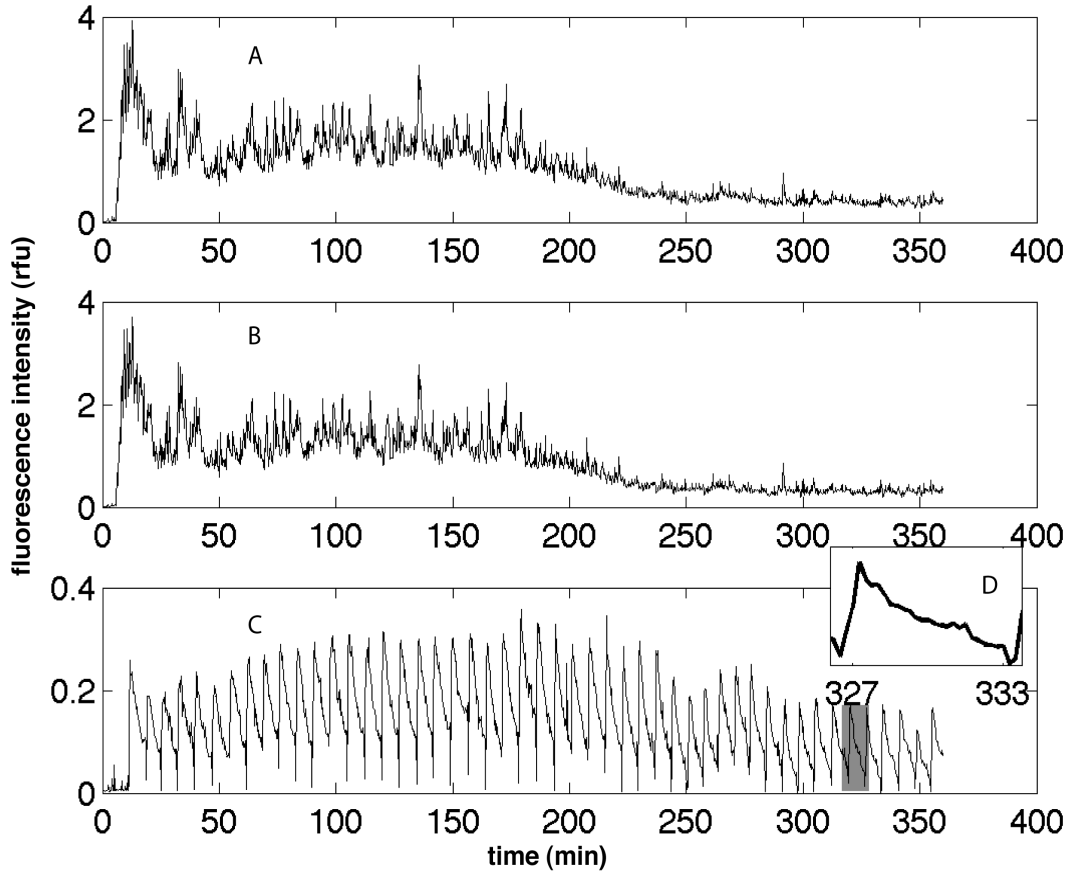

Figure 2-3: *An example of fluorescence time series obtained from the gut of a single individual over ~ 6 h.* (A) Bulk gut fluorescence, (B) UMG, (C) PMG. (D) Detail of the PMG pattern, magnified from the shaded region in (C), and spanning ~6 min.

Common features and individual differences in bulk gut content time series

Even though feeding conditions were identical and copepods had similar acclimation, individual bulk gut content curves varied markedly in both amplitude and rhythm (Fig. 2-4). There were, however, some common features among many if not all

individuals, shown by an average gut content time series (Fig. 2-4, thick black line). Comparing this average to the individual time series showed that there were large differences between outliers and the mean signal, by factors ranging ~0.1 – 5 (Fig. 2-4, thick grey lines). The mean signal showed an initial peak in gut content (see also Fig. 2-3) that occurred in the first tens of minutes after feeding begins. The average gut fluorescence decreased, and the curve reached an equilibrium level.

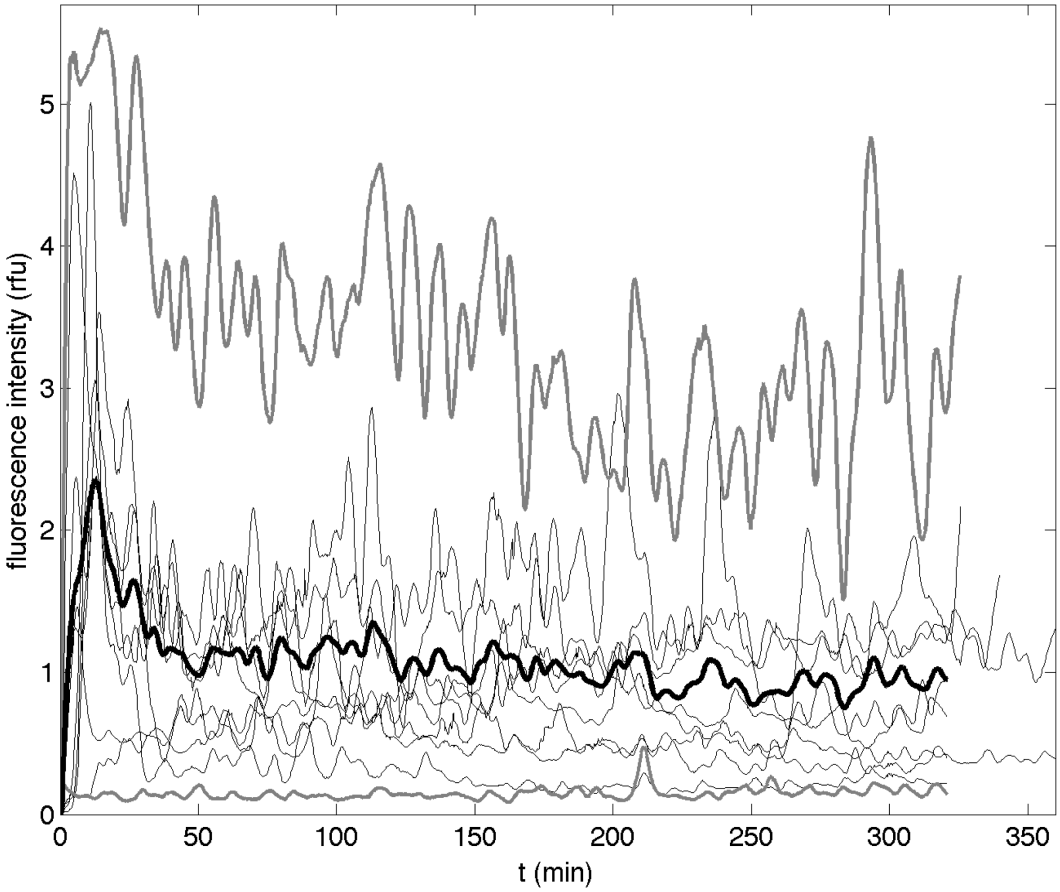

Figure 2-4: *Bulk gut content time series* from 10 individual copepods (thin lines), the weakest and strongest feeders outlined (thick grey lines), and the mean of all the individual signals (thick black line). Time 0 was when food was first introduced to the copepods.

Patterns of gut dynamics

The bulk of digestive hydrolysis occurs in the UMG while the final products of digestion are absorbed in the PMG (Arnaud et al. 1978). As mentioned earlier, mechanically, this translates into accumulation of ingested material in the UMG, and a regular transfer of a food bolus into the PMG to rapidly replace a previously evacuated pellet. When plotted against time, the average PMG gut fraction increased progressively from the moment feeding began (Fig 2-5). This curve was in good agreement with a

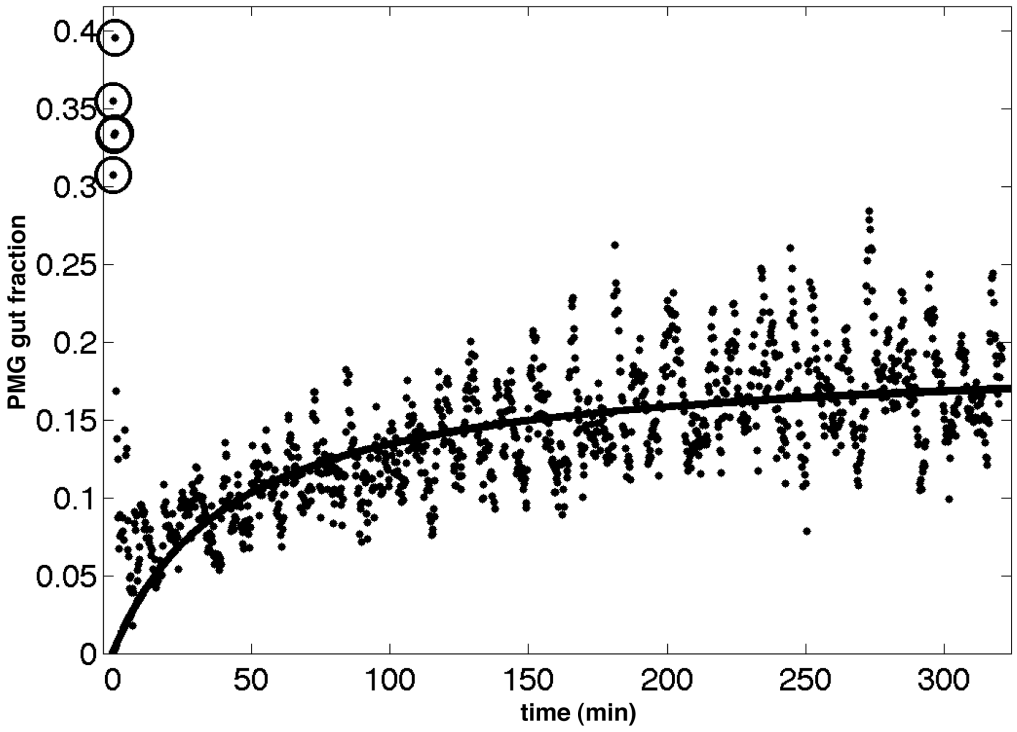

Figure 2-5: *Average PMG gut fraction from 10 copepods.* The black line is a rectangular hyperbola fit to the data: $P = P_{max}\, t / (k_p + t)$, where P is PMG gut fraction as a function of time, t, P_{max} is the maximum gut fraction, and k_p is a half saturation constant. The fit yields $P_{max} = 0.193$, $k = 43.5$ min, $r^2 = 0.50$. Circled points are outliers > 3 SD away from the mean.

saturation model, characterized by an asymptote close to 19%, and a half-saturation time of ~ 44 min (Fig 2-5). Thus at steady state the average copepod evacuates ~1/5 of its gut content with every fecal pellet. However, this steady state is not reached until several tens of minutes after feeding began, during which a smaller fraction of the gut content was evacuated.

Gut Throughput Time

Though the *GTT* time series varied widely among individuals, some common trends were apparent. 6 out of 10 copepods (Fig. 2-6A, C, F, H, I, J) showed a clearly decreasing transit time after they began feeding; two copepods showed a slight overall decrease in their *GTT*, with occasional bouts of increasing *GTT* spanning tens of minutes (Fig. 6B, G); two copepods showed an increasing *GTT* after they began feeding (Fig. 2-6D, E). In many cases, the *GTT*'s tended toward ~15-20 min after beginning feeding, with a transition time that lasted from 20 min (Fig 2-6B) to the duration of an entire experiment (~5 hrs, Fig. 2-6H). In most cases the *GTT*'s were fairly close to their 'equilibrium' level after about 50 min of feeding. The majority of individual copepods had a *GTT* significantly less than the 28 min predicted for 12°C (Dam and Peterson 1988, verified for C. pacificus feeding on *T. weissflogii* by Landry et al. 1994). Only two individuals had a median *GTT* longer than 28 min: 45 and 52 min (Fig 2-7A). When the *GTT* data from all individuals were pooled together, the mode was 20 min (Fig 2-7B).

We tested (Spearman's rho) the potential effect of size, quantified as prosome length (ranging from 2.29 to 2.74 mm) and time since collection on both the median and mode of the individual *GTT*s. Testing for an effect of time since collection was necessary because we were only able to conduct experiments on two copepods per day, one

copepod per experiment. The remaining animals were kept under the acclimation conditions until their turn came. We did not find a significant effect of prosome length on *GTT* median ($p = 0.44$) or *GTT* mode ($p = 0.59$). While there appeared to be a slight decreasing trend in median *GTT* as a function of time since collection (Fig 2-7A), the relationship was not significant ($p = 0.31$). The same was true for *GTT* mode ($p = 0.57$); however, omitting one copepod (6th individual, Fig. 2-7A) reinforced the relationship, though not enough to be considered statistically significant ($p = 0.083$). Discarding the same animal did not change the significance of the other tests.

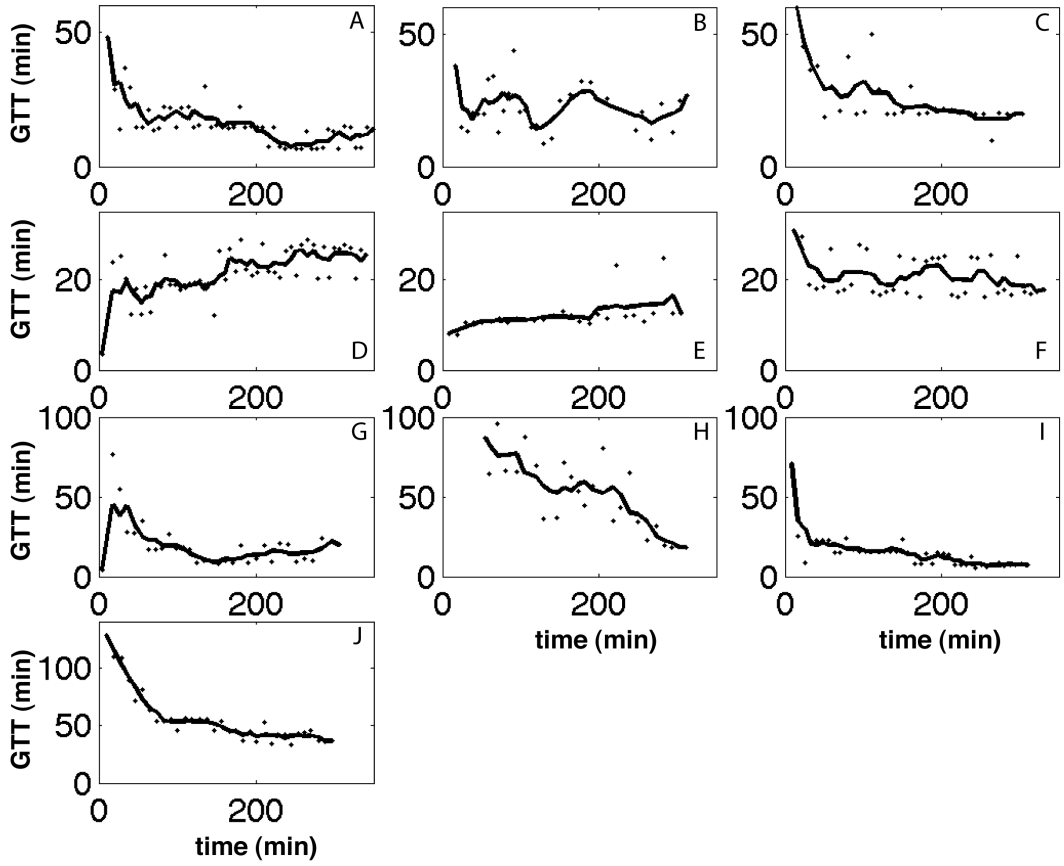

Figure 2-6: *GTT time series of individual copepods* that have resumed feeding after ~18 h of starvation. Data points are actual GTT calculated as described in the text. Lines show a 5-point running mean of the data to highlight the trends.

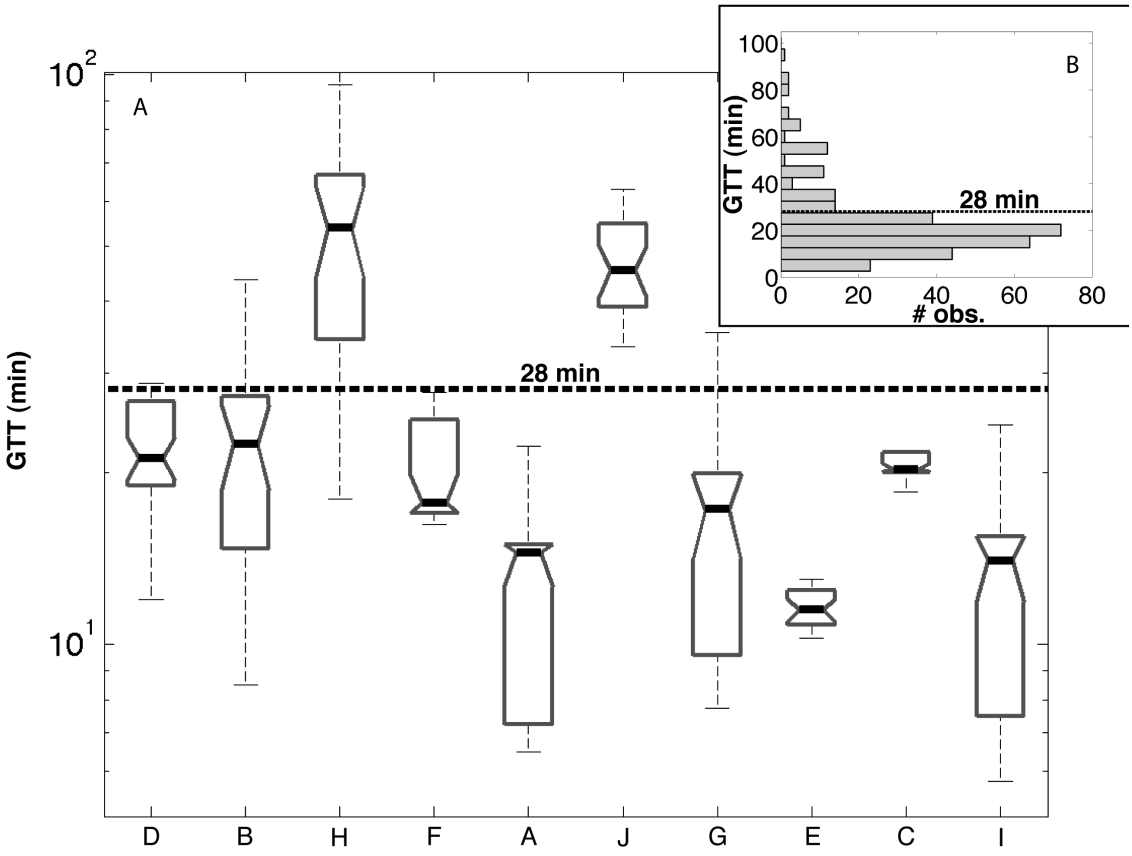

Figure 2-7: *Statistics of individual copepods' GTT's.* Data presented here exclude the first 50 min of an experiment, during which all copepod GTT's showed a trend (see Fig. 2-6). Each box and whisker summarizes the GTT data for one copepod. Letters relate copepods to plots in Fig. 2-6. Top and bottom of the boxes are the upper and lower quartiles of an individual's GTT, respectively. The thick black line is the median; side notches mark 95% confidence intervals; dispersion whiskers are equivalent to 1.5 times the interquartile distance. The horizontal dashed line references the expected GTT, given the experimental temperature (12 °C, 28 min, Dam and Peterson 1988). Inset: histogram of the number of occurrences of different values of GTT pooled over all the copepods.

A significant correlation ($p << 0.001$) was found between GTT and PMG pigment decay time scale (1/decay rate, Fig. 2-8). We failed to find any significant correlation between PMG pigment decay and either copepod size or time since collection.

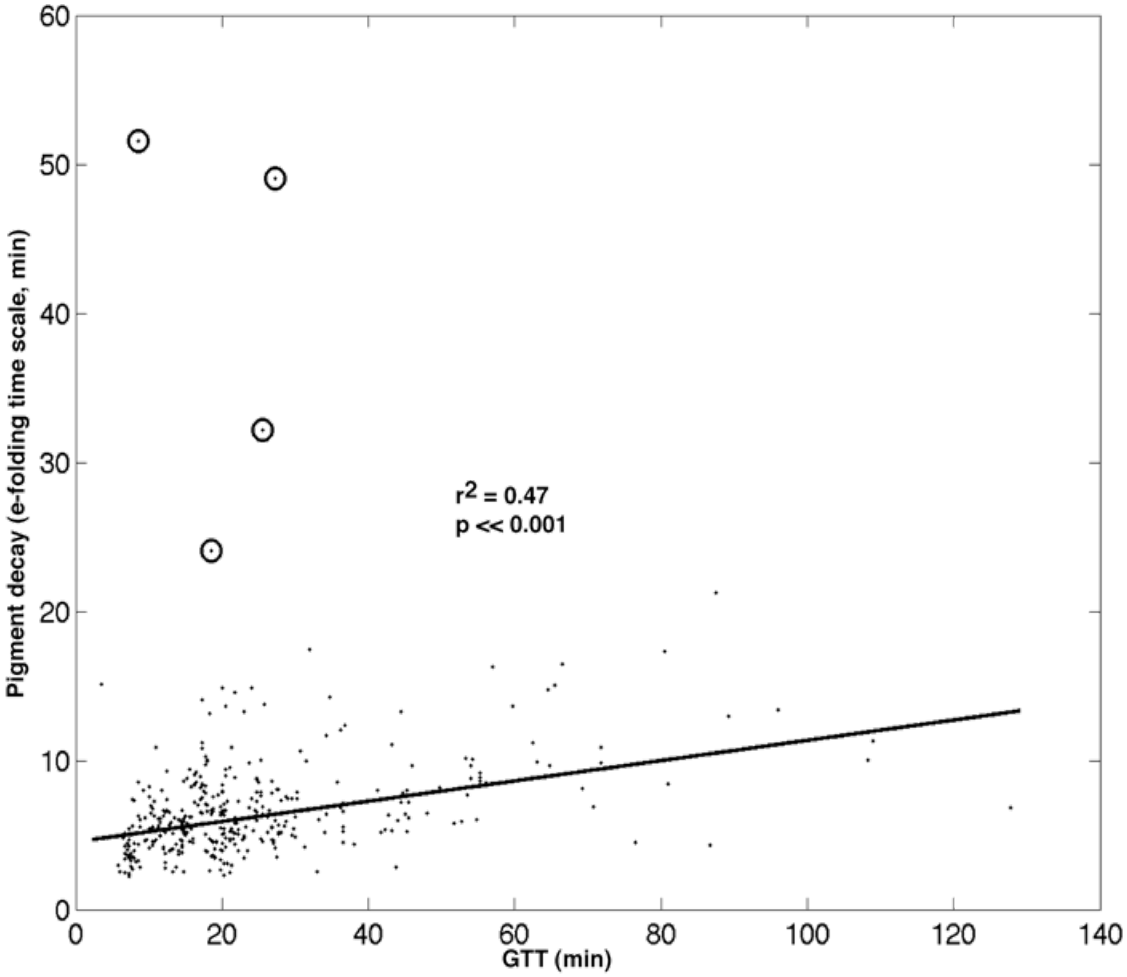

Figure 2-8: *Comparison between GTT and corresponding PMG pigment decay time scale*, for all copepods tested. Circled data points indicate outliers that were beyond 3 SD of the data when the trend was removed. Thick black line shows the linear fit.

Ingestion

Individual mean ingestion rates (Table 2-1) varied between ~0.91 – 3.68 μg C h^{-1}, with an overall mean ingestion rate of 2.21 μg C h^{-1}. To put these numbers in context, we consider a scenario common for C. pacificus, where a 12-hour non-feeding period at 8 °C is followed by a 12-hour feeding period at 12 °C, with no food limitation. Energetic requirements for this scenario were calculated from Vidal (1980), with the assumption

that metabolic expenditure during the refractory period was approximately halved (ibid.). Daily requirements for the copepods used here ranged from 6.83 to 10.9 µg C. Assuming a C assimilation of 75%, given the acclimation conditions (Landry et al. 1984), the time required for individual copepods to acquire an adequate daily ration ranged between 2.94 and 13.8 h (Table 2-1), with a mean of 6.38 h.

Table 2-1*: Estimation of ingestion rate,* comparison of total ingestion to a theoretical daily ration, and resulting feeding time required for satiation for 10 individual copepods, taking into account an assimilation rate of 75% (Landry et al. 1984).

Mean Ingestion (µg C h^{-1})	Daily Requirement (µg C)	Required Feeding Time (h)
2.03	8.13	5.34
2.81	7.82	3.71
1.74	**6.83**	5.23
2.36	**10.9**	6.16
3.68	8.13	**2.95**
3.09	10.0	4.32
1.04	7.49	9.60
0.91	9.39	**13.8**
1.98	10.3	6.94
2.43	10.6	5.82

Discussion

Individual adult female C. pacificus feeding on saturating levels of T. weissflogii showed dramatic variations in gut content during 4- to 6-hour long experiments. In many cases, the largest variations occurred during the first tens of minutes of an experiment in the form of a pronounced peak reminiscent of a hunger response. This initial peak was clearly visible in the gut content time series averaged over all the individuals (Fig. 2-4). Two hypotheses have been proposed to explain hunger response (Mackas and Burns

1986): a synchrony at the beginning of feeding among copepods that had been starving, and/or a higher initial feeding rate. Synchrony is not a factor here since we examined individual copepods. A higher initial feeding rate was found in C. pacificus individuals (Mobley 1987). However, when we take into consideration that the average PMG content increased progressively, toward an asymptote of ca. 19% of the total gut content, then a third possibility, not in contradiction with the other two, comes to mind; the gut content peak may be in fact the result of food retention in the gut.

A potential advantage of food retention in the gut comes from the fact that C. pacificus dwells in a heterogeneous environment, where its survival will depend on the uncertain encounter with the next food patch. Once a copepod has located a patch, it could reduce its predation risk by ingesting until its gut was full, sinking temporarily while digesting, then swimming back up to renew foraging (Pearre 2003). With this behavior, long food retention may ensure a more thorough breakdown of food, making more nutrients available for assimilation. In addition, when feeding starts after a several hour-long starvation period, copepod guts may experience a delay before reaching peak digestive performance; during this delay, it would be to their advantage to retain food for subsequent digestion.

The first evidence of such a delay comes from the progressive increase in the PMG gut fraction. PMG gut fraction indicates how much of the gut content has been processed and will be either absorbed or evacuated. An often tacitly made assumption is that on average, when food type and concentration are held constant, the amount evacuated should be linearly related to the total gut content (e.g. Timonin et al. 1992,

Tseitlin 1994). Here we see that on average this relationship requires several tens of minutes after the animals start feeding before it stabilizes.

A second indicator of progressively increasing digestive performance is provided by the GTT decrease we observed in 8 of 10 copepods after they began feeding; this despite unaltered environmental factors, including temperature (Irigoien 1998), and food quality or quantity (Tirelli and Mayzaud 2005). Theoretical studies of digestion for a variety of taxa including copepods (Mitra and Flynn 2007) have postulated that assimilation should at least partly depend on GTT, where in general the longer the residence time in the gut, the greater the assimilation. The wide intra-individual variability in GTT we observed here suggests that as feeding continued, digestive performance was changing. If so, other digestive factors might co-vary with changes in GTT. The decay rate in the PMG fluorescence appears to be such a factor.

Fluorescence decay in the PMG could result from the destruction of pigments by digestive enzymes – possibly one or more proteases – synthesized in the UMG (Arnaud et al. 1978) and carried through the gut with a bolus of food into the PMG where they remain active (Nott et al. 1985). Note that in all likelihood pigment fluorescence decay occurs throughout the midgut; the decay is only visible in the PMG because it is not obscured by the complex mixing patterns that occur in the UMG. If the rates of fluorescence decay in the PMG before an evacuation event are related to enzyme levels packed in the fecal pellet, and these PMG enzyme levels are indicative of enzyme levels in the entire midgut, then these decay rates could provide a means of quantifying digestive performance. Assuming there is a relation between PMG decay rates and midgut enzyme levels, our data suggest that digestive enzymes vary in conjunction with

gut dynamics. Feeding history is known to affect digestive enzyme levels over relatively long periods (weeks, Mayzaud and Poulet 1978). More recently Kreibich et al. (2008) showed that proteolytic enzyme levels could decrease significantly in the small calanoid copepod Temora longicornis within starvation periods as short as 24 hrs. However there is no reason why enzyme levels should not vary over shorter time scales. The significant correlation that we found between *GTT* and PMG decay rates (Fig. 8) could reflect an increase in enzyme output when previously starved copepods fed. In other words, the induction of digestive enzymes is related to short-term (tens of minutes to hours) feeding behavior. A reduction in digestive enzyme output during starvation might be expected given that pellet production and evacuation continues to occur when animals are not feeding (ibid.) in the form of mostly empty membrane-encased pellets (Reeve 1963). Enzymes present in the gut lumen would also be voided in these pellets, representing an unnecessary metabolic cost. A potential link between GTT and enzyme availability has been posited previously (Mayzaud and Poulet 1978); our data support this hypothesis.

Along with the intra-individual variability described above, we found significant differences among individuals in spite of a similar feeding history and replicated feeding conditions. The observed variability suggests a corresponding variability in feeding behavior with no apparent environmental explanation. We recognize that we could have made better measurements of physiological characteristics of the copepods we tested. For instance, although we selected gravid females prior to beginning the acclimation process, we did not examine whether there were eggs still present in the ovaries and if they were present, at what stage they were immediately prior to an experiment; nor did we assess the animal's lipid content. However, such measurements would not have necessarily shed

more light on the observed variability. Peterson (1986) found significant variability in the size of C. marshallae females raised to adulthood in the laboratory under controlled conditions, and could not link these variations to genetic differences. While we attempted to heed Båmstedt's (1988) recommendation to ensure that feeding histories were controlled, a 10-day acclimation period might not have been sufficient. Moreover, we could only conduct experiments at the rate of two animals per day while the others continued to be incubated, which might have resulted in further individual departures in conditioning. No strong correlation was found between individual *GTT* and the time elapsed between collection and experimentation. In addition, pairs of copepods experimented upon the same day did not show significant similarities. Nevertheless, the existence of a weak decreasing trend in *GTT* as a function of time since capture suggests there might still be a residual effect of earlier conditions encountered in the field by these copepods. An imaging system similar to the one we used could prove adequate to study some aspects of feeding history (cf. Huntley 1988).

Most studies quantifying copepod feeding yielded averages of feeding rates and digestive performance, and thus highlight average behavior and physiology. Average measurements tend to hide individual variability and outliers. Recently there has been an effort toward incorporating gut dynamics and digestive performance into models (e.g. Mitra and Flynn 2007) to better understand processes that control ecosystem dynamics (Flynn 2009). These models are parameterized with available data, usually average measurements. Using only average parameters such as gut transit time and assimilation efficiency without an understanding of their dispersion could yield unrealistic results. Numerous field studies have documented the importance of considering individual

differences to explain patterns in population dynamics. Recruitment in fish, for instance often depends on the individual growth rate of larvae (Rice et al. 1987); the survivors were found to have a greater than average growth rate, conferring them a relative advantage against predation. Furthermore, there are strong theoretical arguments supporting the potential importance of outliers and individual variability. Lomnicki and Sedziwy's (1989) pioneering work showed that relatively active individuals that monopolize resources tend to positively impact population stability and persistence. In more recent work that takes into account rapidly changing resource availability – not unlike a copepod's environment – Grimm and Uchmanski (2002) stress that the entire regulation of a population depends on the individual differences among its members.

In the present study, individual ingestion rates suggested that some copepods would fulfill their theoretical energetic requirements faster than the average. In a situation where copepods migrate upward to shallow layers to feed and migrate downward to reduce the risk of visual predation, we would expect fast feeders to migrate out of the feeding layer earlier, increasing their chances of survival. Those that were slower in obtaining a sufficient daily ration would continue to forage, resulting in a progressively higher proportion of slow feeders in shallow layers as time passed and fast feeders became satiated. In short-term laboratory experiments, feeding rates of pre-starved copepods are initially high and decline subsequently (e.g. Mackas and Burns 1986). Our data suggests the possibility that after a few hours of feeding, satiated fast feeders would cease to feed while slow feeders would continue to forage, resulting on average in a lower measured feeding rate. Slower feeding is not necessarily a disadvantage, if it results in enhanced detection ability of hydrodynamic disturbance. In copepods the

chances of avoiding predation are more dependent on the ability to detect an approaching predator than on the capacity to escape from an attacking predator (Viitasalo et al. 1998). Thus the high variability in ingestion rates could be the manifestation of alternative strategies to avoid predation during feeding: feed rapidly to reduce time spent in a potentially dangerous location, or feed at decreased intensity and thus increase chances of detection of approaching predators.

In conclusion, even in homogeneous trophic conditions, gut dynamics of previously starved copepods change as they continue feeding. In particular, an initial peak in gut content observed during the first tens of minutes of feeding and an initially slow transit of food through the gut appears to be a transition period during which digestive performance increases. During this transition period *GTT* decreases progressively, accompanied by an increase in the rate of PMG decay. We speculate that PMG decay is indicative of pigment destruction by one or more digestive enzymes. While this is the general trend we observed there are significant differences among individuals, which cannot be currently explained.

References

Arnaud, J., Brunet, M., and Mazza, J. 1978. Studies on the midgut of Centropages typicus (Copepod, Calanoid). I. Structural and ultrastructural data. Cell Tissue Res. 187: 333-353.

Baars, M.A. and Oosterhuis , S.S. 1984. Diurnal feeding rhythms in North Sea copepods measured by gut fluorescence, digestive enzyme activity and grazing on labeled food. Netherlands Journal of Sea Research 18(1/2): 97-119.

Båmstedt, U. 1988. Ecological significance of individual variability in copepod bioenergetics. Hydrobiologia 167/168: 43-59.

Besiktepe, S. and Dam, H.G. 2002. Coupling of ingestion and defecation as a function of diet in the calanoid copepod Acartia tonsa. Mar. Ecol. Progr. Ser. 229: 151-164.

Dam, H.G. and Peterson, W.T. 1988. The effect of temperature on the gut clearance rate constant of planktonic copepods. J. Exp. Mar. Biol. Ecol 123: 1-14.

Durbin, E.G. and Campbell, R.G. 2007. Reassessment of the gut pigment method for estimating in situ zooplankton ingestion. Mar. Ecol. Progr. Ser. 331:305-307.

Flynn, K.J. 2009. Food-density-dependent inefficiency in animals with a gut as a stabilizing mechanism in trophic dynamics. Proc. R. Soc. B Biol.l Sci. 276: 1147-1152.

Grimm, V. and Uchmanski, J. 2002. Individual variability and population regulation: a model of the significance of within-generation density dependence. Oecologia 131: 196-202.

Huntley, M. 1988. Feeding biology of Calanus: a new perspective. Hydrobiologia 167/168: 83-99.

Irigoien, X. 1998. Gut clearance rate constant, temperature and initial gut contents: a review. J. Plankton Res. 20(5): 997-1003.

Karaköylü, E.M., Franks, P.J.S., Tanaka, Y., Roberts, P.L.D. and Jaffe, J.S. 2009. Copepod feeding quantified by planar laser imaging of gut fluorescence. Limnol. Oceanogr. Methods 7: 33-41.

Kreibich, T., Saborowski, R., Hagen, W., and Niehoff, B. 2008. Short-term variation of nutritive and metabolic parameters in Temora longicornis females (Crustacea, Copepoda) as a response to diet shift and starvation. Helgol. Mar. Res. 62: 241-249.

Landry, M.R., Lorenzen, C.J. and Peterson, W. 1994. Mesozooplankton grazing in the Southern California Bight. II. Grazing impact and particulate flux. Mar. Ecol. Progr. Ser. 115: 73-85.

Landry, M.R., Hassett, R.P., Fagerness, V., Downs and Lorenzen, C.J. 1984. Effect of food acclimation of assimilatino efficiency of *Calanus pacificus*. Limnol. Oceanogr. 29(2): 361-364.

Lomnicki, A. and Sedziwy, S. 1989. Do individual differences in resource intakes without monopolization cause population stability and persistence? J. Theor. Biol. 136:317-326.

McCullough, D.A., Minshall, G.W. and Cushing, C.E. 1979. Bioenergetics of a stream 'collector' organism Tricorythodes minutus (Insecta: Ephemeroptera). Limnol. Oceanogr. 24: 45-58.

Mayzaud, P. and Poulet, S.A. 1978. The importance of the time factor in the response of zooplankton to varying concentrations of naturally occurring particulate matter. Limnol. Oceanogr. 23(6): 1144-1154.

Mackas, D.L. and Burns, K.E. 1986. Poststarvation feeding and swimming activity in Calanus pacificus and Metridia pacifica. Limnol. Oceanogr. 31(2): 383-392.

Mackas, D.L. and Bohrer, R. 1976. Fluorescence analysis of zooplankton gut contents and an investigation of diel feeding patterns. J. Exp. Mar. Biol. Ecol. 25: 77-85.

Mitra, A. and Flynn, K. J. 2007. Importance of interactions between food quality, quantity, and gut transit time on consumer feeding, growth, and trophic dynamics. Am. Nat. 169(5): 632-646.

Mitra, A., Flynn, K.J. and Fasham, M.J.R. 2007. Accounting for grazing dynamics in nitrogen-phytoplankton-zooplankton models. Limnol. Oceanogr. 52(2): 649-661.

Mobley, C.T. 1987. Time-series ingestion rate estimates on individual Calanus pacificus Brodsky: interactions with environmental and biological factors. J. Exp. Mar. Biol. Ecol. 114: 199-216.

Murtaugh, P.A. 1984. Variable gut residence time: problems in inferring feeding rate from stomach fullness of a mysid crustacean. Can. J. Fish. Aquat. Sci. 41: 1287-1293.

Nott, J.A., Corner, E.D.S., Mavin, L.J. and O'Hara, S.C.M. 1985. Cyclical contributions of the digestive epithelium to faecal pellet formation by the copepod Calanus helgolandicus. Mar. Biol. 89: 271-279.

Pearre, S. Jr. 2003. Eat and run? The hunger/satiation hypothesis in vertical migration: history, evidence and consequences. Biol. Rev. 78: 1-79.

Peterson, W.T. 1986. Development, growth, and survivorship of the copepod Calanus marshallae in the laboratory. Mar. Ecol. Progr. Ser. 29: 61-72.

Reeve, M.R. 1963. The filter-feeding of Artemia. III. Faecal pellets and their associated membranes. J. Exp. Biol. 40: 215-221.

Rice, J.A., Crowder, L.B. and Holey, M.E. 1987. Exploration of mechanisms regulating larval survival in Lake Michigan bloater: A recruitment analysis based on characteristics of individual larvae. Trans. Am. Fish. Soc. 116:703-718.

Strzepek, R.F and Price, N.M. 2000. Influence of irradiance and temperature on the iron content of the marine diatom *Thalassiosira weissflogii* (Bacillariophyceae). Mar. Ecol. Prog. Ser. 206: 107-117.

Tirelli, V. and Mayzaud, P. 2005. Relationship between functional response and gut transit time in the calanoid copepod Acartia clausi: role of food quantity and quality. J. Plankton Res. 27(6): 557-568.

Timonin, A.G, Arashkevich, E.G., Drits, A.V., and Semenova, T.N. 1992. Zooplankton dynamics in the northern Benguela ecosystem, with special reference to the copepod Calanoides carinatus. S. Afr. J. Mar. Sci. 12: 545-560.

Tseitlin, V.B. 1994. Simulating measurements of copepod gut passage time. Oceanology 34(1): 66-71.

Vidal, J. 1980. Physioecology of Zooplankton. III. Effects of Phytoplankton Concentration, Temperature, and Body Size on the Metabolic Rate of Calanus pacificus. Mar. Biol.56:195-202.

Viitasalo, M., Kiørboe, T., Flinkman, J., Pedersen, L.W. and Visser, A.W. 1998. Predation vulnerability of planktonic copepods: consequences of predator foraging strategies and prey sensory abilities. Mar. Ecol. Progr. Ser. 175: 129-142.

Yearsley, J., Tolkamp, B.J. and Illius, A.W. 2001. Theoretical developments in the study and prediction of food intake. Proc. Nutr. Soc. 60: 145-156.

Wolesensky, W., Joern, A., and Logan, D.J. 2005. A model of digestion modulation in grasshoppers. Ecol. Model. 188: 358-373.

Wotton, R.S., Malmqvist, M. and Ashelford, K. 1995. The retention of particles intercepted by a dense aggregation of lake-outlet suspension feeders. Hydrobiologia 306:125-129.

CHAPTER 3

Temperature-dependence of gut dynamics in continuously feeding individual *Calanus pacificus* (Copepoda: Calanoida)

Abstract

I tested the effect of temperature on a number of variables describing different processes of feeding in individual *Calanus pacificus* females, as they fed. These processes included ingestion, gut throughput time, evacuation rate, gut contents, and pigment decay in the posterior midgut (PMG). Experiments were conducted at 8, 12, and 16 ºC, on the same 9 individuals, to obviate problems of interpretation due to inter-individual variability. In particular, average ingestion rates at 8, 12, and 16 ºC were 1.17, 3.14, and 4.87 μg C h^{-1}, respectively. However, individual ingestion rates varied between 0.34 – 2.3 μg C h^{-1} at 8 ºC, 1.1 – 4.5 μg C h^{-1} at 12 °C, and 0.85 – 10 μg C h^{-1} at 16 ºC. Similarly, average gut throughput times (GTT) at 8, 12, and 16 ºC were 25, 20 and 18 min, respectively. However, individual *GTT* varied between 13 - 39 min at 8 °C, 11 - 54 min at 12 ºC, and 10 - 40 min at 16 ºC. Such large range among individuals suggests average measurements may have little value in representing ongoing processes. Ingestion Q_{10} was 5.2; gut throughput time (i.e. clearance rate) had a Q_{10} of 1.5; evacuation rate had a Q_{10} of 2.2; PMG decay had a Q_{10} of 1.9. Thus, these various processes, the interplay of which determines gut dynamics, may not be at equilibrium over time scales of several minutes relevant to foraging, though some feedback mechanisms appear to exist. As a result, a single descriptor, usually gut throughput time in most published studies, may not be sufficient to completely describe the effects of temperature on copepod feeding.

Introduction

One of the principal goals of biological oceanography is the accurate measurement of zooplankton feeding rates. Among zooplankton, copepods are often the dominant taxa. Herbivorous copepods constitute a crucial link between autotrophs and higher heterotrophs including many commercially important species. In spite of its importance, we still do not fully understand copepod feeding, in particular the reasons for the observed variability in feeding rates.

Since its introduction (Nemoto 1968), the gut fluorescence measurement technique has been a commonly used approach to quantify feeding in copepods (Mackas and Bohrer 1976, Tseng et al. 2009), as it is easily employed both in the laboratory and at sea. Typically, pre-fed copepods are incubated in filtered seawater; a number of animals are drawn at distinct time intervals and their gut contents assessed. The gut clearance rate is calculated from the decrease in gut fluorescence over time. This is taken as a representative rate for animals encountered in the environment, and ingestion rates are calculated by multiplying gut contents by gut clearance rate.

A key assumption of the gut fluorescence method is that gut clearance during feeding is the same as during starvation. A number of authors argue that this may not be so (e.g. Kiørboe et al. 1985, Wang and Conover 1986) and propose taking only the first few tens of minutes of an experiment as truly representative of gut clearance during feeding (e.g. Kiørboe et al. 1985); it is still not clear whether this makes for a more accurate estimate. In addition, the method provides a snapshot of clearance rates averaged over a relatively coarse time interval. Thus, it is not clear how representative the inferred ingestion rates are because copepods are known to be intermittent feeders (e.g. Rosenberg

1980) that graze asynchronously relative to each other (e.g. Rodriguez and Durbin 1992) at very different intensities even under the same conditions. (Karaköylü and Franks, submitted ms.). As Båmstedt et al. (1992) remarked, the reasons behind this variability are not well understood. Yet, this can result in compromised estimates of ingestion rates (Tseitlin 1994).

A number of studies have looked at individual variability in feeding copepods. Paffenhöfer et al. (1995), while continuously observing ingestion of phytoplankton and fecal pellet release in individual *Paracalanus aculeatus* at different food concentrations, could not find a clear relationship between ingestion and pellet release rates. Because ingestion and pellet release are linked by gut dynamics, it is conceivable that the observed variability could be at least in part be explained by gut dynamics. Quantifying gut dynamics is not logistically feasible, as it would require continuous sampling of the gut contents of copepods without interrupting their feeding.

In this paper, we combine continuous direct observations of individual copepods with the gut sampling capability offered by gut fluorescence to quantify gut dynamics during feeding. For this purpose, we use a non-invasive near-continuous gut fluorescence imaging method (Karaköylü et al. 2009) to investigate individual *Calanus pacificus* gut dynamics during feeding, in relation to temperature. Temperature, as with any living organism, is an important factor affecting copepod physiology in general (e.g. Vidal 1980a-d), and gut processes in particular (Dam and Peterson 1988). Because copepods are likely to encounter a range of temperatures during foraging over a day, and in their lifetime, this aspect of copepod feeding remains of particular interest.

Methods

Preparation

Copepods were collected in a single vertical tow using a 1m opening net, 2 miles offshore of La Jolla, California. Gravid *Calanus pacificus* females were selected and transferred into 1L jars at 12 °C under a 12/12 light cycle. Equal amounts of *Thalassiosira weissflogii* were added to all jars. Copepods were transferred to new media every day. This acclimation phase lasted 10 days. The morning of the day before the experiment, 1 jar was selected; two copepods were tethered, and transferred to a 1L jar containing filtered seawater and incubated at the experimental temperature. Each tether was color coded for identification.

Feeding experiments

For each set of two copepods, three pairs of 4- to 6-hour experiments were conducted on three consecutive days. On each day a different experimental temperature was used; 8, 12, or 16 °C, a typical range *C. pacificus* is likely to encounter in Southern California. Each pair of copepods was assigned a different order of the 3 experimental temperatures. In all, six pairs of copepods were used to cover all possible 3-temperature permutations (Table 3-1).

A few hours prior to the experiments, filtered seawater that had been pre-cooled overnight to the desired temperature was poured into a 4L clear acrylic tank. A chiller was used to keep the water at the desired temperature via fresh water flowing through steel pipes of 8 mm inner diameter. The steel pipes ran along the top, bottom, and corners of each side of the tank. Water temperature was measured at the center of the tank, approximately where the copepod tether was to be positioned. Once the temperature

stabilized at the desired level, one of two tethered copepods was selected and placed in the center of the tank. A solution containing saturating levels of *T. weissflogii* (>10,000 cells mL^{-1}) was injected directly in front and slightly above the copepod, using a peristaltic pump. A pulsing (30 ms on, 15 s off) 3W green (532nm) laser sheet completely illuminated the copepod and its immediate surroundings; thus, both the ingested phytoplankton and the phytoplankton caught in feeding currents were induced to fluoresce. A highly magnified (20 μm pixel side resolution), highly sensitive Charge-Coupled Device Camera (Cook Corp.) was centered on the copepod. Electronically synchronized to the laser pulse, and equipped with a red (680 nm bandpass, 20 nm bandwidth) filter, the camera recorded the distribution of the pigment fluorescence inside the copepod. This imaging system's resolution allowed us to distinguish between functionally distinct midgut compartments. A more detailed description of this setup can be found in Karaköylü et al. (2009). At the end of the experiment, the copepod was returned to filtered seawater and brought to the next experiment's temperature during an 18-hour starvation period. The tank was cleaned and the experiment was re-set. When the water temperature was deemed satisfactory, the second experiment of the day was conducted as described previously with the second copepod of the pair. Each experiment lasted between four and six hours, yielding over a thousand images.

Image Analysis

Table 3-1: *Copepod pairs and corresponding experimental temperature sequence*

Copepod #	Temperature Sequence
1,2	12-16-8
3,4	8-12-16
5,6	16-8-12
7,8	16-12-8
9,10	8-16-12
11,12	12-8-16

We only consider the midgut for two reasons. Firstly, passage of matter through the other compartments is too fast to be resolved adequately by our system. Secondly, the midgut is the principal site of digestion and is therefore likely to be an important internal source of feedback in the foraging behavior of the copepod. Two main midgut compartments, separated by a constriction were distinguished in the analysis. The first and larger of these is the upper midgut (UMG), where ingested food is broken down. The second is the posterior midgut (PMG), where nutrients are absorbed and undigested material is packed into fecal pellets. The fluorescence was integrated over the UMG and the PMG in each image, yielding an estimate of the food in each midgut compartment at that time. An experimental data set consisted of a *UMG* time series, a *PMG* time series, and a time series of bulk gut contents (*G*) that is the sum of the *UMG* and *PMG* signals.

Quantification of gut dynamics

The following characteristics of gut dynamics were quantified; pellet output rate, fraction of bulk gut contents in the PMG (i.e., *PMG*/G), *GTT*, ingestion rate, and the rate of fluorescence decay observed in the *PMG* signal. The flow of matter through the midgut is a principal determinant of gut dynamics, and depends at least in part on PMG kinetics as a function of gut contents. This relation is examined by expressing *PMG* as a fraction of total gut contents (*PMG*/*G*).

GTT was calculated by considering how long it would take a copepod to evacuate a given gut contents measured at t^*, $G(t^*)$. Thus,

$$\sum_{k=1}^{n} P_k \geq G^*(1 - e^{-1}) \qquad (1)$$

corresponding to elapsed time t_n

$$t_n = \sum_{k=1}^{n} t_k \qquad (2)$$

Here k indexes the evacuation events at time t_k, subsequent to t^*, and P_k is the fluorescence proxy for the amount of material transferred from *UMG* and *PMG*. Once (1) is satisfied, *GTT* is calculated from (2):

$$GTT = t_n - t^* \qquad (3)$$

The above specifies an e-folding time scale of gut clearance, i.e. the time required to evacuate ~63% of $G(t^*)$ given the evacuation rate and amounts transferred to fecal pellets that followed. Expressing an e-folding scale makes results reported here comparable to a

large fraction of work previously published, where *GTT* is estimated by fitting an exponential loss model to gut clearance data (e.g. Mackas and Bohrer 1976).

Ingestion - We assumed that the flow of food through the gut was matched by the amount ingested. This allowed us to calculate individual instantaneous ingestion rates (from here on referred to as ingestion rates) by dividing bulk gut contents by concurrent *GTT* such that

$$I(t) = G(t) \times GTT(t)^{-1} \qquad (4)$$

where $I(t)$ is the ingestion rate at time t. Data were converted to $\mu g\ C\ t^{-1}$, as described in the previous chapter.

PMG decay

A striking characteristic of the data is an exponential decay in the *PMG* signal between evacuation events. Because they could represent digestion, *PMG* decay rates were evaluated by fitting an exponential function to the decaying portions of the *PMG* signal, starting from the peak marking the transfer from *UMG* and ending just short of the trough resulting from the evacuation of a fecal pellet.

Unless mentioned otherwise, we used Friedman's non-parametric repeated measures multiple comparison test to compare central tendencies of individuals between the three temperature treatments. The median was used as central tendency, except in the case of *GTT* where a decrease is often seen from the beginning of feeding, lasting a variable amount of time, depending on the individual (cf. previous chapter).

Results

Description of the initial data

Only those copepods that yielded complete data sets for all three temperatures were retained. Out of 12 copepods, 9 copepods satisfied this requirement resulting in a total of 27 data sets, each data set comprising >1200 images. All image sequences and the

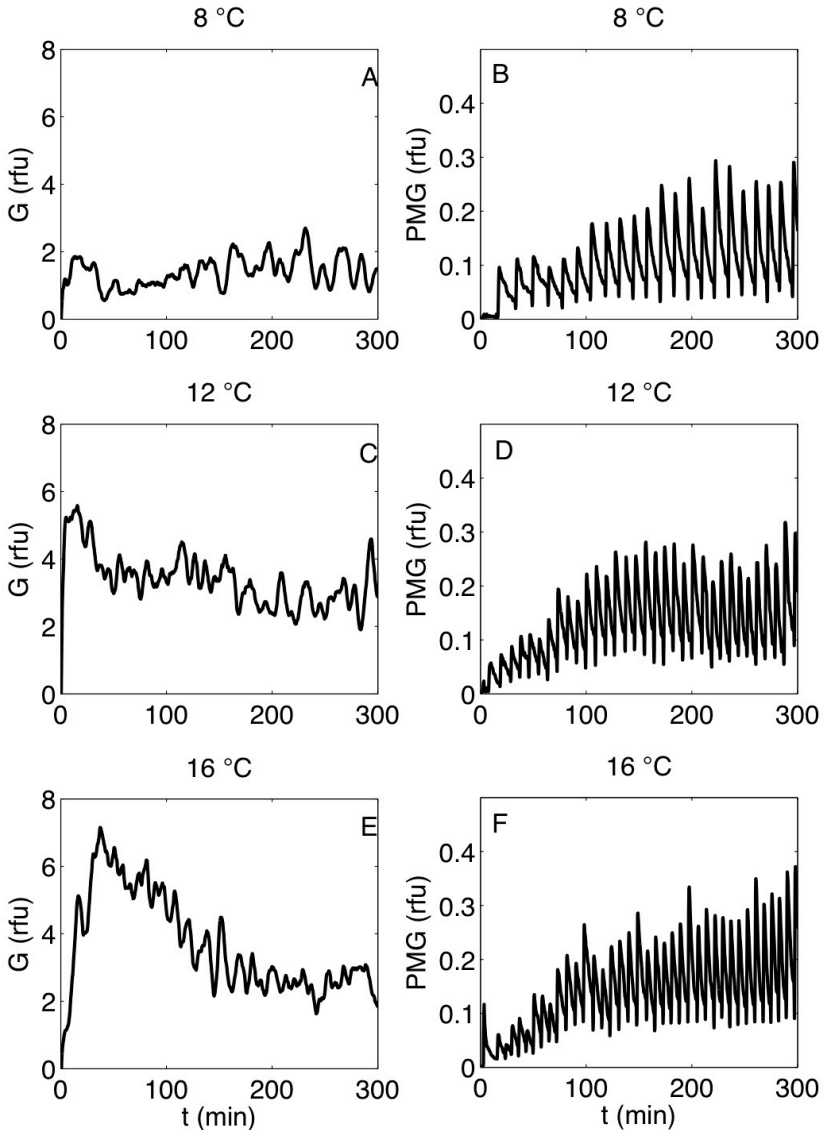

Figure 3-1: *Gut content of a copepod, measured at three different temperatures*. Data in raw fluorescence units (rfu). Left column: total gut content (*G*); panels A, C, E show *G* measured at 8, 12 and 16 °C, respectively. Right column: posterior midgut (*PMG*); panels B, D, F show *PMG* measured at 8, 12 and 16 °C, respectively.

resulting raw gut contents time series, the analyses of which are presented here, are available from the corresponding author upon request. Comparisons of the unprocessed time series collected from the same individual copepod at three different temperatures are shown in Fig. 3-1. The bulk gut contents increased with temperature. An initial peak could often be seen during the first tens of minutes. While total gut contents *G(t)* often showed long-term (hours) trends, the data fluctuated between peaks and troughs of varying amplitude and slope. The *UMG* signal was highly variable both among individuals and within an individual. We could not relate this variability to differences in temperature. The *PMG* signal on the other hand was characterized by a repeating pattern (Figs. 3-1 and 3-2). This pattern consisted of an initial peak when a bolus from UMG was transferred to PMG, a decay period, and a sharp trough marking the evacuation of the bolus as a fecal pellet. The trough rarely reached zero in our data as boluses usually replaced their predecessors in less time than our temporal resolution (15 s). Temperature did affect the amount of material transferred from UMG to PMG, although the effect was not statistically significant. At 8 ºC the overall median amount transferred from the UMG to the PMG was 52.03 ng C; at 12 ºC, the median amount transferred was 82.85 ng C; at 16 ºC, the median amount transferred was 98.18 ng C.

Average gut content and PMG fraction

Average gut content, $\bar{G}(t)$, time series, calculated by averaging the individual signals at each temperature, showed a positive relationship with temperature (Fig 3-3). There was a rapid increase during the first tens of minutes before the curves tended toward an equilibrium level. Oscillations in the average gut signals indicate changes in feeding synchrony among individuals. After >2 h of feeding these oscillations became

apparent, indicating a departure from synchrony among copepods. Comparison of the individual medians between treatments – with the first hour discarded to avoid including post-starvation effects (*cf* Chapter 2) – showed that temperature affected the gut content significantly (p <0.05), but only between the 8 and 16 ºC groups.

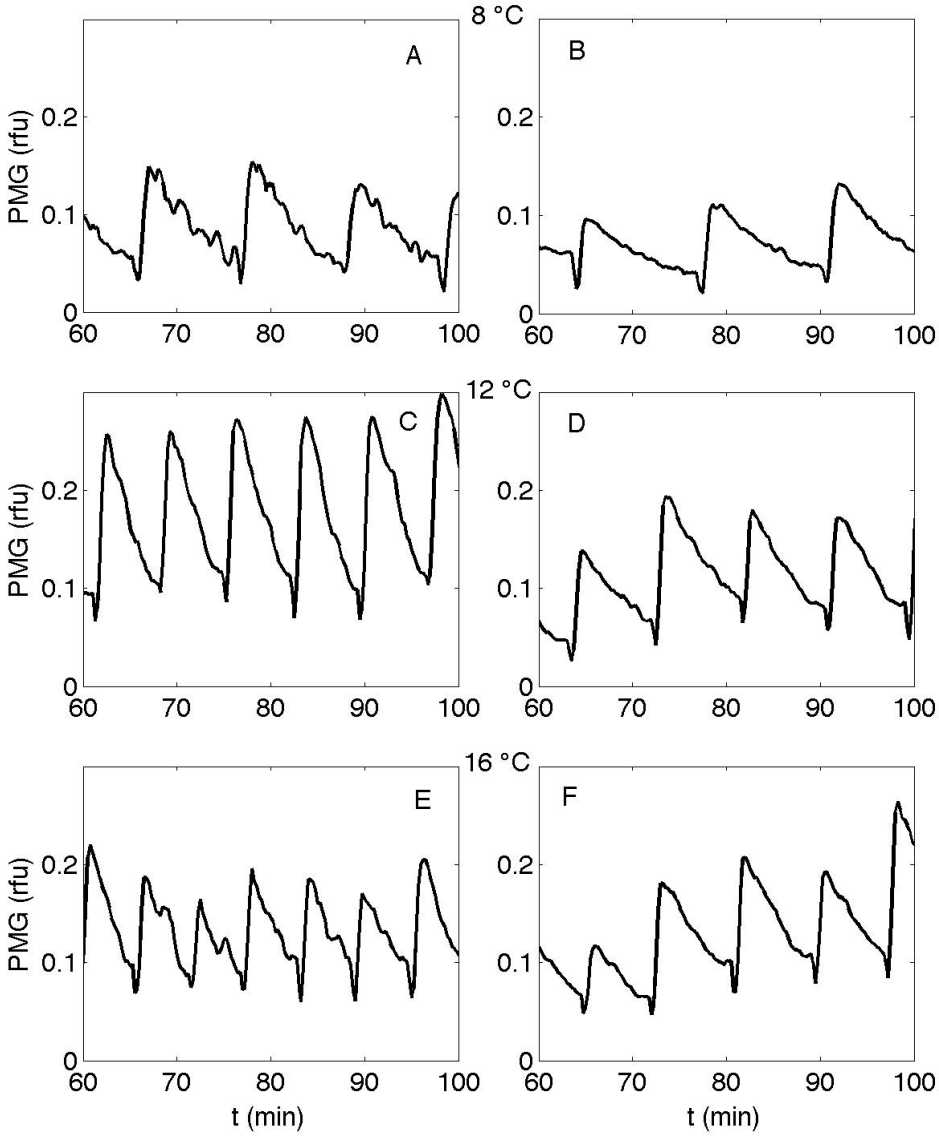

Figure 3-2: *Comparison of PMG oscillations of two copepods observed at three different temperatures.* Data in raw fluorescence units (rfu). Panels A, C and E are from one copepod at 8, 12 and 16 °C, respectively, while panels B, C and F are from another copepod for the same temperatures.

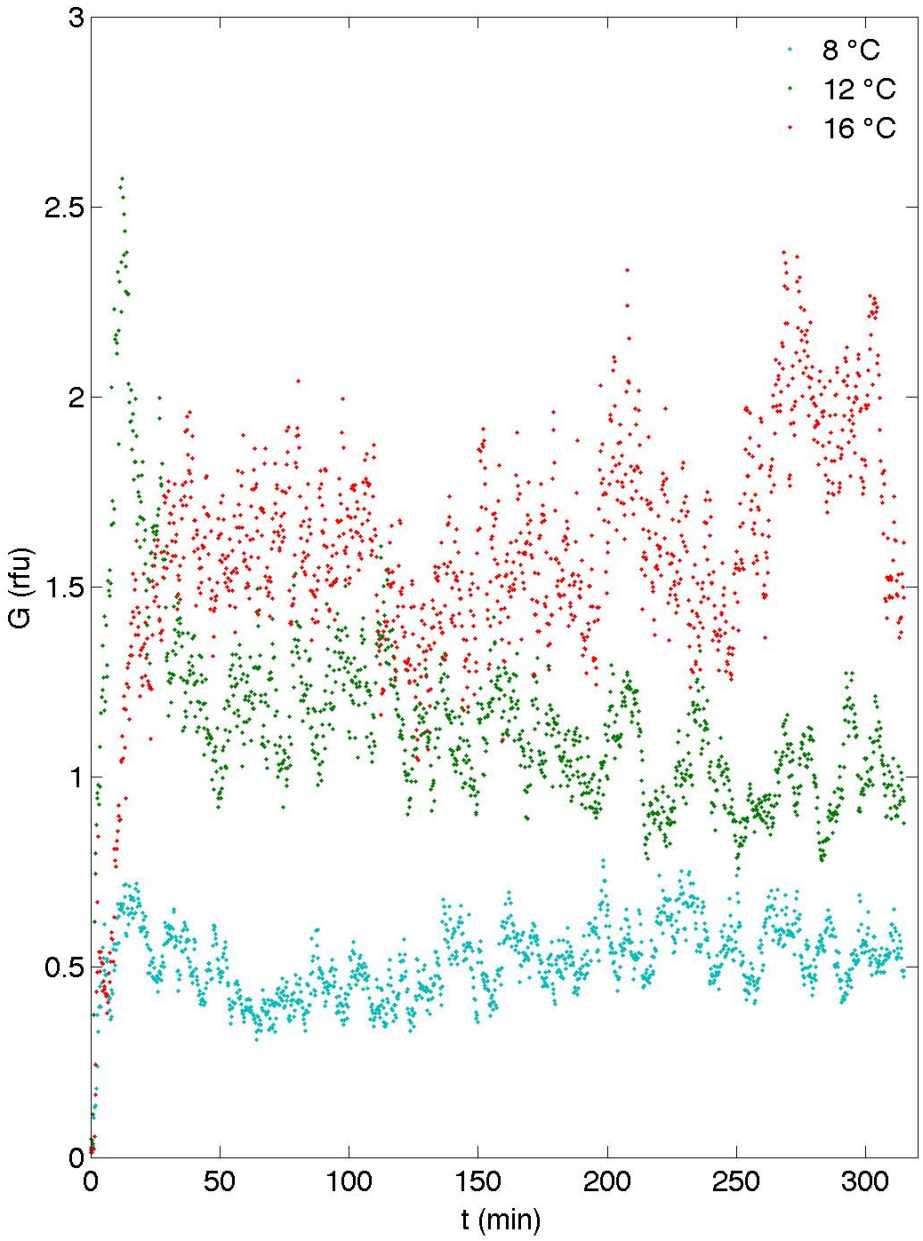

Figure 3-3: *Average gut content G(t) time series*. Data from experiments at three different temperatures; 8, 12, 16 °C, in blue, green red, respectively.

PMG fractions show whether transport through the gut reached a steady state: a steady state is indicated by an approximately constant *PMG* fraction. The *PMG* fraction followed the same temporal pattern at all three temperatures (Fig 3-4). The initial *PMG*

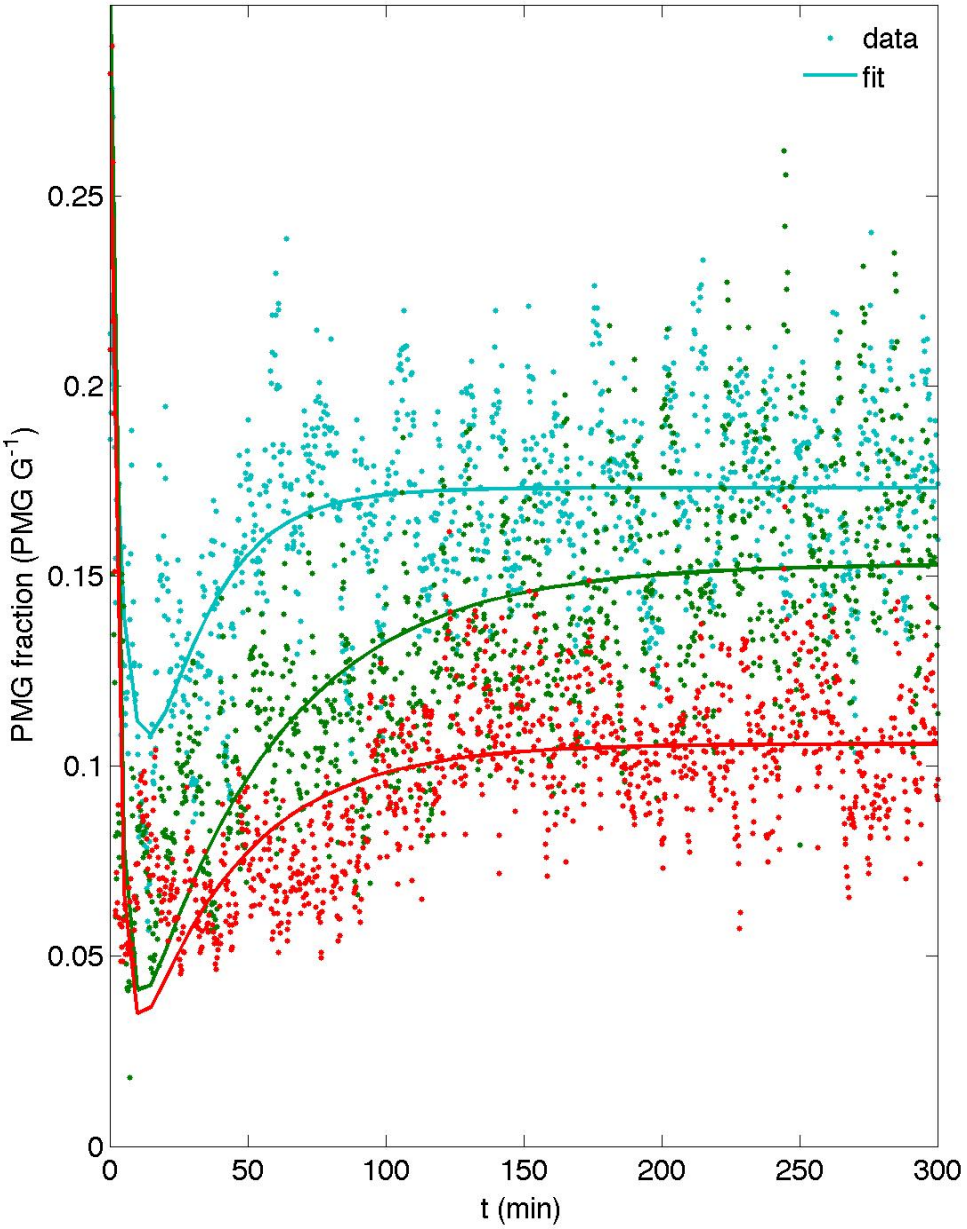

Figure 3-4: *Average PMG fractions*. 8, 12, and 16 °C data in blue, green, red, respectively. PMG fractions calculated as PMG contribution to total gut signal, and are an indicator of food processing capacity. Lines represent bi-phasic model fits.

fraction peaked at ~25% within a few minutes. An examination of image sequences shows that this high fraction occurred because during the first minutes of feeding, food made its way through to the PMG with very little time spent in the UMG. Soon after, an initial defecation occurs, causing the *PMG* fraction to plummet to about ~11 % at 8 ºC,

and ~ 4% at 12 and 16 ºC. This value is not zero because different individuals release pellets at somewhat different rates, so the average *PMG* was never zero. As feeding continued, the average *PMG* fraction then increased, though not as fast as the initial increase, and reached an asymptote close to 17% at 8 ºC, ~15% at 12ºC, and ~ 11% at 16 ºC. The temporal patterns in *PMG* fraction *P(t)* were modeled as a bi-phasic system with two rate-limiting steps:

$$P(t) = P_1 e^{-k_1 t} + P_2(1 - e^{-k_2 t}) \qquad (5)$$

P_1 is the first-phase (fast) *PMG* fraction, k_1 is the rate at which the *PMG* fraction decreases during the first phase, P_2 is the second-phase (slow) *PMG* fraction asymptote, and k_2 is the rate at which P_2 is reached, (Table 3-2). k_1 varies positively with temperature, so that P_2 is reached faster as temperature increases. On the other hand, P_2 varies negatively with temperature, so that the equilibrium *PMG* fraction is lower with higher temperature. None of these relationships is statistically significant, however.

Table 3-2: *PMG* fraction fitting parameters

Temperature (°C)	P_1	k_1	P_2	k_2	r^2
8	0.22	0.15	0.17	0.05	0.33
12	0.31	0.32	0.15	0.02	0.46
16	0.28	0.33	0.11	0.03	0.43

Evacuation rates

The difference in evacuation rate from one temperature to the next varied among copepods. At 8 ºC output rates spanned on average ~0.05 – 0.11 pellet min^{-1}, ~0.09 – 0.15 pellet min^{-1} at 12 ºC, and ~ 0.11 – 0.22 pellet min^{-1} at 16 ºC. In the case of three copepods, there was overlap in their evacuation rates at different temperatures (Fig 3-5A; copepod #2, 8 and 12 ºC; #9, 12 and 16 ºC; #10, 8 and 12 ºC). Comparing individual medians across temperature showed there was a significant difference only between 8 and 16 ºC ($p < 0.001$). For a given temperature, there were often significant differences in evacuation rate among copepods. This inter-individual variability increased with increasing temperature; at 8 ºC 3 out of 9 copepods had significantly different defecation frequencies, 5 at 12ºC, and 6 at 16 ºC (Fig 3-5A), in agreement with the greater interquartile range of overall averages (Fig 3-5B). Overall average evacuation rates were significantly different at different temperatures. At 8 ºC, the median evacuation rate was 0.082 min^{-1}, 0.114 pellet min^{-1} at 12 ºC, and 0.154 pellet min^{-1} at 16 ºC (Fig 3-5B).

Gut throughput time

There was considerable individual variability in *GTT*. Individual average *GTT* varied between 13 - 39 min at 8 ºC, 11 - 54 min at 12 ºC, and 10 - 40 min at 16 ºC. Eight out of 9 copepods showed a lower *GTT* at 16 °C than 8 °C; of these, 5 animals showed significant differences (copepods 1, 2, 5, 9, 11, Fig. 3-6A). Data from the 12 ºC experiments generally overlapped either the 8 or the 16 ºC data, occasionally both. Some individuals exhibited an opposite trend to the expected higher temperature – shorter *GTT* trend (Irigoien 1998). For instance, copepods 3 and 7 had a shorter *GTT* at 8ºC than at 12 ºC, Fig. 3-6A). Only three individuals maintained the expected pattern of decreasing *GTT*

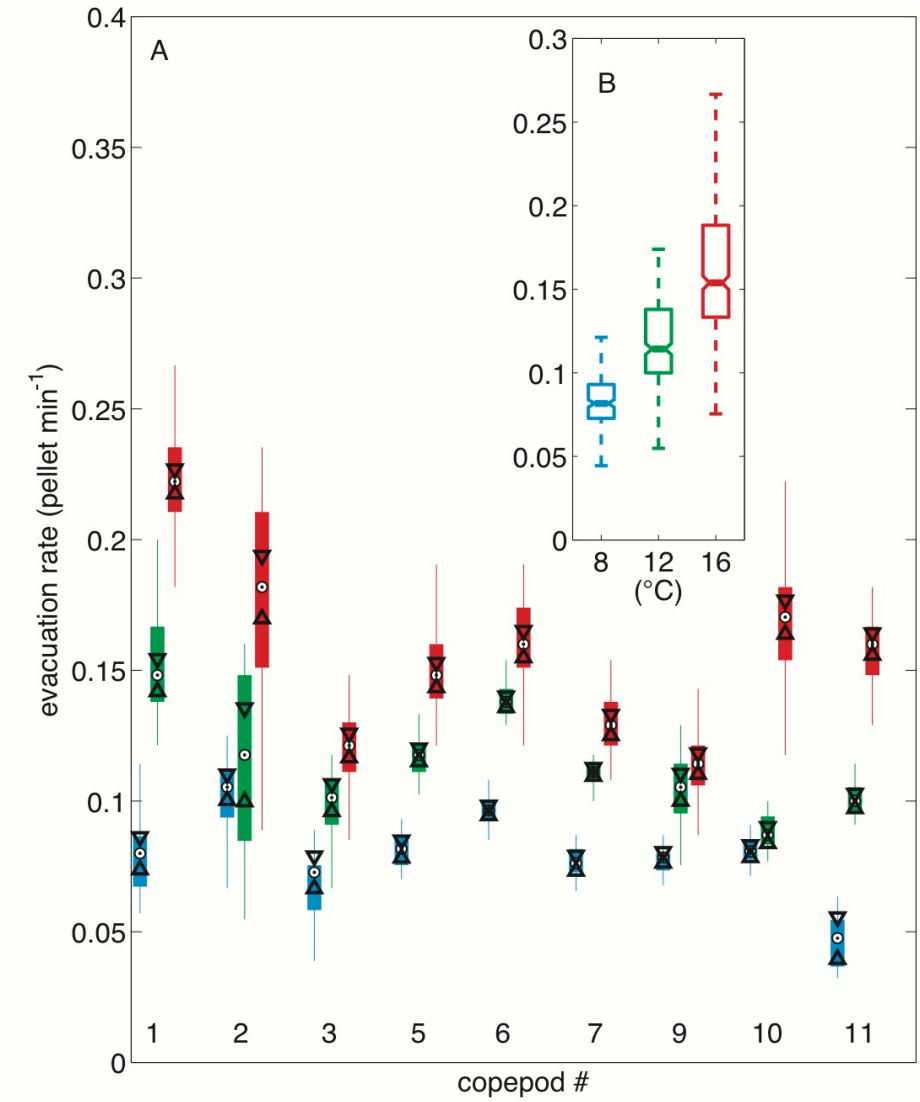

Figure 3-5: *Individual (A) and average (B) evacuation rate box plots.* Box length indicates intra-individual variability, with box bottom and top marking 1st and 3rd quartile, respectively. 95% confidence intervals are black triangles in A and notches in B. Black and white circles in A and central line in B indicate the median.

with increasing temperature (copepods 1, 5, 11) for all three temperatures, and of these only one showed a significant difference among all three temperatures (copepod 5, Fig. 3-6A). There was considerable inter-individual variability. At 8 ºC, 5 out of 9 copepods were significantly different from each other in their *GTT*. At 12 ºC, 4 out of 9 copepods were significantly different from each other in their *GTT*. At 16 ºC, 5 out of 9 copepods

were significantly different from each other in their *GTT*. Temperature affected *GTT*, though this effect was significant only between the 8 and 16 ºC treatments (p <0.005).

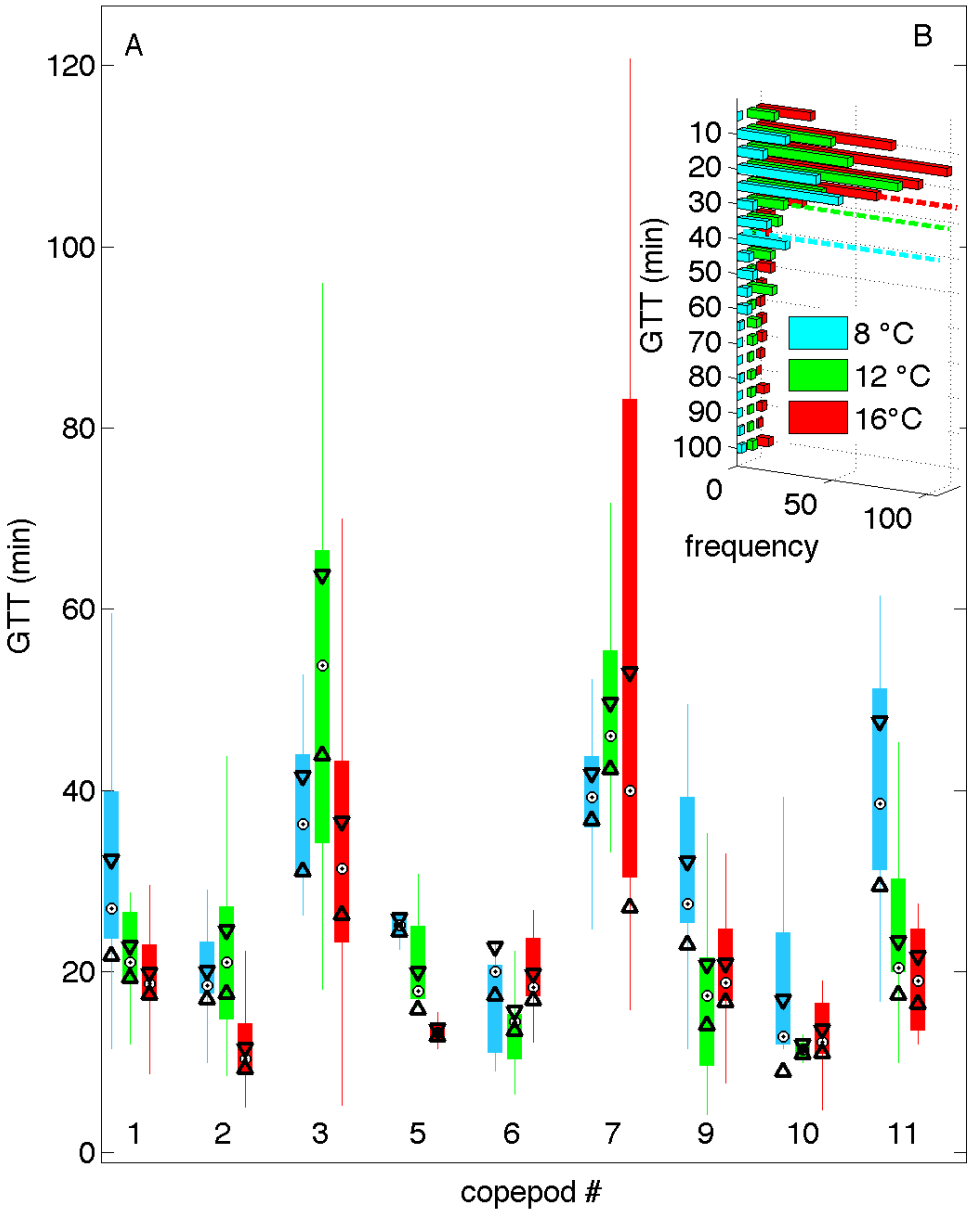

Figure 3-6: *Gut Throughput Time (GTT).* (A): Individual *GTT* box plots. Box length indicates intra-individual variability, with box bottom and top marking 1st and 3rd quartile, respectively. Black triangles are 95% confidence intervals. Whiskers span the interquartile range. (B): *GTT* histogram for all individuals tested. *GTT* modes for 8, 12, and 16 °C are 25, 20 and 18 min, respectively. Dashed lines indicate previously published *GTT* values, estimated from non-feeding copepods; approx. 35, 30, 25 min at 8, 12, and 16 °C, respectively.

Overall GTT modes were 25 min at 8ºC, 20 min at 12 ºC, and 18 min at 16 ºC (Fig. 3-6B). Fitting the data to a line using robust linear least squares with bi-square weights yielded a slope of –095 ºC min $^{-1}$ and a y-intercept of 32.7 min (r^2 = 0.69).

Ingestion rate

Ingestion rates were generally higher at higher temperatures (Fig 3-7A). Individual averages varied between 0.34 – 2.3 μg C h^{-1} at 8 ˚C, 1.1 – 4.5 μg C h^{-1} at 12 ˚C, and 0.85 – 10 μg C h^{-1} at 16 ˚C. The ingestion rate of one copepod relative to the others at one temperature was not a good predictor of its ingestion rate relative to the others at a different temperature. For instance, copepod #1 had the second smallest ingestion rate at 8 ˚C (0.65 μg C h^{-1}) but had the highest ingestion rate at 16 ˚C (10 μg C h^{-1}) (Fig 3-7A). In all but one case (copepod 9, Fig 3-7A) individual ingestion rates were significantly different between 8 and 16 ˚C. This pattern was maintained – although less clearly – when the temperature difference was less (e.g., between 8 and either 12 or 16 ˚C). Individual median ingestion rates were significantly different (p<0.005) at different temperatures. At 8 ˚C the average ingestion rate was 1.17 μg C h^{-1}, 3.14 μg C h^{-1} at 12 ˚C, and 4.87 μg C h^{-1} at 16 ˚C. The data were fit to a line using robust linear least squares with bi-square weights yielding a slope of 0.42 and a y-intercept of -1.92 μg C h^{-1} (r^2 = 0.45).

PMG decay rates

A total of 1083 decay patterns were fit to an exponential decay model and the corresponding decay rates calculated. Among these fits, one had an r^2 ~0, 16 had an r^2 < 0.50, 78 had $0.5 \leq r^2 \leq 0.75$, the remaining 989 fits had $r^2 > 0.75$. Of these fits, those with $r^2 \geq 0.50$ were analyzed. *PMG* decay rates increased with increasing temperature (Fig 3-

8). These trends were consistent for all individuals when comparing data from 8 and 16 ˚C; the relationship between these data and data from the 12 ˚C experiments was more variable. Rates varied between 0.08 – 0.18 min^{-1} at 8 ˚C, 0.09 – 0.21 min^{-1} at 12 ˚C, and 0.11 – 0.40 min^{-1} at 16 ˚C (Fig 3-8A). Average decay rates were significantly different at

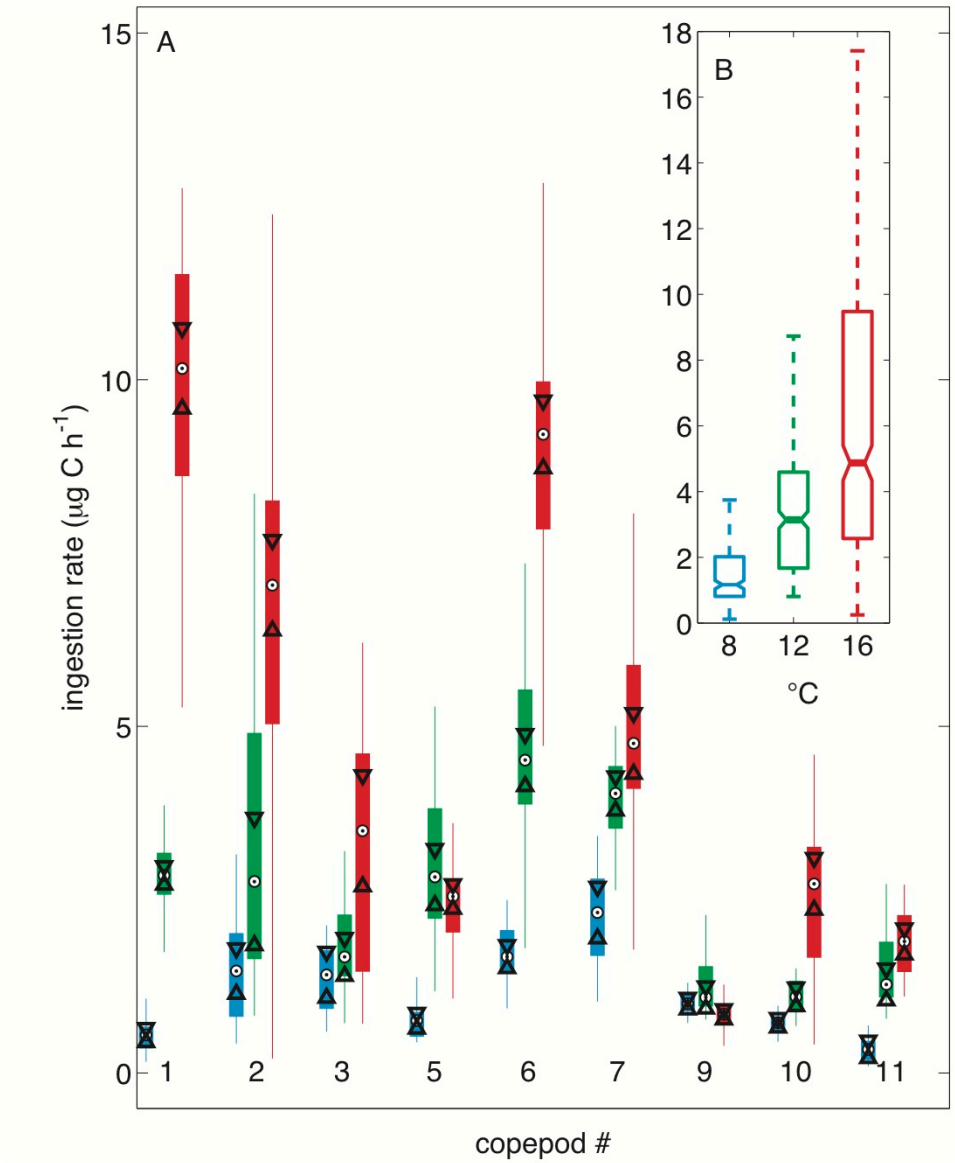

Figure 3-7: *Ingestion rates.* A: individual rates; B: average rates. Box length indicates intra-individual variability, with box bottom and top marking 1st and 3rd quartile, respectively. 95% confidence intervals are black triangles in A and notches in B. Black and white circles in A, and central line in B, indicate the median.

different temperatures (p <0.005). At 8 ˚C the overall median decay rate was 0.116 min^{-1}. At 12 ˚C the median decay rate was 0.160 min^{-1}. At 16 ˚C the median decay rate was 0.194 min^{-1} (Fig 3-8B).). A significant correlation was found between ingestion rate and PMG decay rate (Spearman's rho, p<0.01, Fig. 3-9).

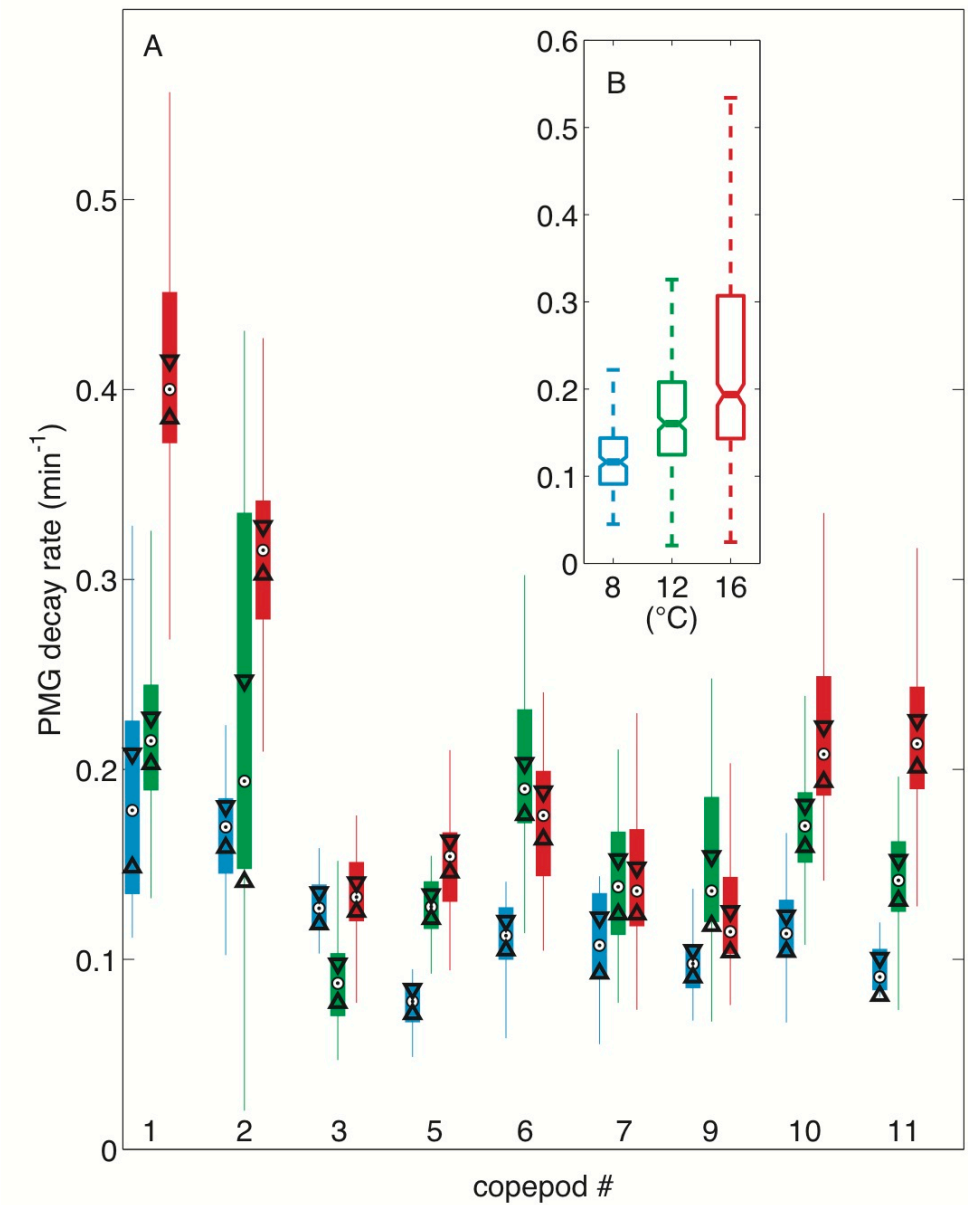

Figure 3-8: *PMG decay rates.* A: individual rates; B: average rates. Box length indicates intra-individual variability, with box bottom and top marking 1st and 3rd quartile, respectively. 95% confidence intervals are black triangles in A and notches in B. Black and white circles in A, and central line in B, indicate the median.

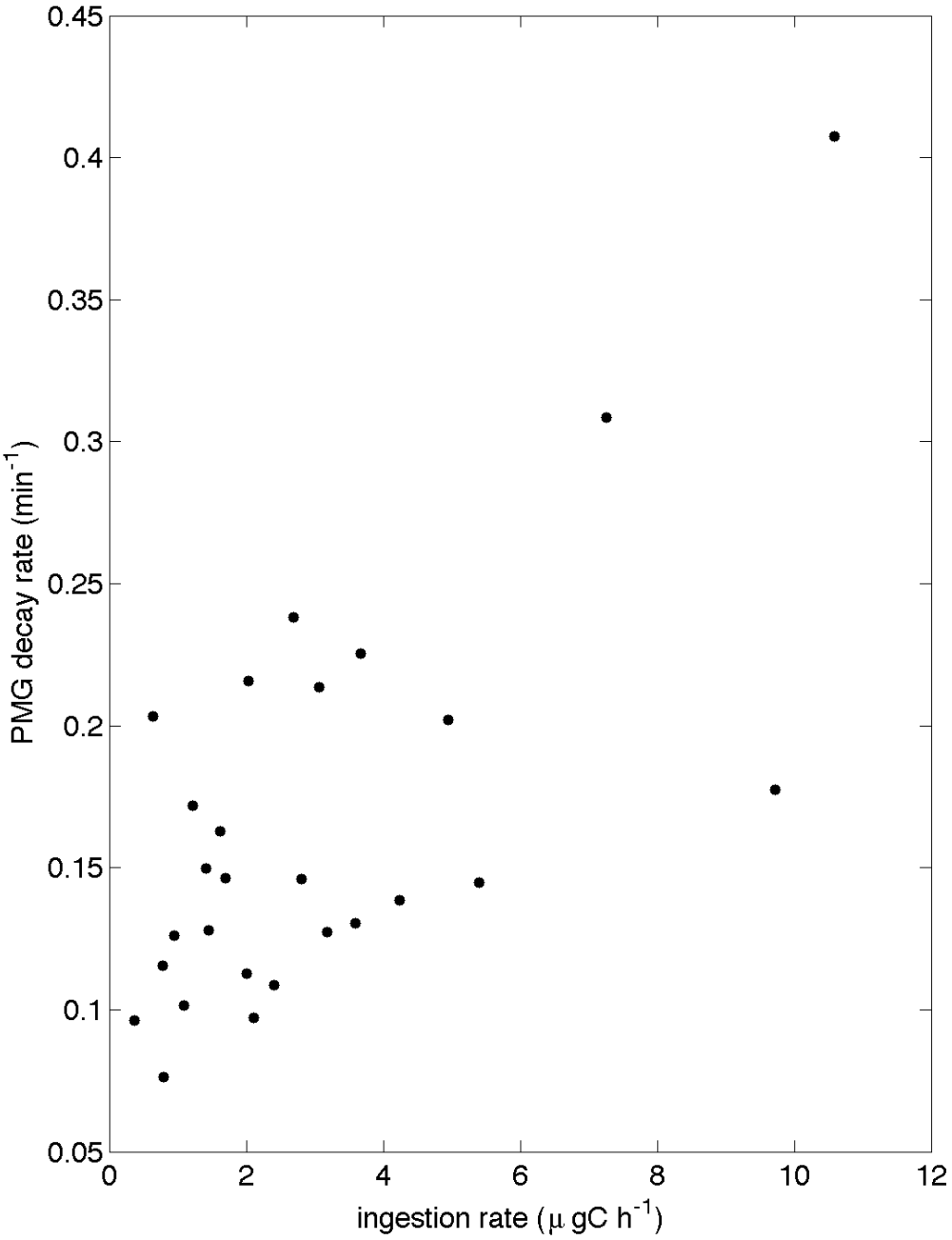

Figure 3-9: *PMG decay rates vs. ingestion rates.* Data are individual averages; all treatments (8, 12, 16 ˚C) included.

Gut dynamics temperature coefficients (Q_{10})

To summarize the above analyses we calculated individual and average Q_{10} coefficients for evacuation gut clearance (GTT^{-1}), ingestion, and *PMG* decay rates

between 8 and 16 ˚C (Table 3-3). The Q_{10} for individual evacuation rate ranged between 1.6 and 4.5 with a group average of 2.2. Individual gut clearance rate (GTT^{-1}) Q_{10} ranged between 0.8 and 2.6 with a group average of 1.5. The Q_{10} for ingestion rate ranged between 0.8 and 39 (8.6 when 39 was considered an outlier), and the group average was 6.0 (5.2 when the outlier was omitted). *PMG* decay Q_{10} ranged between 1.1 and 2.9; the group average was 1.9. A comparison between Q_{10} calculated for the different processes showed differences were significant between GTT^{-1} and ingestion, and between *PMG* decay and ingestion ($p < 0.01$); all other pair-wise comparisons showed no significant differences. We also tested for a possible size dependence of the data using prosome length (data displayed in Table 3-3); no significant effect was detected.

Table 3-3: *Individual and mean Q_{10}* for evacuation, gut clearance (GTT^{-1}), ingestion, and *PMG* decay rates, between 8 and 16 ˚C. In the case of ingestion, the parenthesized group average was calculated by omitting the outlier (copepod 1). Prosome length (*PL*) is also included.

Q_{10}		Evacuation	GTT^{-1}	Ingestion	*PMG* Decay
Copepod #	PL (mm)				
1	2.42	3.6	1.6	**39**	2.7
2	2.40	2.0	2.3	7.1	2.2
3	**2.29**	2.0	1.5	3.1	**1.1**
5	**2.74**	2.1	**2.6**	4.6	2.3
6	2.44	1.9	**0.8**	8.4	1.7
7	2.64	1.9	1.0	2.5	1.3
9	2.35	**1.6**	1.7	**0.8**	1.2
10	2.56	2.5	1.5	5.3	2.1
11	2.67	**4.5**	2.2	**8.6**	**2.9**
Group Average		2.2	1.5	6.0 (5.2)	1.9

Discussion

One of the principal motivations for conducting these experiments was to obtain data on gut dynamics *during* feeding. Through the use of the gut clearance method, a large body of data on copepod feeding has been collected on copepods that were in fact not feeding. Copepods that are not feeding have slower gut throughput times than when they are actively ingesting (e.g. Baars and Oosterhuis 1984). As a result, Kiørboe et al. (1985) estimated that the gut clearance method could underestimate grazing by up to 50 %. It was not clear, however, whether this discrepancy would change with temperature. According to the relationship calculated by Dam and Peterson (1988) – reported to work well for *C. pacificus* pre-fed with *T. weissflogii* (Landry, 1994) – the expected *GTT* at 8, 12, and 16 °C would be ~38, 30, and 25 min, respectively. These are substantially higher than our results (25, 20, 18 min for 8, 12, and 16 °C, respectively), suggesting that the use of the gut clearance method does indeed underestimate ingestion rates. This discrepancy between *GTT* in feeding and non-feeding copepods decreased with temperature, however.

The fact that *GTT* had the lowest Q_{10} can perhaps be explained by a high variation in GTT within each temperature. For instance GTT would be longer in cases of reduced feeding, no matter the temperature; and vice versa during bouts of intensive feeding. Temperature had a measurable effect however. Under colder conditions, the fraction of gut content transferred to the *PMG* was depressed suggesting that digestion slowed down as well. In addition, colder temperature resulted in the decrease of evacuation rates, which imply a longer residence time of food boluses in *PMG*, where the products of digestive hydrolysis are absorbed. Finally, the above also in agreement with the decrease

in the *PMG* decay rates that, if PMG decay is the result of digestive action (*cf.* Chapter 2), show a less intense digestive enzyme action under colder conditions.

Because several hours passed between subsequent experiments where the same individual was exposed to different temperature, it is not clear whether the observed temperature-driven changes would occur over the relatively short time scales of change in a field situation – for example when a copepod crosses a strong thermocline on its way to forage after spending a day at colder depths.

Q_{10} coefficients have been calculated for *GTT* of various species of copepods. Dam and Peterson (1988) report a Q_{10} of 2.21; Kiørboe et al. (1982), 3.3; Christoffersen and Jespersen (1986), 4.01. and Dagg and Wyman (1983), 5.4. In contrast the *GTT* Q_{10} of 1.5 calculated in this study appears rather modest. However, the works cited above included pre-acclimation periods that either spanned several days, or were seasonal (i.e. copepods were incubated at the temperature of the waters from which they were collected). The present study on the other hand included an acclimation period of less than 24 hrs. Consequently, the data presented here are closer to what a copepod might experience during its daily foraging ambit. The lower Q_{10} indicates a lower sensitivity to temperature effects suggesting that the copepod had not fully adapted to the different temperature regime. Thus, during sufficiently extensive vertical displacement a potential thermocline crossing may not cause a large difference in *GTT* if the copepod continues to feed. On the other hand, this difference could become substantial if such a crossing comes with an interruption (or initiation) of feeding, depending on the food and temperature structure. Consider for illustrative purposes a copepod that feeds in a shallow layer at 12 °C, giving a *GTT* of 20 min; if this copepod then migrates to a lower layer of 8

°C where food concentrations are low enough that feeding is interrupted, its *GTT* would lengthen to 38 min. The corresponding "Q_{10}" would be ~5 instead of 1.5.

The different Q_{10} values of the different gut processes indicate that temperature affected the different variables of gut dynamics differently. Harrison and Fewell (1995) found significantly different Q_{10} coefficients for different variables related to feeding and digestion in grasshoppers. Specifically, these authors found that for variables closer to ingestion – chewing and crop-filling – rates were lower (Q_{10} ~2) than the longer-term variables related to digestion (gut throughput and defecation, Q_{10} ~5). This is the first time such a discrepancy has been recorded for copepods. This means that – contrary to what had been previously assumed – a change in *GTT* with temperature does not imply a similar change in ingestion. In fact, ingestion was the most temperature-sensitive variable. Among variables that describe feeding, ingestion was also the most directly linked to short-term (seconds to minutes) behavior. All other variables described the longer-term (several tens of minutes) digestive process. Thus, in this case, the more removed a variable was from the immediate effects of behavior, the less it was affected by temperature; conversely, the more a variable was likely to be directly affected by behavior (ingestion), the more it was affected by temperature. This could be an adaptation to the patchy environment in which copepods forage. In such an overall dilute but vertically structured environment, a change in temperature may signal a significant increase in food availability, which the copepod should rapidly take advantage of. Thus when taking temperature into account, copepod feeding should be not be approached as a single-action phenomenon, but rather as an interaction of mechanisms – ingestion, digestion, and evacuations – each with its own particular response to temperature

changes. These mechanisms are therefore not necessarily in equilibrium over short time scales (minutes), and *GTT*, on its own, may not be a sufficient descriptor of the effects of temperature on grazing.

Chapter 3, in full, is currently being prepared for submission for publication of the material. Karaköylü, Erdem; Franks, Peter J. S. The dissertation author was the primary investigator and author of this material.

References

Arnaud, J. Brunet, M., and Mazza, J. 1978. Studies on the midgut of *Centropages typicus* (Copepod, Calanoid). I. Structural and ultrastructural data. Cell Tiss. Res. 187:333-353.

Båmstedt, U., Eilertsen, H.C., Tande, K.S., Slagstad, B. and Skjoldal, H.R. 1991. Copepod grazing and its potential impact on the phytoplankton development in the Barents Sea. Polar Research 10:339-353.

Dagg, M.J. and Wyman, K.D. 1983. Natural ingestion rates of the copepods *Neocalanus plumchrus* and *N. cristatus* calculated from gut contents. Mar. Ecol. Progr. Ser. 13: 37-46.

Dam, H.G. and Peterson, W.T. 1988. The effect of temperature on the gut clearance rate constant of planktonic copepods. J. Exp. Mar. Biol. Ecol. 123: 1-14.

Doyle, S.R. and Momo, F.R. 2009. Effects of body weight and temperature on the metabolic rate of Hyalella *curvispina* Shoemaker, 1942 (Amphipoda). Crustaceana 82(11):1423-1439.

Fernandez, F. 1978. Metabolismo y alimentación en copépodos planctónicos del Mediterráneo: Respuesta a la temperatura. Inv. Pesq. 42(1): 97-139.

Gauld, D.T. 1957. A peritrophic membrane in calanoid copepods. Nature 179 (4554): 325-326.

Harrison, J.F. and Fewell, J.H. 1995. Thermal effects on feeding behavior and net energy intake in a grasshopper experiencing large diurnal fluctuations in body temperature. Physiol. Zool. 68: 453-473.

Head, E.J.H. and Harris, L.R. 1996. Chlorophyll destruction by *Calanus* spp. grazing on phytoplankton: kinetics, effects of ingestion rate and feeding history, and a mechanistic interpretation. Mar. Ecol. Progr. Ser. (135): 223-235.

Irigoien, X. 1998. Gut clearance rate constant, temperature and initial gut contents; a review. J. Plankton Res. 20(5): 997-1003.

Karaköylü, E.M, Franks, P.J.S., Tanaka, Y., Roberts, P.L.D., Jaffe, J.S. 2009. Copepod feeding quantified by planar laser imaging of gut fluorescence. Limnol. Oceanogr. Methods 7: 33-41.

Kiørboe, T. Møhlenberg, F. and Riisgård. 1985. In situ feeding rates of planktonic copepods: a comparison of four methods. J. Exp. Mar. Biol. Ecol. 88: 67-81.

Landry, M.R., Lorenzen, C.J. and Peterson, W. 1994. Mesozooplankton grazing in the Southern California Bight. II. Grazing impact and particulate flux. Mar. Ecol. Progr. Ser. 115: 73-85.

Mackas, D. and Bohrer, R. 1976. Fluorescence analysis of zooplankton gut contents and an investigation of diel feeding patterns. J. Exp. Mar. Biol. Ecol. 25: 77-85

Mitra, A. and Flynn, K.J. 2007. Importance of interactions between food quality, quantity, and gut transit time on consumer feeding, growth, and trophic dynamics. Am. Nat. 169(5): 632-646.

Morris, R.W. 1962. Body size and temperature sensitivity in the cichlid fish *Aequidens portalegrensis* (Hensel). Am. Nat. 96(886): 35-50.

Nemoto, T., 1968. Chlorophyll pigments in the stomach of euphausiids. J. Oceanogr. Soc. Japan 24: 253-260.

Nott, J.A., Corner, E.D.S., Mavin, L.J., O'Hara, S.C.M. 1985. Cyclical contributions of the digestive epithelium to faecal pellet formation by the copepod *Calanus helgolandicus*. Mar. Biol. 89: 271-279.

Paffenhöfer, G.-A., Bundy, M.H., Lewis, K.D., Metz, C. 1995. Rates of ingestion and their variability between individual calanoid copepods: direct observations. J. Plankton Res. 17(7): 1573-1585.

Paffenhöfer, G.-A. 1994. Variability due to feeding activity of individual copepods. J. Plankton Res. 16: 617-626.

Penry, D.L. and Frost, B.W. 1990. Re-evaluation of the gut-fullness (gut fluorescence) method for inferring ingestion rates of suspension-feeding copepods. Limnol. Oceanogr. 35(5): 1207-1214.

Pierson, J.J., Frost, B.W., Thoreson, D., Leising, A.W., Postel, J.R., Nuwer, M. 2009. Trapping migrating zooplankton. Limnol. Oceanogr. Methods 7: 334-346.

Rao, K.P. and Bullock, T.H. 1954. Q_{10} as a function of size and habitat temperature in poikilotherms. Am. Nat. 88(838): 33-44.

Rodriguez, V., and Durbin, E.G. 1992. Evaluation of synchrony of feeding behaviour in individual *Acartia hudsonica* (Copepoda, Calanoida). Mar. Ecol. Progr. Ser. 87: 7-13.

Rosenberg, G.G. 1980. Filmed observations of filter feeding in the marine planktonic copepod *Acartia clausii*. Limnol. Oceanogr. 25:738-742.

Tseitlin, V.B. 1994. The modeling of experiments on measuring copepods gut passage time. Okeanologiya 34(1): 73-78.

Tseng, L.-C., Dahms, H.-U. , Chen, Q.-C., Hwang, J.-S. 2009. Copepod feeding study in the upper layer of the tropical South China Sea. Helgol. Mar. Res. 63: 327-337.

Vidal, J. 1980a. Physio-ecology of zooplankton. 1. Effects of phytoplankton concentration, temperature, body size on the growth rate of *Calanus pacificus* and *Pseudocalanus* sp. Mar. Biol. 56(2): 111-134.

Vidal, J. 1980b. Physio-ecology of zooplankton. 2. Effects of phytoplankton concentration, temperature, and body size on the development and molting rates of *Calanus pacificus* and *Pseudocalanus* sp. Mar. Biol. 56(2): 135-146.

Vidal, J. 1980c. Physio-ecology of zooplankton. 3. Effects of phytoplankton concentration, temperature, and body size on the metabolic rate of *Calanus pacificus*. Mar. Biol. 56(3): 195-202.

Vidal, J. 1980d. Physio-ecology of zooplankton. 4. Effects of phytoplankton concentration, temperature, and body size on the net production efficiency of *Calanus pacificus.* Mar. Biol. 56(3): 203-211.

Villareal, H. and Ocampo, L. 1993. Effect of size and temperature on the oxygen consumption of the brown shrimp *Penaeus californienisi* (Holmes, 1900). Comp. Biochem. Physiol. 106A(1): 97-101.

Wang, R. and Conover, R.J. 1986. Dynamics of gut pigment in the copepod *Temora longicornis* and the determination of in situ grazing rates. Limnol. Oceanogr. 31(4): 867-877.

CHAPTER 4

Foraging behavior of *Calanus pacificus* (Copepoda: Calanoida): evaluating the foraging sorties hypothesis in Dabob Bay, Puget Sound, WA (U. S. A.)

Abstract

Past field studies of the vertical distribution of copepods showed that copepods with pigments in their gut were not necessarily found in layers of high food concentration. Two hypotheses were proposed to reconcile these seemingly conflicting observations. The stationary feeding hypothesis, states that copepods have acquired their gut contents in situ, in the layer in which they were captured. The foraging sorties hypothesis predicts that copepods will conduct brief grazing forays into a shallow food-rich, predator-rich layer, feed to saturation, and sink away to relative safety as they digest. To evaluate both hypotheses, I developed an individual-based model where copepods do not have a specific foraging behavior built-in, and where the internal state of individuals, represented by hunger, gut content, and food processing capacity, interacts with their external environment, parameterized by food and temperature; food processing constraints were based on gut dynamics calculated in the previous chapters. Simulation results showed that in fact while both mechanisms, foraging sorties and *stationary* feeding, could be occurring, the vertically integrated shallow layer chlorophyll concentration is the most important factor in determining the dominant foraging strategy. This emergent property of the IBM implies that short-term feeding behavior patterns may be broadly predictable from as little as knowing the vertical hydrographic properties of the system studied.

I use this IBM to facilitate the interpretation of data collected during the deployment of the MultI-Spectral Copepod Imaging System (MISCIS) in Dabob Bay (WA). In this system, one channel was used to identify objects that occur in the imaging

volume; the other channel was used to determine whether the particles imaged had any associated fluorescence signature. Using this system, copepods were identified among the imaged particles, and their recent feeding activity was assessed from their gut fluorescence signature. Results show that copepod gut fullness as a function of depth is tightly correlated to the chlorophyll maximum, suggesting that at least under conditions encountered in Dabob Bay foraging sorties did occur, and was at times the likely dominant mechanism.

Introduction

Diel vertical migration (DVM) is a well-known phenomenon that affects the vertical distribution of zooplankton on a diel scale. A large body of literature describes the general patterns of DVM, which, in combination with environmental data contributes significantly to our understanding of proximal *external* cues that control the vertical distribution of zooplankton. However, the effects of concurrent individual behavior and individual conditions (i.e. *internal* cues) on vertical distribution are rarely studied. The main obstacle is the size of the subjects, which makes tracking them in the field currently impossible on time and space scales relevant to individual foraging behavior. The paucity of observations on such scales could hinder our understanding of the dynamics that shape the systems we study. For example, the co-location between predator and prey does not necessarily imply feeding; similarly, the lack of co-location between predator and prey does not necessarily imply lack of feeding. Both situations could result in erroneous estimates of feeding rates.

There are a number of field observations that could be explained by individuals undertaking significant sub-diel vertical movements, aimed at maximizing food intake while minimizing predation pressure or the effect of some other limiting factor such as the anoxic conditions of food-rich layers in certain systems (e.g. De Robertis et al. 2001). Relatively brief incursions by zooplankton into layers different than those in which they reside on longer time scales – and where they are more likely to be captured during sampling – could imply a fundamentally different view of trophic interactions and of the contribution of individuals to biogeochemical cycling, than the one offered by the current paradigm.

Dagg et al. (1997) reported the presence of *Calanus pacificus* with similar gut contents in two adjacent layers of significantly different phytoplankton concentrations. Dagg et al. attributed this to feeding in situ to the layer in which animals were captured, referred to here as stationary feeding (*SF*, Fig. 4-1A). However, in the laboratory, *C. pacificus* followed 1-3 hrs bouts of feeding with refractory periods during which their inactivity caused them to sink to the bottom of their experimental container (Mackas and Burns 1986). In the field, some evidence exists that *C. pacificus* may conduct forays into the shallow, food-rich layer, subsequently sinking or swimming back to the underlying food-poor intermediate layer (Pierson et al. 2009), a strategy here referred to as foraging sorties (*FS*, Fig 4-1B). Because *C. pacificus* is not as transparent when replete as it is during starvation, and because its feeding/swimming currents could create a hydrodynamic signal noticeable to predators (e.g. Pearre 1973, Zaret 1972) FS is a reasonable strategy to minimize predation risks.

Brief feeding incursions have been previously described in zooplankton. For example, de Robertis et al. (2001) reported that the amphipod *Orchomene obtusus* conducts incursions into the food-rich, predator-poor anoxic benthos layer to feed, subsequently returning to the oxygen-rich water column. More recently Tarling and Johnson (2006) observed stationary that the Antarctic krill could alternate its upward swimming behavior with a "parachuting" sinking mode. They showed in the laboratory that the latter was significantly associated with a half-full to full gut content. The above is in accordance with the hunger/satiation hypothesis (reviewed by Pearre, 2003), which in simplified terms states that hunger is the most likely proximal cue for individuals at depth to swim into and forage in a food-rich layer; conversely satiation is the most likely

proximal cue for individuals at depth to swim away from the food-rich layer in which they were foraging.

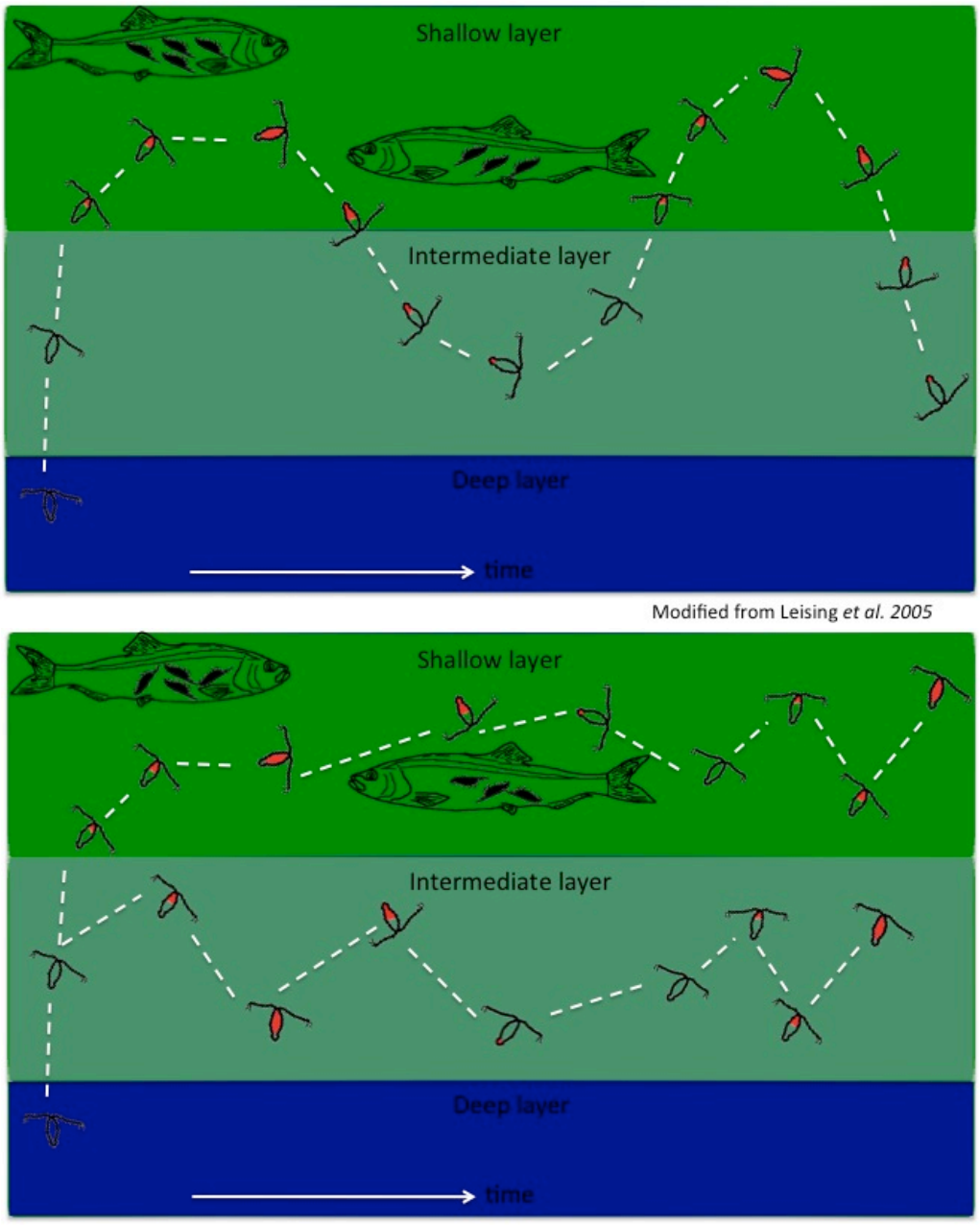

Figure 4-1: *Alternative foraging strategies* – A: *Stationary feeding (SF),* where copepods migrate to any layers where they can forage and reside in that layer without further significant vertical displacement. Copepod gut content is shown in red. B: *Foraging sorties (FS),* where copepods migrate to the shallow food-rich predator-rich layer, feed to saturation, and sink while they digest. Once their gut is cleared past a threshold, they return to the shallow layer and repeat this cycle.

In this chapter, I evaluate the foraging sorties (FS) and the stationary feeding (SF) hypotheses. For this purpose, I developed an individual-based model (IBM) that includes a gut module, formulated according to the gut dynamics data acquired in the laboratory (cf. earlier chapters), to reasonably constrain the individuals' foraging ambit. Forcing the model with a series of vertical chlorophyll (chl) and temperature profiles – including some acquired during a field study in Dabob Bay, WA, I examine the foraging behaviors that result from this interaction between environment and physiology, i.e. between proximal *external* and *internal* cues. I then use this model to interpret data collected in Dabob Bay, WA. These data were collected using a profiling MultI-Spectral Copepod Imaging System (hereafter referred to as MISCIS) that allows the identification of copepods and the assessment of their gut content.

Materials and Methods

Fieldwork

The approach I used to evaluate the foraging sorties hypothesis required the determination of the location of copepods in the water column, and at the same time, estimate their gut content. For this purpose, the FIDO-ϕ (Franks and Jaffe 2008) was reconfigured. Two highly sensitive Cooke CCD cameras were used for this project. One camera was equipped with a 532nm filter to image light scatter. The other camera was equipped with a 680 nm filter to image a volume illuminated by a 3W laser, also the same used in previous chapters. This laser was fanned at an angle of 15°, and projected straight down between two cameras resulting in an imaging volume of 9.8cm x 7.4 cm x 0.6 cm,

37.3 cm from the laser porthole, and 30 cm from either cameras. This resulted in a resolution of 71.4μm by 74.0μm pixel^{-1}. Because of the small imaging volume (43.5 cm^3), a 1m opening 500 μm net was attached under the main frame, with the tail end opening onto the imaging volume. This was successful in funneling and concentrating copepods that were subsequently imaged. At midpoint during the cruise in Dabob Bay, the net was lost and was replaced with a funnel manufactured made of canvas, with a 0.5m opening. While this meant that sampling efficiency was reduced, this replacement still allowed for the imaging of a sufficient number of copepods that the project could be continued.

In addition to the imaging system, there was a Seabird-19 CTD, equipped with a Wet Labs fluorometer, mounted onto the frame.

The fieldwork took place during the week of May 5-12, 2007, in Dabob Bay, Puget Sound (WA), from the R/V Thomas G. Thompson. The sampling protocol consisted in 3 nightly deployments; at dusk, midnight, and dawn. Each deployment consisted of multiple profiles spanning around 90 minutes, which approximated the available battery lifetime. During a deployment, the MISCIS was tethered to a winch. The winch was operated manually, with the controller determining the extent of the cast, as well as the speed. Two types of deployment protocols were followed; one that consisted in few (4 -5) but deep (~60m) casts; the other consisted in many (10-20) but shallow (~30m) casts. The operator attempted to maintain an even and slow descent rate, approximating ~10 cm s^{-1}, in an attempt to minimize the number of smeared images. During the descent, a pair of images (light scatter and fluorescence) was collected simultaneously every second on the downcast. Images were retrieved from the MISCIS at

the end of each deployment. In addition to the work conducted from the R/V Thomas G. Thompson, Prof. B.W. Frost and members of his laboratory at the University of Washington were concurrently deploying directional traps and taking vertical tows from the R/V Barnes, with the same goal of evaluating the foraging sorties hypothesis.

Image analysis

Image analysis was performed using Matlab (The Mathworks) and its Image Processing Toolbox (IPT). The first step was to prepare images for analysis. The original images were 1040 x 1376 pixels. From these, a central square of 900 x 900 was used for analysis. A threshold was applied to the images so that the excess scatter signal that caused objects to lose their original shape could be eliminated. A similar threshold was applied to the fluorescence images to eliminate background noise. The same thresholds were found to be applicable to all deployments.

Image streaking was relatively common and presented the particular challenge that the smeared image of a particle looks very much like a copepod. This problem was dealt in a similar fashion as in Franks and Jaffe (2008, 2001): each image was sub-sampled, and a 2D Fast Fourier Transform (FFT) was applied; the resulting geometric shape of the 2D FFT contours varied from circular (non-streaked) to elliptic (streaked). The eccentricity of the contours was quantified using IPT. An eccentricity criterion of 0.86 was used to categorize images as streaked and non-streaked. Only non-streaked images were retained for further analysis.

Corresponding fluorescence and light-scatter images were co-registered using IPT. Sample images from a deployment were used to create control points from which a spatial transformation matrix was created. From the same test deployment a different

batch of images were used to test this spatial transformation. A piecewise linear transformation was found to work best as there appeared to be local differences between the fluorescence and light-scatter images, probably on account of the filters used. The final spatial transformation matrix thus created appeared to work well with images from other deployments. Images from this test deployment were not used beyond this point.

Copepod identification and assessment of gut fullness

To identify *Calanus* in light-scatter images, I used some morphological constraints. These were length, length-to-width ratio, and asymmetry along the longitudinal axis. The targets were required to range between 1.5 and 3 mm in length, to account for possible bending of the urosome; expected length to-width-ratio was ~2.5, close to Kiørboe's proposed average aspect ratio for pelagic copepods of 0.38 (Kiørboe, submitted); the asymmetry constraint was in accordance with the fact that the cephalosome represents the wider part of the body. The above meant that only copepods that were imaged with their longitudinal axis parallel to the long sides (9.8 cm x 7.4 cm) of the imaging volume could be identified. This is because given the resolution used, the differentiation of copepods, imaged with their radial axis parallel to the long sides of the imaging volume, from other particles is highly uncertain.

Gut fullness was measured by integrating the fluorescence signal within the copepod. This number was compared to the range of gut fluorescence encountered in all deployments. The maximum gut fullness was then assumed to be 30 ng of pigment (Mackas and Burns 1986). The gut fullness of individuals was then classified on a linear scale, according to the following categories; 1: ≤ 25 % of the maximum gut fullness, 2: >25% and ≤ 50%, 3: >50% and ≤ 75%, 4: > 75%. Copepod vertical distribution profiles

were then constructed for each gut fullness category. Because of the scarcity of data in certain sections of the water column, I used a non-parametric Kernel-Smoothing Density Estimator (Bowman and Azalini 1997) to extrapolate from discrete points to a continuous vertical frequency distribution of copepods in the water column. Here I used a Gaussian kernel, and let Matlab's automatic bandwidth selector chose the bandwidth; however, after each computation I examined the resulting density and judged by eye whether the distribution was either under-smoothed (i.e. inexplicably spiky) or over-smoothed (suspiciously rounded). If that was the case, I reran the kernel smoothing density estimator with a manually entered bandwidth that I modified accordingly. Generally, the bandwidth, automatically or manually selected, ranged between 0.5 and 2 m. This procedure was repeated for all four gut-fullness categories.

Modeling of copepod foraging behavior

The structure of the IBM I developed is shown in the flowchart below (Fig 2). In this model, copepods begin at 75 – 125 m (Frost 1988) and start to migrate upward. At each time step, a random number generator modified by the local concentration of food experienced by individual copepods determines whether foraging begins; the higher the food concentration, the higher the probability that a copepod will begin foraging. Once foraging has begun ingestion is modeled as a saturation response such that

$$I = I_{\max}\left(\frac{chl}{k_s + chl}\right) \qquad (1).$$

Here I is ingestion, I_{max} is the maximum rate of ingestion k_s is a half-saturation constant and *chl* is the local food concentration experienced by the individuals. Individual swimming behavior is formulated as an area restricted search that relates to the ingestion function such that

$$z = \alpha z_{\max}\left[1 - \left(\frac{chl}{k_s + chl}\right)\right] \quad (2).$$

Here z is step length, α is a randomized direction (up or down) parameter, z_{max} is maximum step length. (1) and (2) are complementary, and share a common half-saturation constant to model the fact that a copepod uses the same appendages to feed and swim (e.g. Leising 2000). Food processing is determined by gut throughput time (*GTT*). *GTT* is a function of feeding activity and the ambient temperature experienced by individuals. Temperature dependent *GTT* when the copepod is not feeding is calculated according to Dam and Peterson (1988). Temperature dependent *GTT* during feeding is calculated according to an average fit to the data presented in the previous chapter. The copepod's gut is modeled as a two-compartment system, upper mid-gut (UMG) and posterior mid-gut (PMG), in accordance to the description provided in chapters 2 and 3. *GTT* determines the rate at which food moves through these two compartments. Once the PMG accumulates past a threshold amount of 20% of the gut content, a fecal pellet is evacuated. While not pursued here, this formulation can answer questions regarding the impact of behavior on copepod contributions to the biological pump.

A copepod's feeding bout is formulated as in Leising et al. (2005); specifically a bout lasts until the copepod saturates its gut past a satiation threshold s, beyond which

feeding ceases; the copepod enters a refractory period and sinks or swims downward. Once the gut contents of copepods in the refractory period have cleared past a hunger threshold, copepods return to feeding. Unlike the approach in Leising et al. (2005) however, where total feeding time is limited by a pre-determined descent time, here, total feeding is determined by a minimum metabolic requirement (*m*) being fulfilled. As a result copepods that had not ingested enough to assimilate m by the end of a simulation run could still be found near the surface (Huntley and Brooks 1982). The entire model is summarized below (Fig 4-2), and some of the critical parameters are listed along with their assigned value (Table 4-1).

Table 4-1: *Important model parameters*

Parameter		**Value or range**	**Source**
Max ingestion	I_{max}	100 ng chl h^{-1}	Frost (1972)
Half-saturation	k_s	5 µg chl L^{-1}	Frost (1972)
Max. step length	z_{max}	10-30 cm	Landry and Fagerness (1988)
Satiation threshold	*s*	30 ng chl	Mackas and Burns (1986)
Hunger threshold	*h*	5 ng chl	Mackas and Burns (1986)
Daily Metabolic Requirement	*m*	200 ng chl	Vidal (1980)
Assimilation coefficient	*a*	75%	Landry et al. (1984)
$GTT_{FEEDING}$*		32.7 – 0.95T	Karaköylü, previous chapter
$GTT_{REFRACTORY}$**		$(0.0117 + 0.001794T)^{-1}$	Dam and Peterson (1988)

* GTT, both during and between feeding bouts, is expressed as a function of temperature, T.

** Dam and Peterson (1988) give the relationship as gut clearance rate (i.e. GTT^{-1})

Two types of simulations were run. The first type consisted in the model being forced with an idealized environment consisting of 3 distinct homogeneous food layers. The second type consisted in the model being forced using real *chl* and temperature data from CTD casts conducted during the fieldwork in Dabob Bay. Note that while

temperature is taken into account in the simulation, because of the relatively small difference in temperature between layers, its effect on foraging behavior is not analyzed here. Model results were evaluated in term of total numbers of foraging sorties conducted during a run, as well as a count of the number of foraging sorties conducted by individual copepods. For this purpose, a ‘gate’ was placed at the bottom of the food-rich layer; this gate recorded and tagged downward swimming copepods that were temporarily satiated. For runs where the model was forced using real profiles of *chl* and temperature, the results were sampled repeatedly at simulation times corresponding approximately to times at which the imaging system was deployed. Following the procedure described above for the field data, copepods were categorized according to their gut content, and their distribution was estimated using again a kernel-smoothing density estimator.

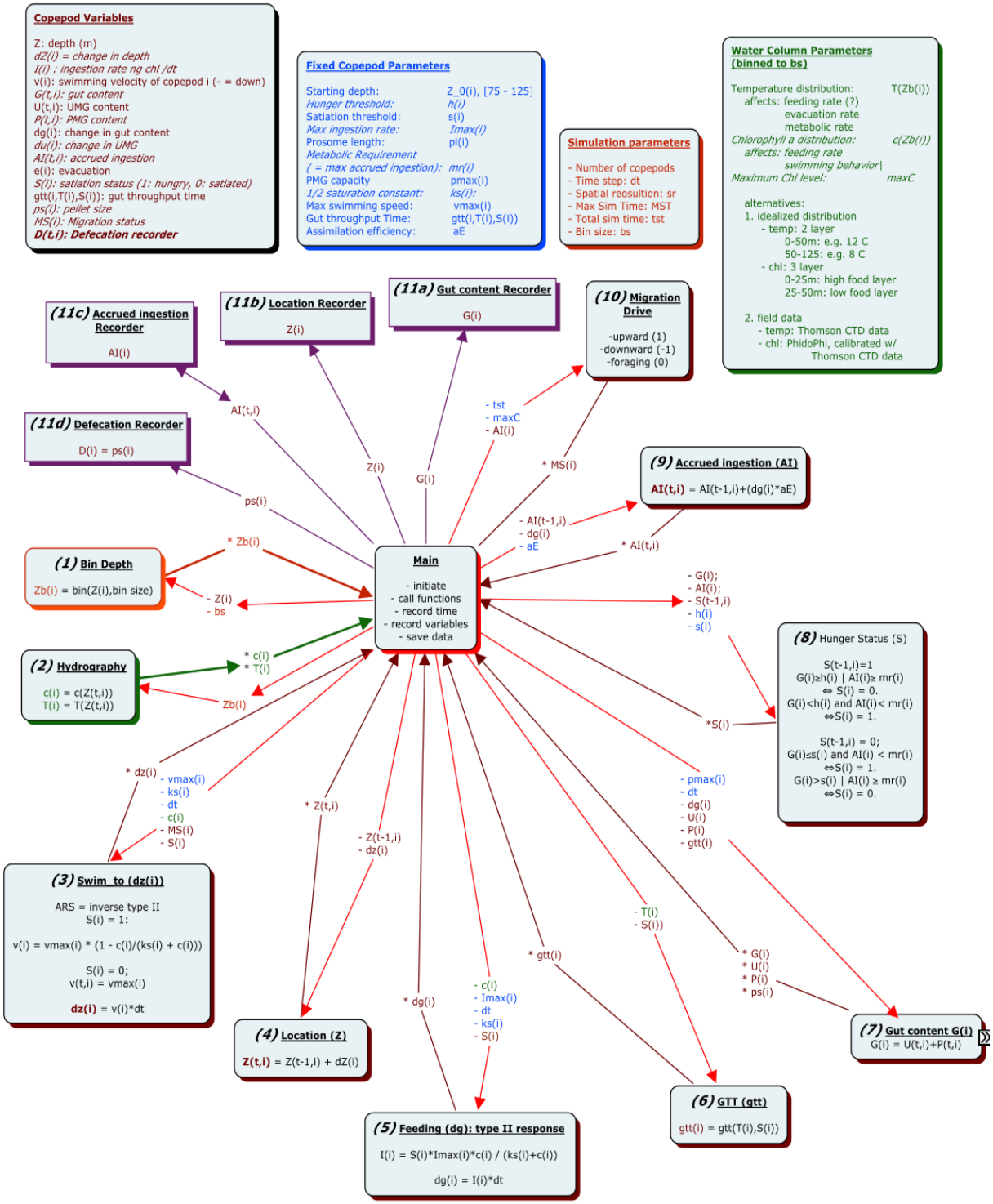

Figure 4-2: *Individual-Based Model flowchart* – Green: hydrographic properties. Blue: copepod parameters. Brown: copepod variables/functions. Other colors: pre-processing, model control, and storage. Arrows are inputs and outputs.

Results

Modeling foraging behavior: hydrographic conditions

A number of hydrographic scenarios were used to force the model. As stated earlier, these scenarios were idealized and emulated the three-layer food environment depicted earlier, or were constructed from actual hydrographic conditions sampled in the field. The shallow layer food concentration was either 5 μg chl L^{-1} (Fig 4-3A) from 0 to 15 m, or 10 μg chl L^{-1} (Fig 4-3B); in both cases the intermediate layer has a food concentration of 2 μg chl L^{-1} and span the 15 to 50 m depth range. In both scenarios, temperature is 12 °C from 0 to 50 m and 8 °C below 50 m. The deep layer extends from 50 to 125 m. The other two scenario types were from data sampled in Dabob Bay and have smoother transitions than the previous ones. One of the scenarios retains essentially the three-layer property with in this case a chl maximum of 11 μg chl L^{-1} located at 18m (Fig 4-3C); the other scenario type is characterized by a thin food-rich layer, in this case with a chl maximum of 11.5 μg chl L^{-1} at a depth of 8m. The latter two hydrographic profiles are much more heterogeneous within the different food layers than the idealized scenarios.

Model results

Each model run included 1000 copepods. Three types of behavior were observed, that resulted in fundamentally different vertical trajectories and gut content time series (Fig. 4-4). A copepod could conduct FS exclusively (red line, Fig 4-4A), or SF exclusively (blue line, Fig 4-4A). Some copepods however conducted a mixture of the two (black line, Fig 4-4A). Copepods that conducted FS exclusively had a gut content that saturated at a rate that depended on food concentration and temperature (red line, Fig

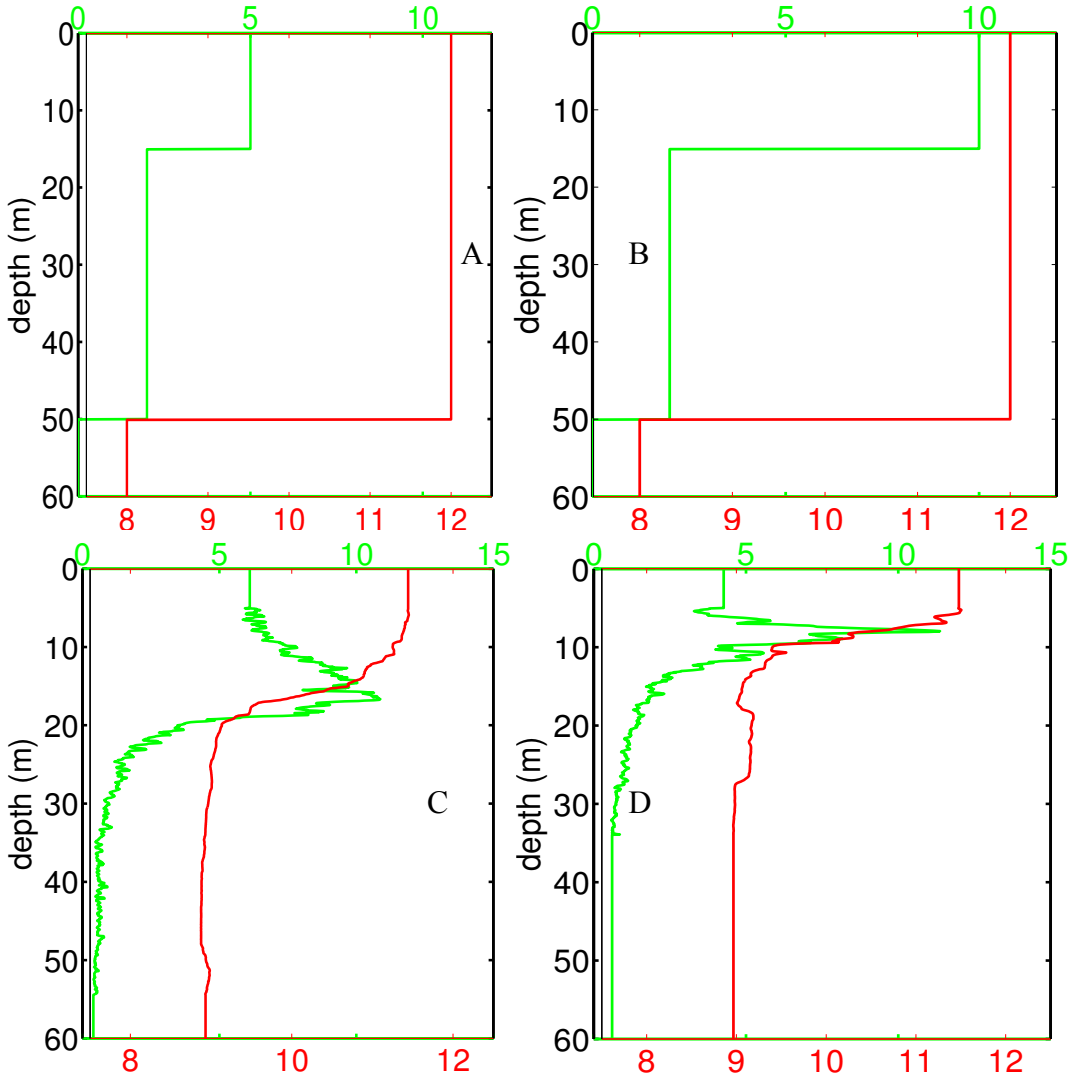

Figure 4-3: *Hydrographic conditions* – Examples of scenarios used chl distribution shown in green, temperature in red. A and B: Idealized scenarios with slab-shaped layers. C and D: real hydrographic data sampled during a cruise in May 2007 in Dabob Bay, WA. **— temperature (ºC) — chl (µg L^{-1})**

4-4B). Copepods that conducted SF exclusively remained in one layer and fed continuously (blue line, Fig 4-4B). Because, under circumstances favorable to SF gut throughput matched ingestion, the gut of these copepods never saturated. Note that these copepods never occurred in the shallow layer when it was slab-shaped, homogeneous and of sufficient concentration. However, when the model was forced with real hydrographic

data, where food distribution was much more heterogeneous in its distribution, ISF conducting copepods could occur in the shallow food-rich layer.

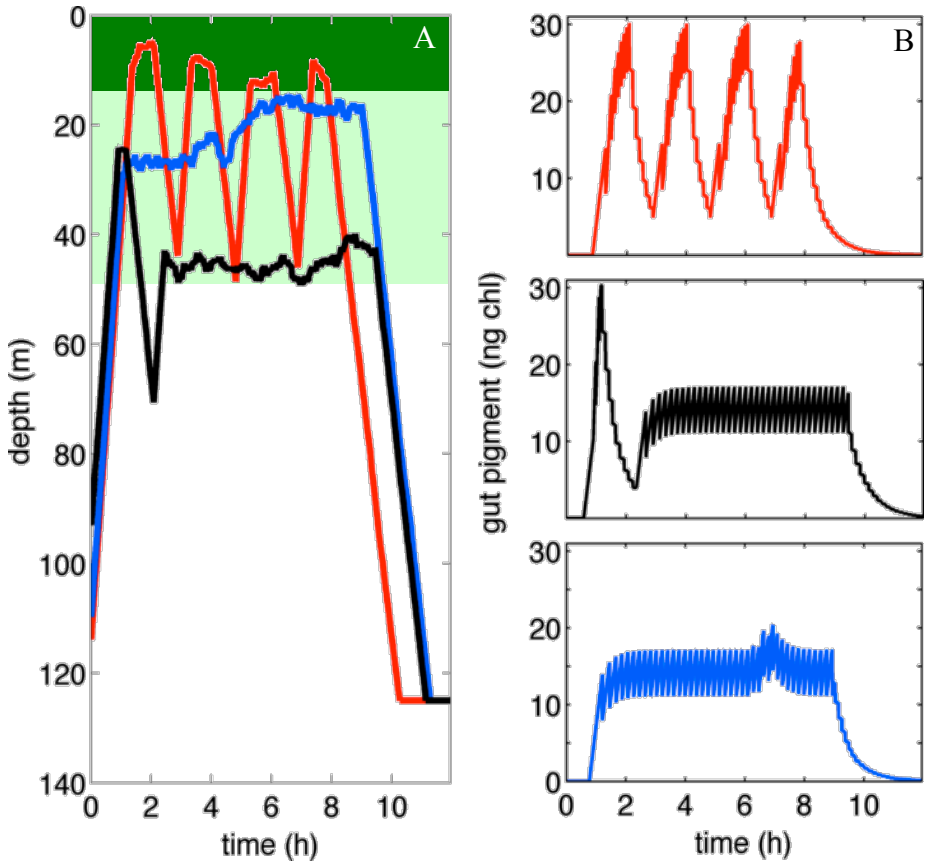

Figure 4-4: *Types of copepod vertical trajectories and corresponding gut content time series* – A: trajectory. —: FS. —: ISF. —: Mixed behavior. B: gut content.

Analyses of model runs showed that the dominance of FS as a strategy depended on the hydrographic profile the model was forced with. Relative dominance was quantified using frequency distributions of numbers of foraging sorties: the proportion of the individuals undertaking a given number of foraging sorties. When the mode of this distribution was 0 or 1, SF was designated the dominant strategy. As the frequency distribution shifted toward the right, the (Fig 4-5), FS became increasingly dominant. When the model was forced with the four vertical structures described earlier, the results

showed that for the first three scenarios (Fig 4-3 A-C), where the *chl* maximum increased (5, 10, 11 µg chl L^{-1}) there was an expected shift in the distributions of numbers of foraging sorties toward FS (Fig 4-5 A-C). However in the case of the fourth scenario, which had the highest chl maximum (11.5 µg chl L^{-1}), the dominant strategy was SF (Fig 4-5 D). Testing this for several scenarios by regressing numbers of foraging sorties against the *chl* maximum revealed that the dominant strategy could not be predicted from the food concentration at the *chl* maximum (r^2 = ~0, p = 0.99, n = 9, Fig 4-6A). However, there was a significant relationship between the integrated chlorophyll in the shallow layer (mg m^{-2}) and the number of foraging sorties conducted during a model run (r^2 = 0.68, p = 0.01, n = 9, Fig 4-6B).

Gut content time series for all four scenarios were mapped together as a composite to demonstrate the implications of FS and SF (Fig 4-7). In all simulation runs, feeding began in synchrony. If the foraging strategy that dominated the system was FS, then the resulting gut content composite was dominated by a pattern of bands that marked alternating feeding and refractory modes. This was the case for the first three scenarios (Fig. 4-7A-C). These bands are particularly clear in the idealized scenarios A and B, as a result of the homogeneous distribution of food in each layer. The alternating bands are thicker in A than B because copepods needed to feed for longer durations in scenario A as a result of the lower food concentration in the shallow layer. Copepods in A needed a minimum of approx 1 hr and 30 of continuous feeding in the shallow layer to saturate their gut. Copepods in B needed only half as much. The pattern in scenario C (Fig 4-7C), though largely made of bands like the first two, is much noisier as a result of the heterogeneous distribution of food in the water column, including the shallow layer, and

the patterns show highly variable feeding times that could vary between 1 h and 30 min, and 20-30 min. Scenario D was dominated by SF. This is clearly visible (Fig 4-7D) in the data where there are very few alternating bouts of hunger and satiation.

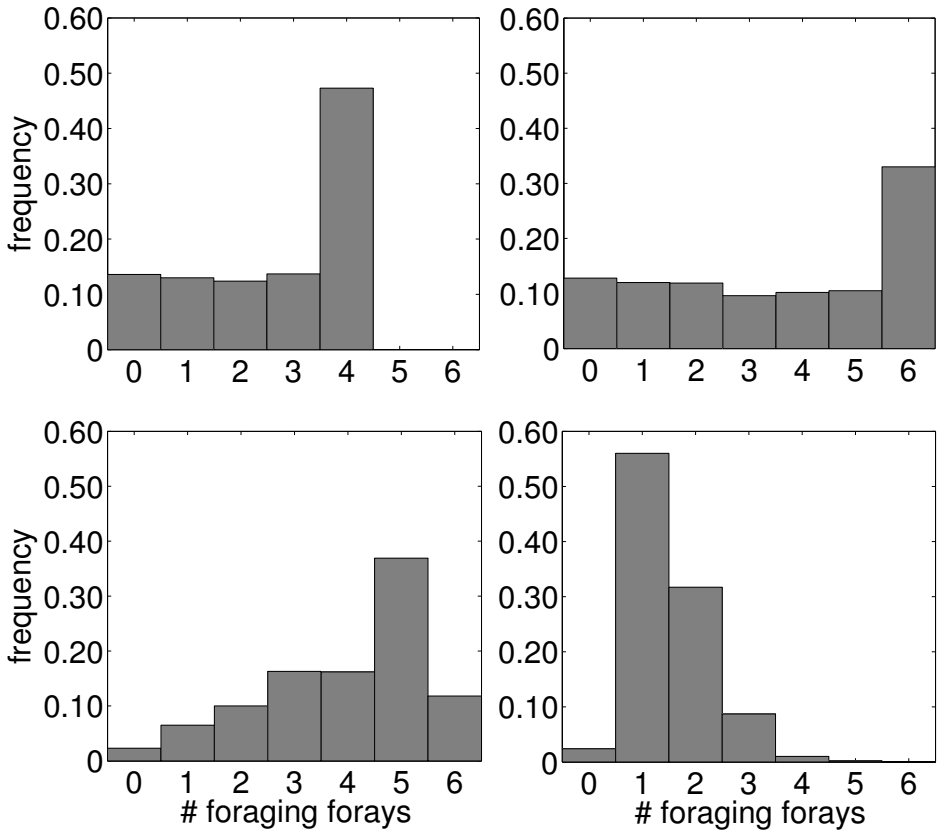

Figure 4-5: *Foraging sorties distribution frequency* – Panels A-D correspond to panels in Fig 3. A and B: idealized hydrography; C and D: real hydrography. A-C: increasing shift toward FS; D: ISF is dominant.

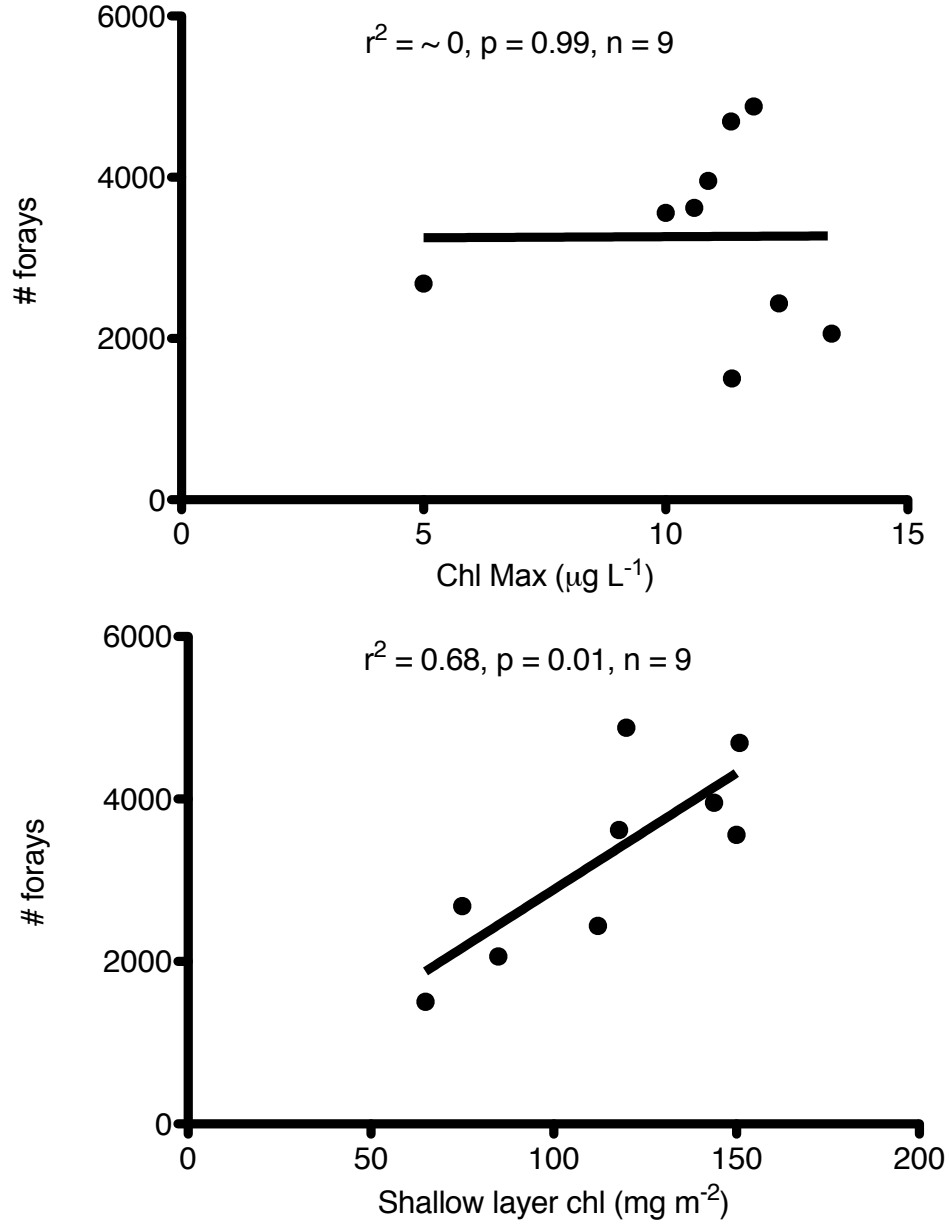

Figure 4-6: *Model regression against hydrographic data* – A: regression of numbers of foraging sorties against *chl* maximum concentration. B: regression of numbers of foraging sorties against the integrated chlorophyll in the shallow layer.

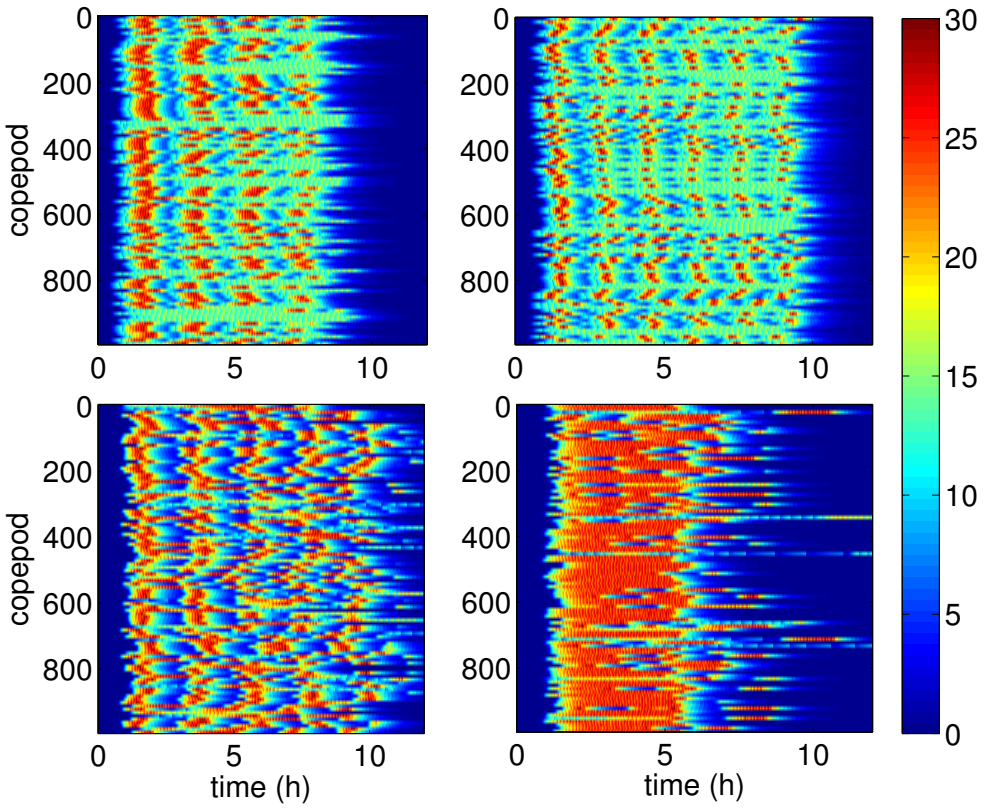

Figure 4-7: *Composite of gut pigment time series* – Rows show individual copepod gut content through time. Panels A-D correspond to panels in Figs 3 and 5. Colorbar scales gut contents, with warmer colors indicating fuller guts; i.e., red→satiated, blue → hungry. Maximum gut content is 30 ng pigment. Alternating bands of warmer and colder colors are diagnostic of synchronized foraging sorties. Width of bands indicates time spent in feeding/refractory modes.

The composite of copepod trajectories (e.g., Fig 4-4A) in the water column show the predominance of bands of alternating depths, indicating the importance of FS (Fig 4-8). As expected, there are again obvious differences between the four scenarios. Patches of dark blue are particularly interesting in that they are assumed to represent an increased risk in predation (cf. Fig 4-1). Panels A-C (Fig 4-8) show bands, the width and the coloration of which changes depending on the scenario. In A, large ~1 h and 30 min wide

dark blue bands alternate with narrow ~10-20 min red bands, indicating a total time spent near the surface of up to ~ 6 h during the 12 h simulation period. In B the blue bands are <1 h wide, and not as blue, showing that copepods spent up to ~3 hours in the shallow layer, though not as close to the surface as in A. Panel C is noisier than A or C, suggesting that the heterogeneity of the food distribution increases the variability of copepod vertical distribution. In panels A-C numerous light blue – orange streaks parallel to the x-axis can be seen, indicating the continued presence of copepods conducting SF at various depths, even when FS was the dominating foraging pattern. Similarly to Fig 4-7, scenario D was characterized by a long residence in the surface layer as a result of a lack of gut saturation resulting from the relative paucity of food in the shallow layer.

The time taken to satisfy a pre-determined metabolic requirement was analyzed by producing a composite of food accrued through time (assuming an instantaneous absorption) (Fig 4-9). Here the cost/benefit associated with either FS or SF can be analyzed in terms of time necessary to satisfy daily requirements. In scenarios A and B where dominance of FS increases clearly from scenario A to B, copepods attained their daily requirements after on average ~7 h and 9 h respectively (Fig 4-9A and B). In the more heterogeneous environment of scenario C, the average time was still ~9 h, but there were copepods that were able to acquire their ration in as little as 6 h. Finally in scenario D, where SF was dominant, copepods were able to fulfill their daily quota on average in ~5.5 h. Thus in conditions similar to those encountered in Dabob Bay, copepods conducting FS overall take longer to satisfy their daily quota than copepods conducting SF.

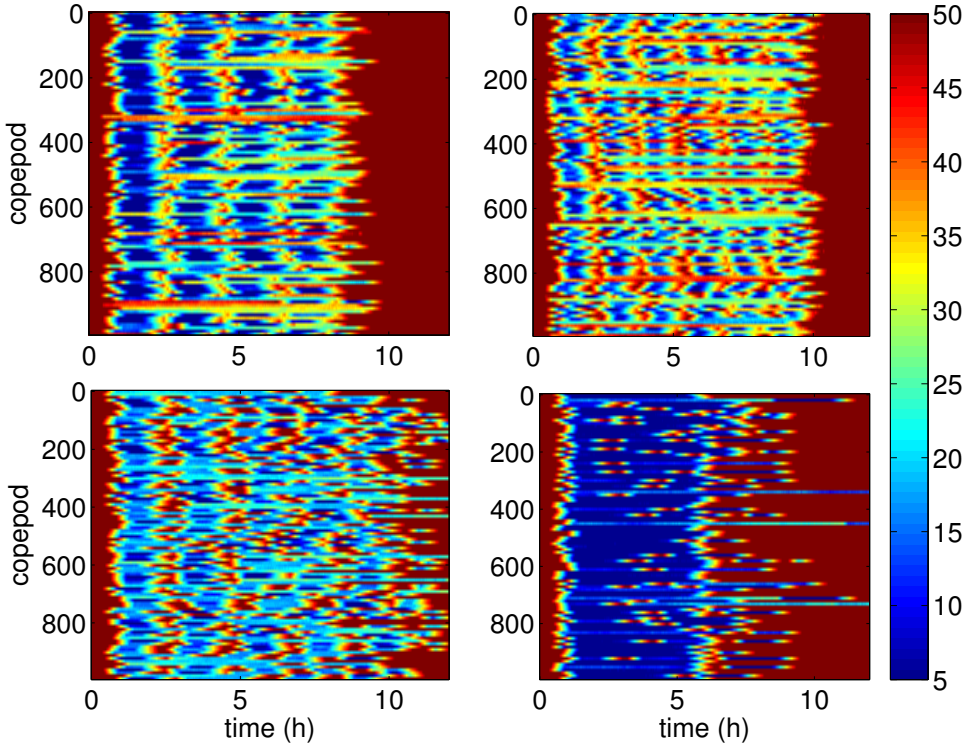

Figure 4-8: *Composite of copepod trajectories in the water column* – Rows report individual copepod vertical location through time. Panels A-D correspond to scenario panels in Fig 3 and results panels in Fig 5. Warmer colors indicate deeper location; colder colors imply a shallow station; i.e. following Fig 1, red→relative safety, blue → relative danger. Depth range includes the shallow and intermediate layer. Alternating bands of warmer and colder colors are diagnostic of foraging sorties. Width of bands indicates time spent at either surface or depth.

Testing the model using field data

Because tracking individual copepods is not an option in the field, a similar analysis is not possible with data collected from the field. Thus to test the model, I compared the vertical distributions of copepods observed using MISCIS to model copepods from a run forced with measured hydrographic data acquired from the same profiles. Modeled and observed copepods were categorized by their gut fullness. For the model/data comparison I used data from one night during which 3 deployments were conducted; dusk, dawn, and midnight. Each deployment yielded 4-5 profiles, resulting in thousands of images.

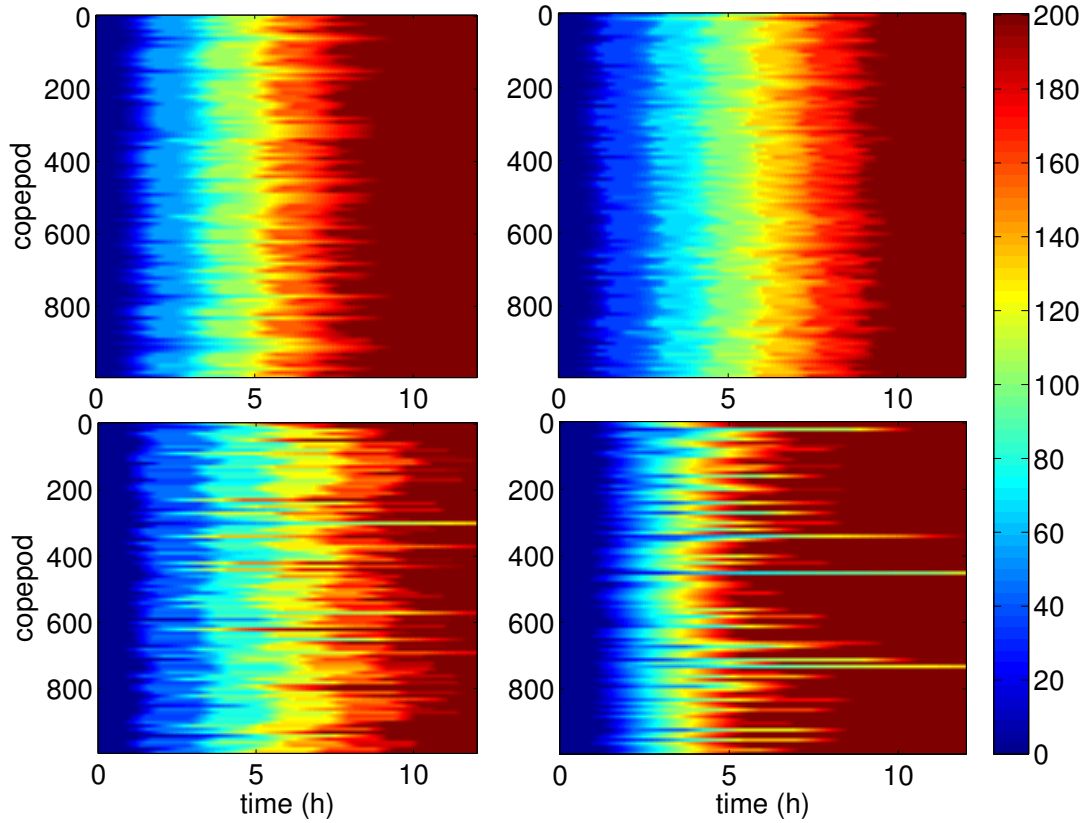

Figure 4-9: *Composite of accrued food absorption, expressed as total ng Chl absorbed*. Warmer colors indicate copepods are close to satisfying their daily requirements, determined to be approx 200 ng Chl d^{-1}.

During the dusk deployment (Fig 4-10), copepods with higher gut content were more strongly confined to the *chl* maximum. This suggests forays into the shallow layer to acquire this high gut content. It also suggests that copepod cleared their guts too rapidly to be able to carry a significant amount to the intermediate layer. There was good qualitative and at times quantitative agreement between model and MISCIS data, particularly comparing modeled and observed copepods having high gut contents. The agreement was not as good when gut contents were low. Interestingly, some features of the model distribution for copepods with <25% gut content agreed better with the MISCIS data for the 25-50% category (Fig 4-10A and B); this suggests that the

relationship between gut content and gut signal might not be linear when there is little algae in the gut. During the midnight deployment (Fig 4-11) the vertical association between the *chl* max and copepods of increasing gut content remained. However copepods with guts more than 50% full could not be found. During the dusk deployment, all categories of gut fullness were present again (Fig 4-12). Agreement between the model and the MISCIS data was weaker, and while the model did predict strong peaks in the distributions of copepods of high gut content seen in the MISCIS data, the model was off by ~ 5 m.

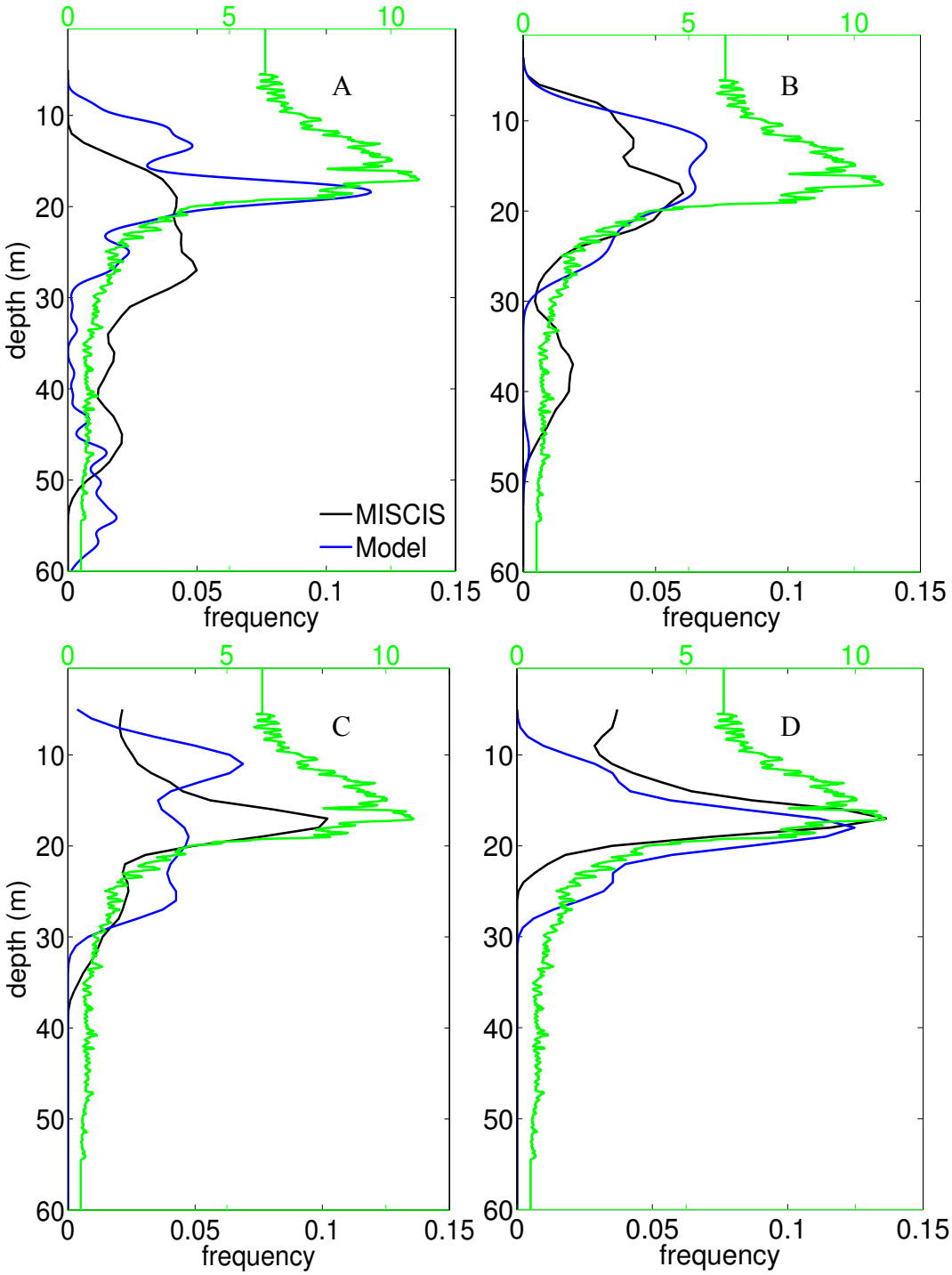

Figure 4-10: *Dusk Deployment* – A: 0 - 25% full copepods; B: 25 - 50%; C: 50 - 75%; D: 75 - 100%. —: MISCIS field data. —: Model data, —: chlorophyll (µg L^{-1}).

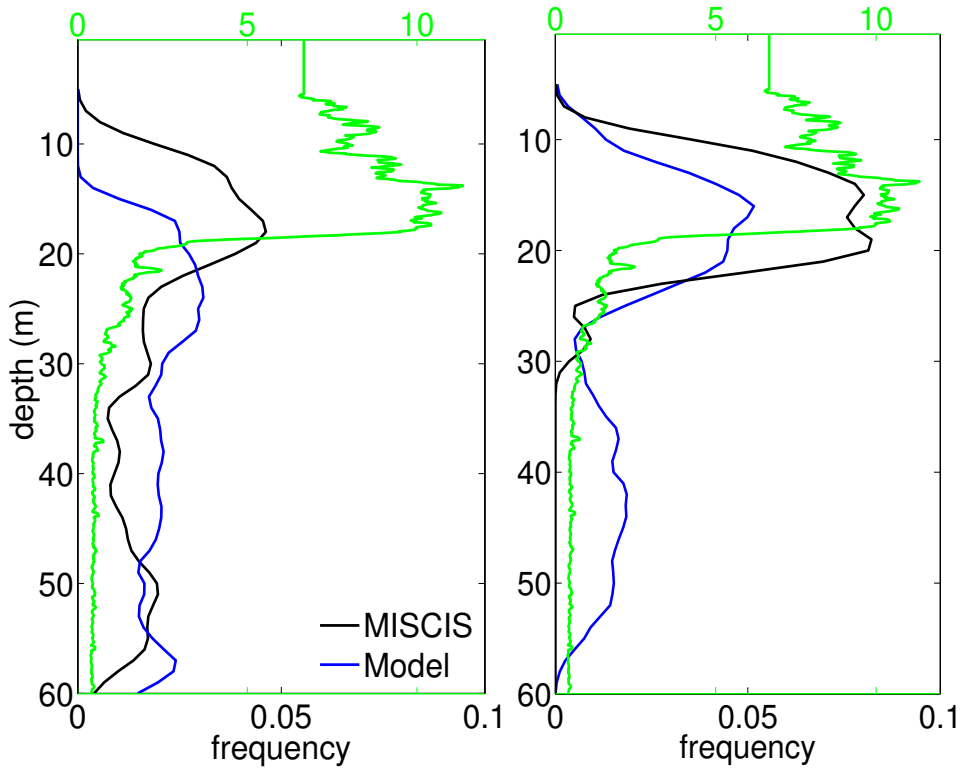

Figure 4-11: *Midnight deployment* – A: 0 – 25% full copepods, B: 25 – 50%. Copepods with higher gut contents could not be found —: MISCIS field data. —: Model data, —: chlorophyll (µg L^{-1}).

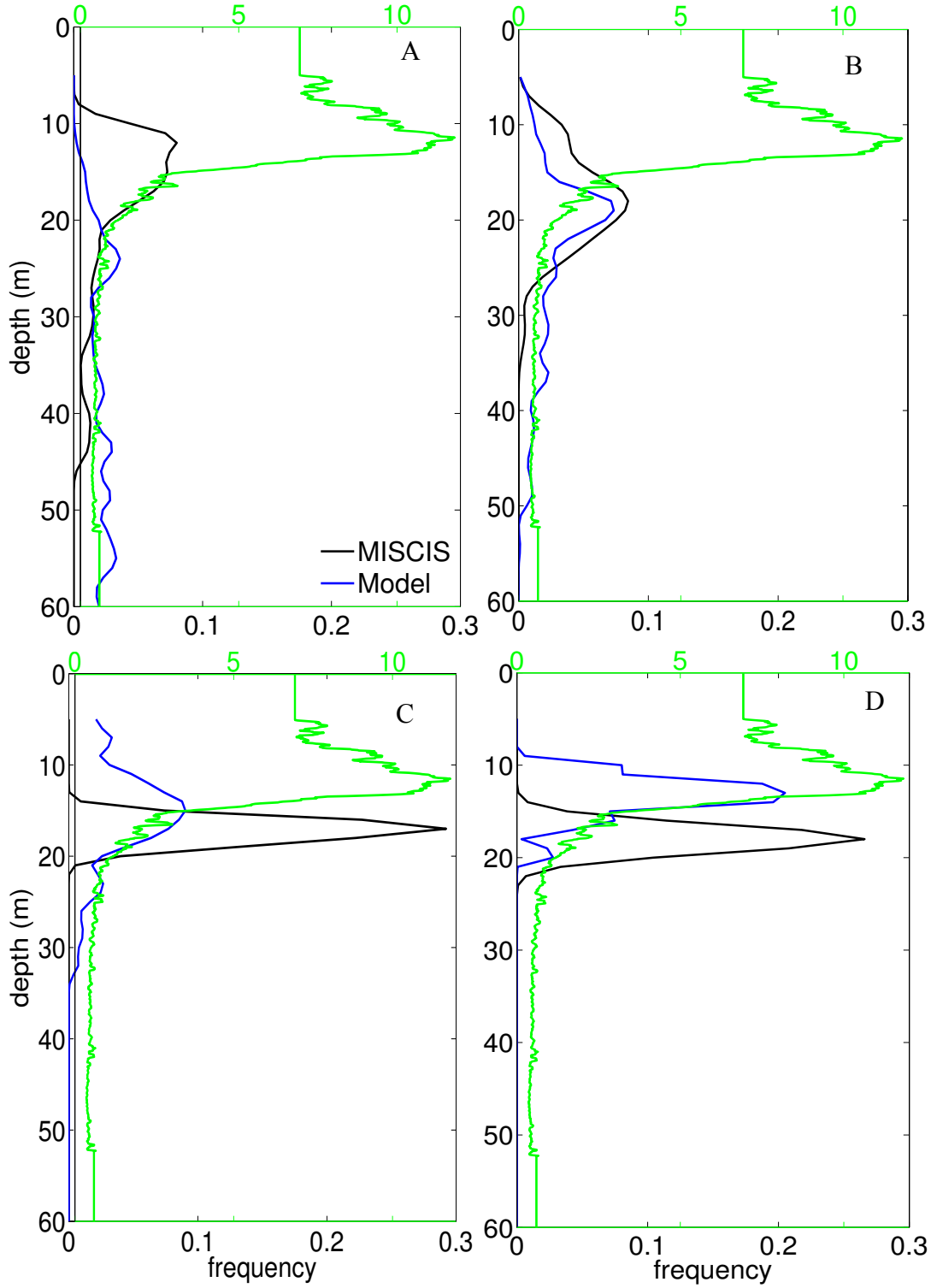

Figure 4-12: *Dawn deployment* – A: 0 – 25% full copepods, B: 25 – 50%. , C: 50 – 75%, D: 75 – 100%. Copepods with a higher gut content could not be found —: MISCIS field data. —: Model data, —: chlorophyll (µg L^{-1}).

Discussion

The IBM presented here did not have any specific foraging strategy built-in. The dominant strategy determined for different scenarios was an emergent property of this model, and resulted from the interaction between the physiology of copepods and the environment they foraged in.

This suggests that copepod behavior could be at least broadly predictable from knowing as little as the distribution of food and temperature in the water column. This simplification may work only in a limited number of situations such as the bloom or near-bloom conditions found in Dabob Bay. In Dabob Bay, the model showed good qualitative, and at times quantitative agreement with data from the MISCIS, suggesting that the essential dynamics were captured. This was particularly true for copepods with high gut content, which tended to aggregate close to the chlorophyll maximum. In such cases, FS was the dominant foraging strategy. Copepods of comparable intermediate gut content were still found in both shallow and intermediate layers. Copepods with maximum, near-saturation gut contents never occurred in the intermediate layer. Intermediate layer food concentrations were sufficiently low that gut throughput always matched ingestion and saturation never occurred. This may a priori seem contradictory to the data presented by Dagg et al. (1997); however, there is no evidence that copepods filled their guts to capacity. Moreover, the study of Dagg et al (1997) took place toward the end of a spring bloom period (night of March 23/24, 1991) and food concentration in the entire shallow layer, shown earlier to be a critical factor in determining the dominant strategy was much lower than the scenarios presented here where conditions were

favorable to FS. Fig. 2 of Dagg et al. (1997) show that the chlorophyll maxima were quite variable throughout the night, ranging between 8 and 17 μg L^{-1}. However, these were usually the peaks of remarkably thin and shallow layers. The17 μg L^{-1} peak for instance was located at ~9-10 m and was ~2 m thick, dropping rapidly back to <5 μg L^{-1}. This is a situation remarkably similar to scenario D (Figs 3D, 5-9D); a scenario where the model predicted ISF to be the dominant foraging strategy.

While this model offers a powerful but simple diagnostic tool for estimating foraging behavior, there are instances when the model does not predict the observed patterns well. This was the case for the copepods with high gut content during the dusk deployment. Here, the MISCIS data showed that copepods of high gut content were 2-3 m below the chlorophyll maximum, and about 5 m below the model-predicted peak (Fig 12D). Moreover, observed copepods from other gut fullness categories appeared to progressively aggregate at that same location, indicative of ISF. This result was not observed in the model. One plausible explanation is that the copepods favored this layer based on the type of food present, rather than opting for the quantity of the food available a few meters above. Active prey selection by *Calanus* is not uncommon, and Leising et al. (2005b) showed that *Calanus pacificus* females often rejected the most abundant phytoplankton in favor of a different prey, with a selectivity ranging from preferring another phytoplankton from the same genus as the abundant prey, to switching to microzooplankton. Another feature not explained by the model is the absence of copepods of high gut content during the midnight deployment, potentially attributable to 'midnight sinking' (Tarling et al. 2002). Simard et al. (1985) documented an instance when *Calanus* left the surface and stopped feeding during the night, returning at dawn.

Tarling et al. 2002 documented a similar nocturnal departure from the surface by *C. finmarchicus* and attributed this migration to a predation avoidance response to the arrival of krill; Pearre (2003b) disputes this conclusion, offering alternative possibilities that included faster feeding, leading to early satiation, and the exploitation of layers of microzooplankton. Given that in this study there were still some copepods with low gut content (< 50%) that remained in the surface layer, predation avoidance is not the likely reason here. More likely, copepods that were satiated left the shallow and intermediate layers, leaving behinds copepods that were either unable to secure a sufficiently concentrated food patch, or that simply were feeding slower than average (cf. chapter 2).

Results of model runs using different scenarios enable a cost-benefit analysis of both strategies. The 'banded' pattern depicted in the trajectory composites (Fig 8) when FS is the dominant strategy show the time copepods need to spend in the shallow layer to obtain a gut full of food. This time of greater exposure to predation is clearly linked to the amount of food available in the feeding layer, as shown by the difference in band thickness (cf Fig 8 A vs Fig 8B), and a shallow layer of higher food concentration implies that the feeding bouts will be shorter, resulting in reduced exposure time per bout; particularly since the feeding currents induced by *Calanus* during feeding could make it more visible to predators (Kislaoglu and Gibson 1976, Wright and O'Brien 1984). Conversely, copepods conducting ISF in the shallow layer, i.e. when food is too scarce even in that layer for copepods to reach saturation, incur the greatest cost in terms of continuous predation risk (see long "risky time" window depicted in blue in Fig 8D). While "better hungry than dead" seems a reasonable strategy for any animal including copepods, evidence exists showing that herbivores (Flik and Ringelberg 1993) including

C. pacificus (Huntley and Brooks 1982) can reside in the shallow layer even during the day when food is scarce. On the other hand, the refractory periods experienced by animals conducting FS implies a decoupling from the prey, resulting in time during which the animal sinks away, digests, resume food searching, but does not feed. As a result, copepods undergoing SF can satisfy their minimum daily requirements in an overall shorter time than copepods undergoing FS. This could imply additional night-time left to accumulate additional reserves, mate or spawn.

Chapter 4, in full is currently being prepared for submission for publication of the material. Karaköylü, Erdem; Franks, Peter J. S. The dissertation author was the primary investigator and author of this material.

References

Bowman, A.W., and Azalini, A. 1997. Applied Smoothing Techniques for Data Analysis. Oxford University Press.

Dagg, M.J., Frost, B.W., and Newton, J.A. 1997. Vertical migration and feeding behavior of *Calanus pacificus* Females during a phytoplankton bloom in Dabob Bay, U.S. Limnol. and Oceanogr. 42: 974-980.

Dam, H.G. and Peterson, W.T. 1988. The effect of temperature of the gut clearance rate constant of planktonic copepods. J. Exp. Mar. Biol. Ecol. 123: 1-14.

De Robertis, A. , Eiane, K., and Rau, G.H. 2001. Eat and run: anoxic feeding and subsequent aerobic recovery by *Orchomene obtusus* in Saanich Inlet, British Columbia, Canada. Mar. Ecol. Progr. Ser. 219: 221-227.

Flik, B.J.G. and Ringelberg, J. 1993. Influence of food availability on the initiation of diel vertical migration (DVM) in Lake Maarsseveen. Arch. Hydrobiol. Beih. Ergebn. Limnol. 39: 57-65.

Franks, P.J.S. and Jaffe, J.S. 2008. Microscale variability in the distributions of large fluorescent particles observed *in situ* with a planar laser imaging fluorometer. J. Mar. Sys. 69: 254-270.

Franks, P.J.S. and Jaffe, J.S. 2001. Microscale distributions of phytoplankton: initial results from a two-dimensional imaging fluorometer, OSST. Mar. Ecol. Progr. Ser. 220: 59-72.

Frost, B.W. 1988. Variability and possible adaptive significance of diel vertical migration in *Calanus pacificus*, a planktonic marine copepod. Bull. Mar. Sci. 43: 675-694.

Frost, B.W. 1972. Effects of size and concentration of food particles on the feeding behavior of the marine planktonic copepod *Calanus pacificus*. Limnol. Oceanogr. 6: 805-815.

Huntley, M. and Brooks, E.R. 1982. Effects of age and food availability on diel vertical migration of *Calanus pacificus*. Marine Biology 71: 23-31.

Kislaoglu, M and Gibson, R.N. 1976. Some factors governing prey selection by the 15-spined stickleback, *Spinachia spinachia*. J. Exp. Mar. Biol. Ecol. 25: 159-169.

Landry, M.R. and Fagerness, V.L. 1988. Behavioral and morphological influences on predatory interactions among marine copepods. Bull. Mar. Sci. 43: 509-529.

Landry, M.R., Hassett, R.P., Fagerness, V., Downs, J. and Lorenzen, C.J. 1984. Effect of food acclimation on assimilation efficiency of *Calanus pacificus*. Limnol. Oceanogr. 29: 361-364.

Leising, A.W., Pierson, J.J., Cary, S., and Frost, B.W. 2005a. Copepod foraging and predation risk within the surface layer during night-time feeding forays. J. Plankton Res. 27: 987-1001.

Leising, A.W., Pierson, J.J., Halsband-Lenk, C., Horner, R., Postel, J. 2005. Copepod grazing during spring blooms: Does *Calanus pacificus* avoid harmful diatoms. Progr. Oceanogr 67: 384-405.

Leising, A.W. 2000. Copepod foraging in thin layers using SEARCH (Simulator for Exploring Area-Restricted search in Complex Habitats). Mar. Models 2: 1-18.

Huntley, M. and Brooks, E.R. (1982). Effects of age and food availability on diel vertical migration of *Calanus pacificus*. Mar. Biol. 71: 23-31.

Mackas, D.L. and Burns, K.E. 1986. Poststarvation feeding and swimming activity in *Calanus pacificus* and *Metridia pacifica*. Limnol. Oceanogr. 31: 383-392.

Pearre Jr., S. 2003a. Eat and run? The hunger satiation hypothesis in vertical migration: history, evidence and consequences. Biol Rev.78: 1-79.

Pearre Jr., S. 2003b. When the lights are low: Comment on 'Midnight sinking behaviour in *Calanus finmarchicus*: a response to satiation or krill predation by Tarling et al. (2002). Mar. Ecol. Progr. Ser. 252: 303-305.

Pearre Jr., S. 1973. Vertical migration and feeding in *Sagitta elegans* Verrill. Ecol. 54: 300-314.

Pierson, J.J., Frost, B.W., Thoreson, D., Leising, A.W., Postel, J.R. and Nuwer, M. 2009. Trapping migrating zooplankton. Limnol. Oceanogr. Methods 7: 334-346.

Simard, Y., Lacroix, G., and Legendre, L. 1985. In situ twilight grazing rhythm during diel vertical migrations of a scattering layer of *Calanus finmarchicus*. Limnol. Oceanogr. 30: 598-606.

Tarling G.A. and Johnson, M.L. 2006. Satiation gives krill that sinking feeling. Curr. Biol. 16: R83-R84.

Tarling, G.A., Jarvis, T., Emsley, S. M. and Matthews, J.B.L. 2002. Midnight sinking behaviour in *Calanus finmarchicus*: a response to satiation or krill predation? Mar. Ecol. Progr. Ser. 240: 183-194.

Vidal, J. 1980. Physioecology of zooplankton. III. Effects of phytoplankton concentration, temperature, and body size on the metabolic rate of *Calanus pacificus*. Mar. Biol. 56: 195-202.

Wright, D.I. and O'Brien, W.J. 1984. The development and field test of a tactical model of the planktivorous feeding of white crappie (*Pomoxis annularis*). Ecological Monographs 54: 65-98.

Zaret, T.M. 1972. Predators, invisible prey, and the nature of polymorphism in the Cladocera. Limnol. Oceanogr. 17: 171-184.